

PASI KEINÄNEN

The Effect of Dispersion Quality of Carbon Nanotube Colloids on Physical Properties of Nanocomposites

PASI KEINÄNEN

The Effect of Dispersion Quality
of Carbon Nanotube Colloids
on Physical Properties of Nanocomposites

ACADEMIC DISSERTATION

To be presented, with the permission of
the Faculty of Engineering and Natural Sciences
of Tampere University,
for public discussion in the auditorium SA203
of the Sähköotalo building, Korkeakoulunkatu 3, Tampere,
on the 30th of October, at 13 o'clock.

ACADEMIC DISSERTATION

Tampere University, Faculty of Engineering and Natural Sciences
Finland

<i>Responsible supervisor and Custos</i>	Professor Jyrki Vuorinen Tampere University Finland	
<i>Supervisor</i>	Associate Professor Mikko Kanerva Tampere University Finland	
<i>Pre-examiners</i>	Associate Professor Grzegorz Celichowski University of Lodz Poland	Professor Maurizio Galimberti Politecnico di Milano Italy
<i>Opponents</i>	Associate Professor Grzegorz Celichowski University of Lodz Poland	Senior Scientist Jani Pelto VTT Technical Research of Finland Ltd. Finland

The originality of this thesis has been checked using the Turnitin OriginalityCheck service.

Copyright ©2020 author

Cover design: Roihu Inc.

ISBN 978-952-03-1725-6 (print)

ISBN 978-952-03-1726-3 (pdf)

ISSN 2489-9860 (print)

ISSN 2490-0028 (pdf)

<http://urn.fi/URN:ISBN:978-952-03-1726-3>

PunaMusta Oy – Yliopistopaino
Vantaa 2020

PREFACE

The work was carried out in Materials Science and Environmental Engineering unit in Faculty of Engineering and Natural Sciences at Tampere University. The work of the author was self-funded.

The work was supervised by Professor Jyrki Vuorinen and Associate Professor Mikko Kanerva to whom I address my gratitude. I want to thank all of my co-authors and especially Dr. Amit Das and Mrs. Sanna Siljander for fruitful conversations and co-operation in both theoretical and practical issues.

I also want to thank my wife Anne for putting up with me.

Tampere, August 2020

Pasi Keinänen

ABSTRACT

Carbon nanotubes have been shown to be excellent nano size filler material in dozens of different matrices. They possess many physical features that make them almost optimal for this purpose including high electrical conductivity, mechanical strength and thermal conductivity. There is however one property that makes nanotubes challenging to use; they typically come in aggregates which have high internal binding energies. Therefore in order to generate evenly distributed dispersions one need to use high shear forces and some times chemical modification of the tubes. These process conditions can cause changes in an integrity of the tubes themselves and inhibit the matrix-filler and filler-filler interactions diminishing the physical properties of the nanocomposites.

The main objectives of this thesis were to answer how the development of the dispersion quality of aqueous nanotube colloids can be optimized and monitored during sonication assisted dispersion, how the dispersion quality affects the properties of the nanocomposites, and how the properties can be further improved after composite have already been prepared.

It was observed that depending on the expected feature, maximum dispersion quality is not always needed and one can even benefit from residual pristine filler-filler interaction of the nanotube agglomerates. Another observation was that if surfactants are being used especially in aqueous dispersion to stabilize the colloid, they have inhibiting effect on properties of the solution casted composites by lowering the filler-filler and filler-matrix interaction. By removing the surfactant afterward some of these expected properties can be realized.

TIIVISTELMÄ

Hiilinanoputket ovat nanokokoinen komposiittien täyteaine, jonka toimivuus on osoitettu useilla eri matriiseilla. Hiilinanoputkien erinomainen lämmön- ja sähköjohtavuus sekä hyvät mekaaniset ominaisuudet tekevät siitä lähes optimaalisen materiaalin moneen tarkoitukseen. Täyteaineen käytössä on kuitenkin suuria haasteita, sillä valmistusprosessien johdosta nanoputket muodostavat suuria agglomeraatteja missä niiden välinen sidosenergia on suuri. Tästä syystä hiilinanoputkien dispergointiin käytettävät energiat ovat myös suuria, jotka taas voivat vahingoittaa itse nanoputkia jolloin menetetään niiden erityisiä ominaisuuksia.

Tämän opinnäytetyön tarkoitus on selvittää miten sonikaatioon perustuvaa dispersioprosessia voidaan valvoa ja optimoida siten, että itse prosessi vahingoittaisi nanoputkia mahdollisimman vähän ja tutkia miten dispersiolaatu vaikuttaa hiilinanoputkista valmistettujen nanokomposiittien ominaisuuksiin. Työssä esitellään myös keino miten joidenkin nanokomposiittien ominaisuuksia voidaan parantaa valmistusprosessin jälkeen. Tutkimuksessa havaittiin myös, että dispersiolaadun ei välttämättä tarvitse olla täydellinen jotta saavutettaisiin tiettyjä ominaisuuksia. Joissakin tapauksissa itse agglomeraattien sisäistä sidosenergiaa voidaan jopa käyttää hyödyksi. Toinen havainto oli, että vesipohjaisissa dispersioprosesseissa käytetyt surfaktantit heikentävät dispersioista valmistettujen komposiittien ominaisuuksia ja poistamalla surfaktantit jälkikäteen voidaan komposiittien ominaisuuksia merkittävästi parantaa.

CONTENTS

1	Introduction	17
2	Carbon nanotubes	19
3	Carbon nanotube polymer composites	23
3.1	Mechanical properties	23
3.2	Electrical properties	25
3.3	Carbon nanotube - elastomer composites	27
3.4	Carbon nanotube - cellulose composites	28
4	Carbon nanotube colloids	31
4.1	Sonication	32
4.2	Surfactants	35
4.3	Dispersion quality	37
5	Aims of this study	39
6	Experimental	41
6.1	Materials	41
6.2	Mixing	43
6.3	Nanocomposite manufacturing	43
6.4	Characterization	44
6.4.1	Spectroscopy	44
6.4.2	Electrical measurements	44
6.4.3	Mechanical measurements	45
6.4.4	Microscopy	46

7	Results and discussion	47
7.1	Theoretical framework for dispersion quality	47
7.2	The effect of relative dispersion quality	48
7.3	The effect of surfactants	56
7.4	The effect of aspect ratio	67
8	Concluding remarks	71
8.1	Research question 1	71
8.2	Research question 2	72
8.3	Research question 3	73
8.4	Research question 4	73
8.5	Future topics	74
	References	75
	Publication I	93
	Publication II	111
	Publication III	125
	Publication IV	141
	Publication V	155

SYMBOLS AND ABBREVIATIONS

C_b	chiral vector
E	energy
E_L	longitudinal elastic modulus
E_T	transverse elastic modulus
E_c	elastic modulus of the composite
E_f	elastic modulus of the filler
E_m	elastic modulus of the matrix
R	radius of the cavitation bubble
S	surface tension
T	translation vector
α	opacity
x	system-specific constant related to the concentrations and properties of the chemical components in the colloid
μ_L	dynamic viscosity
ρ_L	density
σ	electrical conductivity
σ_0	scaling factor
φ	volume fraction
φ_c	critical volume fraction
$a_{1,2}$	lattice vector
p	density of conductive sites

p_B	pressure inside the cavity
p_c	critical density of conductive sites
t	dimensionality dependent exponent
AFM	atomic force microscope
AR	aspect ratio
BHKP	Bleached hardwood kraft pulp
CCA	Cluster-cluster aggregation
CMC	Critical micelle concentration
CNT	Carbon nanotube
CTAB	Cetrimonium bromide
DMA	Dynamical mechanical analysis
HLB	Hydrophilic-lipophilic balance
MWNT	Multi walled nanotube
NBR	Nitrile butadiene rubber
NFC	Nano fibrilled cellulose
NR	Natural rubber
PA	Polyamide
PE	Polyethylene
phr	Parts per hundred rubber
PU	Polyurethane
PVAc	Polyvinylacetate
PVC	Polyvinylchloride
RDQ	Relative dispersion quality
SBR	Styrene butadiene rubber
SDS	Sodium dodecyl sulphate
SEM	Scanning electron microscope
SWNT	Single walled nanotube

TEM	Transmission electron microscope
UTS	Ultimate tensile strength
UV-Vis	Ultraviolet to visible light

ORIGINAL PUBLICATIONS

- Publication I P. Keinänen, S. Siljander, M. Koivula, J. Sethi, E. Sarlin, J. Vuorinen and M. Kanerva. Optimized dispersion quality of aqueous carbon nanotube colloids as a function of sonochemical yield and surfactant/CNT ratio. *Helvion* 4.9 (2018), e00787.
- Publication II P. Keinänen, A. Das and J. Vuorinen. Further Enhancement of Mechanical Properties of Conducting Rubber Composites Based on Multiwalled Carbon Nanotubes and Nitrile Rubber by Solvent Treatment. *Materials* 11.10 (2018), 1806.
- Publication III S. Siljander, P. Keinänen, A. Rätty, K. R. Ramakrishnan, S. Tuukkanen, V. Kunnari, A. Harlin, J. Vuorinen and M. Kanerva. Effect of surfactant type and sonication energy on the electrical conductivity properties of nanocellulose-CNT nanocomposite films. *International journal of molecular sciences* 19.6 (2018), 1819.
- Publication IV S. Siljander, P. Keinänen, A. Ivanova, J. Lehmonen, S. Tuukkanen, M. Kanerva and T. Björkqvist. Conductive cellulose based foam formed 3D shapes—From innovation to designed prototype. Vol. 12. 3. Multidisciplinary Digital Publishing Institute, 2019, 430.
- Publication V J. Sethi, E. Sarlin, S. S. Meysami, R. Suihkonen, A. R. S. S. Kumar, M. Honkanen, P. Keinänen, N. Grobert and J. Vuorinen. The effect of multi-wall carbon nanotube morphology on electrical and mechanical properties of polyurethane nanocomposites. Vol. 102. Elsevier, 2017, 305–313.

Author's contribution

- Publication I The author is responsible for the theoretical work, planning the experiments and interpretation of the results. He wrote the article together with Mrs Sanna Siljander. All authors commented on the experimental work, and read and approved the manuscript.
- Publication II The author is responsible of planning and performing the experiments, and interpretation of the results. He wrote the article. All authors commented on the experimental work, and read and approved the manuscript.
- Publication III The author participated in planning the experiments and interpretation of the results. He also participated in writing parts of the article. All authors commented on the experimental work, and read and approved the manuscript.
- Publication IV The author participated in planning the experiments and interpretation of the results. He also participated in writing parts of the article. All authors commented on the experimental work, and read and approved the manuscript.
- Publication V The author participated in planning the experiments and interpretation of the results. All authors commented on the experimental work, and read and approved the manuscript.

1 INTRODUCTION

One special class of materials is called nanocomposites in which at least one of the components have at least one dimension under 100 nm. This enables large surface to mass distribution which have prominent affects on many features of the composites. One of the first literature references of nanocomposite was written by Blumstein in 1965 on his work with montmorillonite clay and methyl metacrylate polymers [1]. First commercial product based on nanocomposites was presented by Toyota Motor Corporation in 1980's which developed nanoclay-polyamide composition to be used in Toyota Camry in 1993 as a timing belt cover material. They discovered that nanocomposite of 95% nylon and 5% clay offered significantly higher tensile strength and heat distortion temperature compared to any other viable solution.

Some of the requirements set for particulate filler nanomaterials are : (i) excellent mechanical properties such as strength and Young's modulus; (ii) high aspect ratio and high surface area which enables high interaction with the matrix, and (iii) easy to disperse [2]. Carbon nanotubes (CNT) discovered about 30 years ago is checking two of these boxes. CNTs possess excellent mechanical properties and they have very high aspect ratio but on the other hand they do agglomerate and are very challenging to disperse. These problems have been recognized as the major reasons why nanotubes have not realized their full potential as a perfect nanocomposite filler material.

Like many new materials they have experienced almost the perfect hype curve, rising from academic work towards the peak and then almost disappearing from the scene. However, CNTs are making a comeback and are now in a phase of volume growth where increasing number of applications utilizing their properties are introduced [3]. Nanotubes are becoming a commodity.

This thesis is focusing on developing tools to understand and optimize aqueous dispersion process of carbon nanotubes, and on post treatment of elastomer and cellulose based CNT composites to enable better nanocomposites from nanotubes.

2 CARBON NANOTUBES

When studying soot from fullerene manufacturing experiment in 1991, Dr. Sumio Iijima discovered cylindrical graphitic formations which he called ‘helical microtubules’ [4]. Soon after the discovery these ‘microtubulae’ were renamed to carbon nanotubes (CNT) and hundreds of thousands of scientific articles later they are still getting significant attention and research funding both from public and private sectors. Carbon nanotubes are extremely small and hollow needle like elemental carbon structures which aspect ratio of length and diameter can be in 10^8 order of magnitude [5]. They can be divided into two major groups: single walled nanotubes (SWNT) and multi walled nanotubes (MWNT). SWNTs are made of single graphene layer rolled up to form a cylinder. The diameter of the cylinder typically varies from 0.5 nm to 5 nm whereas length can be up to 20 cm [5]. MWNTs are formed of concentric SWNTs or from single helical graphene sheet. Depending on manufacturing method and further treatments CNTs can be closed with fullerene cap or they can be open ended. Carbon nanotubes are synthesized from carbon containing chemical compounds or from pure graphite using several different techniques [4, 6–9].

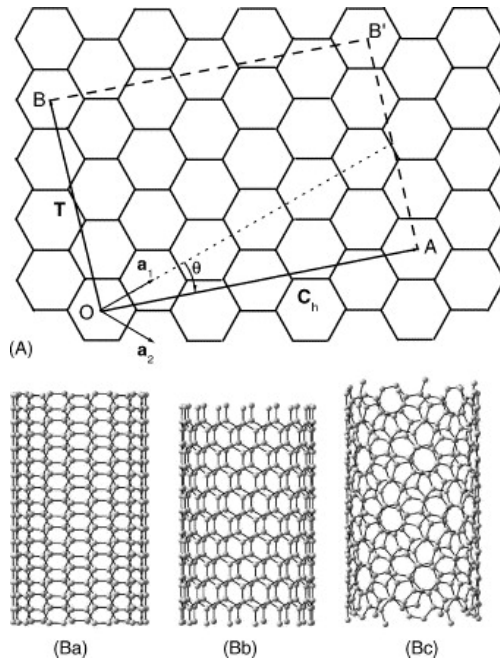


Figure 2.1 Schematic image of the graphene sheet (A) and rolled SWNTs (B). Chiral vector $C_b = na_1 + ma_2$ connects two lattice points O and A which meet after rolling. $T = t_1a_1 + t_2a_2$ is the primitive translation vector of the tube. Ba, Bb and Bc represents special chiralities named armchair, zigzag and chiral respectively [10].

Major reason why CNTs are widely studied can be explained with their physical properties which vary depending on which angle the hexagonal graphene sheet is rolled. For example SWNT can be a semiconductor or metallic depending on its chirality which opens new possibilities in designing carbon based electronic devices [11]. For metallic nanotubes theoretical calculations and measurements show that individual nanotube can carry electric current density over 10^9 A/cm², which is more than metals like copper is capable of [12]. Nanotubes are also excellent thermal conductors, comparable to diamond [13]. For individual carbon nanotube an axial elastic modulus of 1 TPa and a tensile strength of 100 GPa have been measured exceeding the strength of all other natural or synthetic fibres [14] [15]. Despite of being stiff, recoverable radius of curvature of 20 nm have been discovered in manipulations with an atomic force microscope [16]. The same study also revealed that nanotubes can survive multiple repetitions of local strain up to 16%. CNTs have been already demonstrated in several electronic applications including transistors [17], memory elements [18], field-emission electron sources [19], solar cells and batteries [20]. Since SWNTs show large changes in optical and electrical properties

when molecules are adsorbed to nanotube surfaces they have been also used in biological and chemical sensors [21] [22]. Owing to their mechanical properties and high electrical and thermal conductivities, nanotubes have been used as a filler material in many nanocomposite structures.

3 CARBON NANOTUBE POLYMER COMPOSITES

Carbon nanotubes have been mixed with many polymers including epoxy [23, 24], polyethylene (PE) [25], polyvinylacetate (PVAc) [26], polyvinylchloride (PVC) [27], polyamide (PA) [28], several types of elastomers [29–41] and many others. A motivation to mix nanotubes with polymers is to enhance their mechanical and thermal properties and introduce new features like electrical conductivity and electromagnetic shielding, which are typically limited in pristine polymers.

3.1 Mechanical properties

There are several theoretical models describing the mechanical, mainly stress-strain behavior of filler-based nanocomposites in the literature. The basic idea in all of them is to express mechanical properties of the composite, typically elastic modulus, using properties of the matrix and filler as parameters. Depending on model these parameters include moduli and aspect ratio of the filler together with modulus of the matrix. Many of the models are semi-empirical and describe the behavior of the composite in some very narrow regimen regarding filler concentration or elongation.

Originating from Einstein's work with increasing of viscosity caused by a suspension of spherical particles in a viscous fluids, Guth-Smallwood model [42] can be used to estimate the reinforcement factor of the filler E_c/E_m of the composite, where E_c is elastic modulus of the composite and E_m is elastic modulus of the pristine matrix:

$$\frac{E_c}{E_m} = 1 + 0.67AR\varphi + 1.62AR^2\varphi^2 \quad (3.1)$$

where AR and φ are aspect ratio and the volume fraction of the filler.

The equation (3.1) does not take in to account the elastic modulus E_f of the filler, which is assumed to be much higher than of matrix. Therefore Guth-Smallwood model can be used with lower modulus elastomer matrices, but not necessarily with matrices of higher elastic modulus like some polymers, metals and ceramics.

One of the models that encounter E_f as a parameter is called Halpin-Tsai model [43]. For longitudinal direction (L) the reinforcement factor for fiber reinforced composite, with fiber length l and fibre diameter r :

$$\frac{E_L}{E_m} = \frac{(1 + AR\eta_L\varphi)}{(1 - \eta_L\varphi)} \quad (3.2)$$

$$\eta_L = \frac{\frac{E_f}{E_m} - 1}{\frac{E_f}{E_m} + AR} \quad (3.3)$$

for the transverse direction (T)

$$\frac{E_T}{E_m} = \frac{(1 + 2\eta_T\varphi)}{(1 - \eta_T\varphi)} \quad (3.4)$$

$$\eta_T = \frac{\frac{E_f}{E_m} - 1}{\frac{E_f}{E_m} + 2} \quad (3.5)$$

These equations are empirical relationships that have been confirmed by experimental measurements.

In order to calculate elastic modulus E_c for randomly oriented fillers :

$$E_c = a_i E_L + (1 - a_i) E_T \quad (3.6)$$

where for 2D-reinforcement (like in thin films) :

$$a_i = a_{2D} = 0.339 - 0.035\varphi - 0.642\frac{E_m}{E_f} \quad (3.7)$$

and for 3D-reinforcement :

$$a_i = a_{3D} = 0.13 - 0.0815\varphi - 1.669\frac{E_m}{E_f} \quad (3.8)$$

a_i has been traditionally treated as constant, but recent studies have shown that it depends on composite morphology and volume fraction of the filler [43].

3.2 Electrical properties

Electrical properties of CNT/polymer composites are typically estimated by percolation theory :

$$\sigma = \sigma_0(p - p_c)^t \quad (3.9)$$

where σ is electrical conductivity, p is a density of the conductive sites, σ_0 is a scaling factor, p_c is a critical density of conductive sites i.e. percolation threshold and t is an exponent depending on dimensionality of the percolation network. Since the density of conductive sites is related to volume fraction of the CNTs, (3.9) can be written as:

$$\sigma = \sigma_0(\varphi - \varphi_c)^t \quad (3.10)$$

where φ is a volume fraction of the nanotubes and φ_c is a critical volume fraction leading in to sharp increase in conductivity level of the composite. Hundreds of studies have been made to find values for φ_c and for t for CNT filled polymers but consensus is still missing as can be seen from from figure 3.1.

The percolation threshold φ_c as a function of AR can be estimated with:

$$\varphi_c = \frac{1}{2AR} \quad (3.11)$$

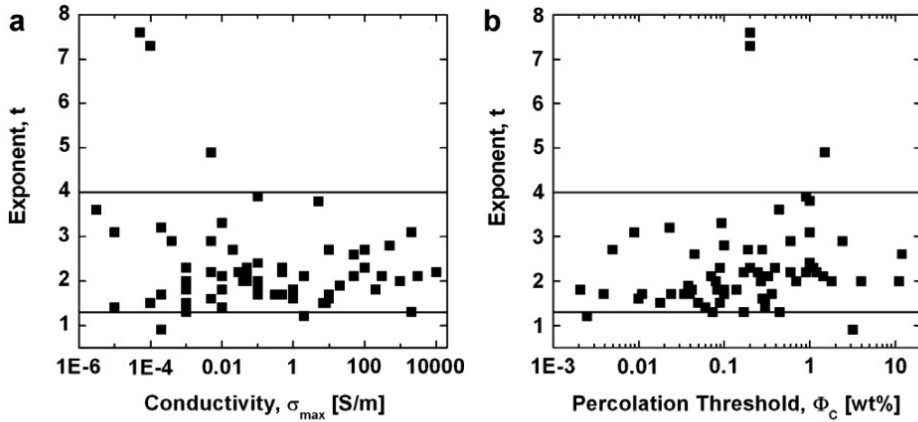


Figure 3.1 Plot of the power law exponent t as a function of (a) the maximum conductivity and (b) the percolation threshold from over 100 reported values for several different matrices. The horizontal lines denote $t = 1.3$ and 4 [44].

There are several factors identified that affect the percolation threshold including purity of the CNT material, chirality of the tubes, aspect ratio, dispersion process and properties of the matrix [45, 46]. From these dispersion process and properties of the matrix are dominating the development of the electrical conductivity of the composite [44]. Typical percolation thresholds for well dispersed carbon nanotubes are below 1 phr [47], so any value above that could indicate poor dispersion of the nanotubes.

The critical percolation φ_c is theoretically inversely proportional to the aspect ratio of the tubes. In reality exception may come from situation where the tubes are long or their morphology differs from stiff and linear form. In this case not only the aspect ratio but also the length of the tubes can affect the results.

The conductivity of randomly oriented CNT networks is dominated by contact resistance between individual carbon nanotubes. Even though internal resistance of nanotubes is very low, the contact resistance is high. This resistance can be even higher if the non-conducting component, the matrix or the surfactants used in dispersion process can penetrate in between the tubes [48]. Due to this barrier the nature of the current in nanotube network is governed by quantum mechanic tunneling resistance which is dependent on distance between tubes and also temperature.

In order to avoid problems of the matrix disturbing the conductivity hierarchial structures can be used. For example selecting cellulose as a carrier for nanotubes enables pristine CNT networks with high local concentrations of conductive paths

leading in to high electrical conductivity of the structure. Unlike polymer matrices cellulose acts as a scaffold supporting and stabilizing CNT network without interfering the nanotube junctions. Structure is still homogeneous enough for most applications and it behaves like a uniform material in macroscopic scale. CNT/cellulose composites are typically manufactured by using water based solution casting method. In order to disperse nanotubes in to water surfactants are needed which can diminish conductivity if not removed afterward.

3.3 Carbon nanotube - elastomer composites

Due to their incompressibility and reversibility under stress, elastomers are widely used in many applications including tires, seals and conveyor belts. In order to enhance their properties even more they are often filled with particulate material like carbon black, silica and carbon nanotubes. Of these the nanotubes have many benefits over two others including better physical properties and lower percolation threshold, which could give applications more durability, weight savings and strenght together with better electrical and thermal properties. Several studies of CNT reinforced elastomer nanocomposites have been made including natural rubber (NR) [29–34], styrene-butadiene rubber (SBR) [35–38], nitrile butadiene rubber (NBR) [39–41] and many others.

It has been noted that one of the limiting factors in realizing the potential of CNT filled elastomers is the dispersion quality. Poorly dispersed nanotubes show three times higher electrical percolation thresholds than composites with better distribution of nanotubes [49]. It also affects the mechanical values and especially failure strain which is typically always smaller with CNT filled elastomers compared to reference values [29]. Another limiting factor is related to the dispersion process itself. Some dispersion processes uses dispersion agents in order to ease the de-agglomeration of the CNTs. If these agents are adsorbed on the surface of the nanotube after the composite has been manufactured it will diminish the mechanical properties by reducing the matrix-filler interaction [29].

3.4 Carbon nanotube - cellulose composites

Cellulose in various forms is abundantly available bio-compatible material which is used as a carrier or scaffold in many functional materials [50]. Electrical conductivity is one examples of the functionality where cellulose can act as a support to which some conductive component is added. Typical conductive components used with cellulose include metal nanoparticles [51, 52], conducting polymers [53–55], graphite [56] and different types of nanocarbons like graphene [57] and carbon nanotubes [58–66]. Regarding electrical conductivity, one of the advantages of carbon nanotubes is their low percolation threshold required to form conductive network. CNT-cellulose composites have been reported to be used as supercapacitor electrodes [59], electromagnetic interference shielding [60, 61], active displays [67], electric heating [66], chemical sensors [62–64] and pressure sensors [65]. In all above applications the level of electrical conductivity is important. The highest reported conductivity for CNT/cellulose composites is 200 S cm^{-1} for anisotropic SWNT nanocellulose films [58]. For isotropic and using more available MWNTs the reported conductivity values are typically between $0.1 - 2.0 \text{ S cm}^{-1}$ [51, 68–70]. Electrical conductivity of randomly oriented CNT networks is dependent on contact resistance between tubes. In case of polymer nanocomposites and perfect dispersion qualities the matrix is typically disturbing these contacts by coating the tubes and diminishing the electron transport at nanotube-nanotube junctions. In case of CNT/cellulose composites the cellulose acts as a scaffold and same type of reduction in conductivity does not appear. However in a case of using surfactant assisted CNT dispersion the surfactant may cause additional resistance in CNT-CNT junctions.

One very simple manufacturing method of CNT/cellulose composites involves dipping the cellulose films or structures in to CNT dispersion to allow nanotubes to impregnate the cellulose scaffold [62, 66, 69, 71–73]. Cultivating cellulose producing microbes in CNT dispersion has also been used [70]. Majority of the reported methods however involves some type of solution casting method after mixing the CNTs and cellulose material together [60–62]. This method is used in paper making process which is more scalable compared to other methods and regarding electrical conductivity is resulting the same characteristics as impregnation method [61].

Regardless of the method CNT colloids are typically prepared separately from cellulose pulp. In our study we found that introducing nanocellulose to the CNT

dispersion process enables homogenous distribution of nanotubes, enhances the adhesion to the macroscopic cellulose fibres which also enhances the electrical conductivity by stabilizing the conductive pathways [Publication IV].

As the size of the cellulose fibres varies, the dispersion quality of the CNT colloids needs to be in a sufficient level in order to proper impregnation to happen. Smaller cellulose fibres equals smaller pores for CNTs to penetrate. In case of nanocellulose this penetration might not even happen regardless of CNT dispersion quality, since both fibres are in a same scale. It has been observed that after proper penetration and evaporation of used solvent the interaction between cellulose and nanotubes is very strong. This interaction is dependent on the quality and quantity of the interface. In many cases nanotubes contain different native or process induced functional groups on the sidewalls. These typically oxygen containing species has high affinity to cellulose fibres [69].

Aqueous CNT dispersion process involves usage of some type of surfactants and high intensity mixing like sonication. Sonication is known to damage the tubes inhibiting their electrical conductivity performance [74]. Surfactants can affect the electrical conductivity of randomly oriented CNT networks by interfering the tube-tube contacts. As a development of dispersion quality is related to available surfactant molecules i.e. the concentration ratio between surfactants and CNTs, it is favorable to have high concentration of surfactants to enable lower sonication energy. On the other hand if the surfactant cannot be removed after nanocomposite has been cast it is also crucial to minimize the usage of it. If it is possible to remove the surfactant it can have significant effect on the performance of the nanocomposite [Publication III][Publication IV].

4 CARBON NANOTUBE COLLOIDS

As-produced non-functionalized carbon nanotube aggregates are challenging to disintegrate. Typical MWNT agglomerates are constructed of randomly oriented nanotube networks in which tubes are crosslinking each other by van der Waals forces. In a typical network having junctions approximately 100 nm apart, the binding energy density for the agglomerate is calculated to be 16 kJ/m^3 or 16 kPa [75]. For SWNTs, which bundle up to form parallel structures and therefore have much more contact area with each other the energy density is estimated to be 100 MPa, significantly more than for MWNTs which makes dispersion of SWNTs more difficult over MWNTs.

In order to disperse CNTs in to a solution or polymer melt, the binding energy densities needs to be overcome by local shear stresses. In optimal case these local shear stresses should be above binding energy of the CNT agglomerates or bundles but still below the fracture resistance of an individual tubes. Too high energy densities causes unwanted chemical modifications, cutting and defect formation to the outer layers of the tubes [74, 76]. There are several techniques demonstrated for dispersing nanotubes including: shear mixing [77], extrusion [78], calendering [79, 80], and sonication [81–83]. Most of the dispersion techniques are dependent on a viscosity of the medium so in order to disperse nanotubes in low viscosity liquids like water, high shear mixing methods simply do not work [75].

In order to optimize the use of CNTs in different matrices their surface chemistry must often be modified. Chemical modification can be covalent attachment of different functional molecules on sidewalls or tube ends [84], or non-covalent for example using surfactants [85]. Modifications changes the mechanical and electrical properties of the outer layer of the tubes which often diminishes their properties.

4.1 Sonication

Sonication is a process in which sound energy is applied to a particular system in order to agitate its molecules. Typical laboratory sonication systems use ultrasound which by definition is a periodic pressure wave with frequency of 20 kHz or more. Equipment can be divided in to two categories: tip sonicators or bath sonicators. The tip sonicator is equipped with a probe which is set to vibrate in ultrasound frequency. The probe is typically made of some inert metal like titanium. This set up enables high concentrations of sound pressure in vicinity of the probe which can lead in to rapid heating of the substance close to the tip. In bath sonicator the vibrating elements are outside of the sample vessel leading in to more isotropic acoustic pressure field. In typical bath sonicators the conducting element is water to which sample vessels are placed.

If the local forces inside liquid induced by the ultrasound exceeds the strength of the liquid itself it causes cavitation, a formation of cavities. Cavitation is analogous to boiling but whereas in boiling cavities are formed by increasing the local temperature above the boiling point, in cavitation cavities are formed by decreasing the local pressure below the saturated vapor pressure of the liquid. It is typical in the literature to use the words cavity and bubble interchangeably although bubble by some definition should always have two surfaces.

Cavitation can have inertial or non-inertial nature. Non-inertial cavitation is a formation of stable bubbles which pulsate in diameter according to external pressure field while the average size remains constant. Inertial cavitation however initiates as a small nucleation which grow in several cycles to a bigger bubble. When growing bubble reaches a critical size it experiences a violent collapse, an implosion, which causes high temperature and pressure gradients. These conditions are capable of creating high shearing and strain rates which are the main reasons sonication is used in dispersing particles into low viscosity liquids.

Strain rates induced by inertial cavitation can be estimated by calculating radial wall velocity of a collapsing cavity from Rayleigh-Plesset (RP) equation [86],

$$R\ddot{R} + \frac{3}{2}(\dot{R})^2 + \frac{4\mu_L}{R}\dot{R} + \frac{2S}{\rho_L R} = \frac{p_B - p_\infty}{\rho_L} \quad (4.1)$$

Where R is time dependent radius of the bubble, μ_L is dynamic viscosity of the

liquid, S is surface tension, ρ_L is a density of the liquid, p_B is uniform pressure inside the cavity and p_∞ is a pressure of the liquid far away from the bubble which in sonication typically a sinusoidal pressure field induced by the sonotrode.

The relationship between strain rate and bubble radius can be seen from 4.1.

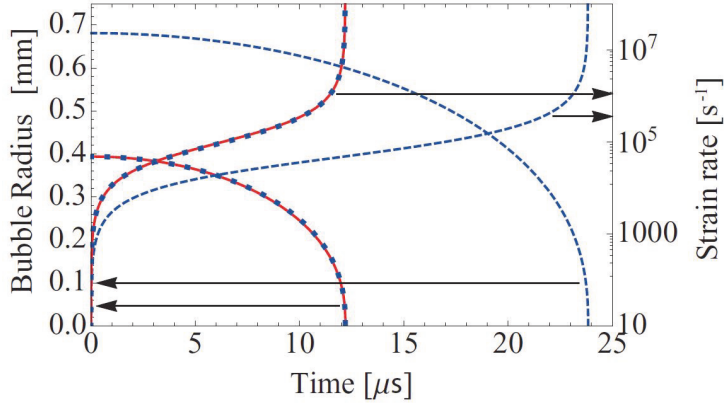


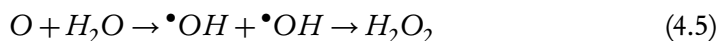
Figure 4.1 The bubble radius and strain rate at the bubble surface as a function of time during the transient collapse of a bubble for a sonication experiment with SWNTs (power 40 W, frequency of 20 kHz, sonicator horn diameter 15 mm.) Dashed blue lines represent the solution as obtained from the empty cavity approximation while the solid red line represents the solution obtained from the Rayleigh-Plesset equation. The solution of the empty cavity approximation, with length and time scales matched to the solution of the Rayleigh-Plesset equation, is represented by the dotted blue line. [87].

Collapsing cavity is capable of producing very high pressures and temperatures which can induce chemical changes in the solution. This phenomenon is called sonolysis and it was discovered already in 1927 by Richards and Loomis [88]. New chemical species generated can react with other components present in the solution which again can cause unexpected results in processes in which the idea is to use sonication purely for mixing. Sonolysis can be categorized into two classes; homogeneous reactions where only one liquid component is being degraded, and heterogeneous reactions where two or more liquid-liquid or liquid-solid systems react with each other. In heterogeneous reactions solid particles also play an important role as preferred nucleation sites for formation of cavities [86]. When water is being sonicated with high enough intensity, it will dissociate into hydroxyl radicals and protons by thermolysis (4.2). It is also possible to receive decomposition of water molecule into

oxygen atom and hydrogen molecule (4.3) [89],



In high temperatures, usually present in collapsing cavities, a proton and oxygen atom can further react with water molecule to produce hydrogen and hydrogen peroxide,



By introducing new species, like hydrogen peroxide, aqueous cavitation alters the chemical reactivity of water which may have a significant role in degradation and chemical modification of components of the dispersion process. Sonolysis induced free radical generation can happen when inertial cavitation is involved [90] and it is linearly dependent on processing time [89]. An upside of all this is that since chemical conversion of water is directly related to inertial cavitation it can be used as a tool to compare different sonication systems. Koda et. al. suggested KI oxidation dosimetry to be used as a calibration tool for generation of inertial cavitation in a system [91].

Nucleation of cavities can be either homogenous nucleation, where cavities are formed inside pure liquids, or heterogeneous nucleation where cavities are formed by external events or by impurities i.e. boundaries. In the real world homogeneous nucleation is practically impossible since ultra pure conditions are very difficult to create and even cosmic radiation induces nucleation so therefore outside theoretical calculations, nucleation is always considered to be heterogeneous. In their studies Keck et al [92] discovered that a presence of quartz particles in water affected the yield of hydrogen peroxide. The formation of hydrogen peroxide was dependent on sonication frequency and concentration of quartz particles. Therefore calibration of sonochemical system by measuring the sonochemical yield without presence of particles, may not give exact information about dispersion conditions of CNTs, but

it still works as a benchmark in comparing different sonication systems.

4.2 Surfactants

By introducing acoustic energy in a form of sonication to aqueous CNT colloids it is possible to disintegrate nanotube agglomerates. After sonication is stopped the nanotubes will rapidly re-aggregate and sediment. To stabilize the system and to prevent re-agglomeration, different types of surfactants such as ionic (anionic and cationic), non-ionic and polymer based are been used [83, 93–114]. Surfactants are adsorbed on the CNTs surface via hydrophobic interactions, $\pi-\pi$ bonds, hydrogen bonds or electrostatic interactions [115, 116]. This arrangement creates an buffer between the tubes inhibiting the aggregation tendency. In case of aqueous dispersions the outer layer of this buffer is composed of hydrophilic functional groups enabling stable dispersions. In water the molecular arrangement happens through entropic forces in which hydrophobic ends are adsorbed on some other hydrophobic surfaces. Hydrophobic end does not repulse water but is lacking of interaction leading in to formation which is energetically more favorable for the system by minimizing the surface area of water. If the concentration of free surfactant in a solution exceeds a specific threshold called critical micelle concentration (CMC), they start to form micelles. Micelles are clusters of molecules where hydrophobic ends coalesce together forming different confined shapes in wich hydrophilic ends are facing the water.

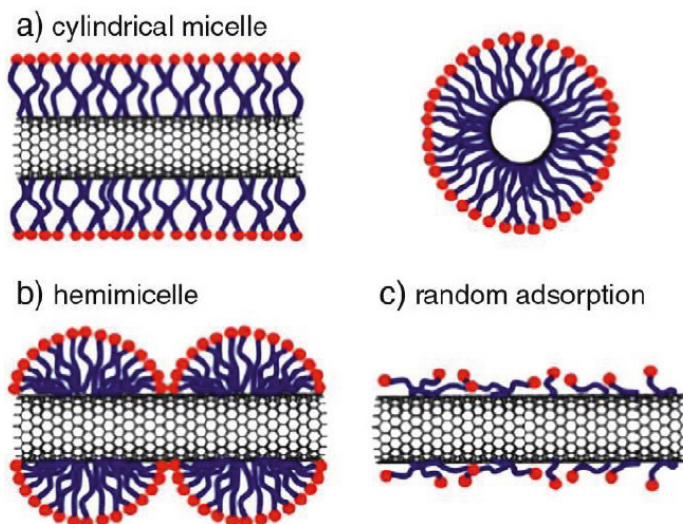


Figure 4.2 Schematic illustration of surfactant assembly on CNT, a) cylindrical micelles, b) hemimicelle, and c) random adsorption [117].

The ability of surfactant to disperse carbon nanotubes is related to length of hydrocarbon chain of the surfactant, presence of benzene rings and the terminal groups [99], concentration [108] and charge [118]. An optimum surfactant-CNT weight ratio has been reported to vary, ranging from 1:1 to 1:10 [99, 119]. It has been reported that an efficient CNT dispersion is possible only when the surfactant concentration is above CMC [113, 120–122], below and equal to their CMC [93, 95, 96, 123] and with 0.5 of CMC [123]. All these above conclusions are related to differences in affinity between micelle formation and hydrophobic-CNT contact. If the micelle formation is energetically more favorable than wrapping the graphitic surfaces, the surfactant is not necessarily capable to disperse nanotubes. Even with a absence of consensus about the required concentration using too much surfactant may affect the properties of CNT network in the end product, using too low surfactant concentration can cause re-aggregation in colloid since a sufficient amount is needed to cover all CNT surfaces with enough surfactant molecules [119]. Below a surfactant specific concentration ratio of surfactant/nanotubes the dispersion does not happen at all. By increasing the ration there is a threshold after which optimal dispersion quality can be achieved [Publication I].

4.3 Dispersion quality

In order to fully utilize the large surface area of nanomaterials, the dispersion quality needs to be controlled. Dispersion quality is describing the fraction of fully dispersed individual particles versus particles staying in the agglomerates. Dispersion quality on 1 means that all particles are being dispersed and interfacial surface area is maximized. Number of methods have been used to study dispersion quality of CNT colloids and nanocomposites. So called ex situ methods include microscopy studies like (AFM) [99] and transmission electron microscopy (TEM) [119] which study dried 2D samples of the 3D colloids. In situ characterization, which could be performed on colloidal samples include UV-Vis spectroscopy [83, 110, 112, 124], different light scattering methods [125, 126] and rheology changes [127]. Of these methods, UV-Vis spectroscopy has been shown to represent the most accessible and versatile method to determine the dispersion quality of CNT dispersions especially for liquid systems. In the method, the light passing through a sample of colloid experiences scattering and absorbance. Both of these phenomena scale linearly with the concentration of colloidal particles and, therefore, the opacity of the dispersion can be used to measure the number of nanotubes (individual tubes or dispersed small aggregates) in the supernatant [110].

In UV-vis spectroscopy there are two distinguished methods: segmental and single point analysis. The absorbance peaks of CNTs are related to different diameters and chiralities of the nanotubes, and a possible red shift of the peak which indicate a presence of agglomerates [128]. Segmental analysis is focusing on these resonance frequencies indicating the concentration of specific and individual dispersed nanotubes. The selectivity of surfactants and dispersion process parameters can be estimated by comparing peak features of different colloids (Figure 4.3) [129]. By calculating the area, height and width of the peak, the concentration and specificity (for example chirality) of the dispersed nanotubes can be resolved.

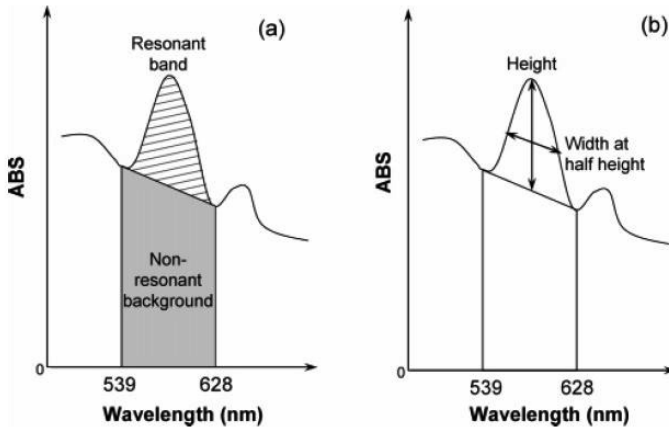


Figure 4.3 Estimation of (a) resonance ratio (area of resonant band)/(area of nonresonant background); (b) normalized width) (width of resonant band)/(height of resonant band) [129].

The single point analysis is focusing on studying the opacity and its development at certain wavelength. Typically the wavelength is selected to be some characteristic absorption peak [83, 118]. However if one is interested only in level of homogeneity of the colloid, it is not necessary to use only the peak frequencies. Opacity is also related to scattering which brings the measured background up as dispersion quality is improved. By using only peak values it is possible that as the peak maximum is shifting it could give inaccurate information about the development of the process.

5 AIMS OF THIS STUDY

The hypotheses behind this work were:

- Disperision quality of CNTs affects the physical performance of the nanocomposites
- A presence of surfactants in CNT nanocomposites affects the physical performance of the nanocomposites
- Characteristics of the carbon nanotubes affects the physical performance of the nanocomposites

The objective of the work was to study how different steps, including filler material selection, surfactants and dispersion quality, in aqueous solution casting method affects the physical properties of carbon nanotube reinforced nanocomposites. The research questions are:

1. What is the theoretical framework in estimating the development of dispersion quality in aqueous CNT dispersions using sonication?
2. How does the dispersion quality of aqueous CNT dispersions affect the physical performance of nanocomposites manufactured with solution casting method?
3. How does the surfactants used in the dispersion process affect the physical performance of the composites?
4. How does the characteristics of the nanotubes affect the performance of the nanocomposites?

First a theoretical framework to study the development rate of dispersion quality in aqueous CNT-dispersion during sonication was created. Developed framework was later used to study relation between relative disperison quality and physical performance of CNT/NBR and CNT/NFC nanocomposites. The role of surfactant used in the dispersion process was studied by comparing physical performance of

CNT nanocomposites before and after the removal of surfactants from the matrix. The affect of characteristics of carbon nanotubes was investigated by manufacturing elastomer nanocomposites using different types of nanotubes.

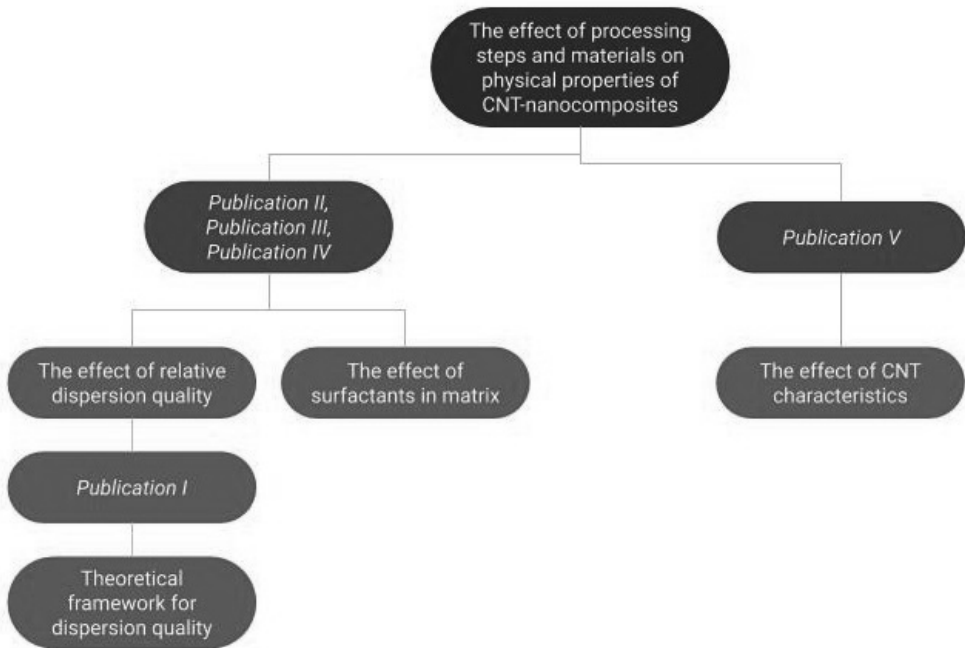


Figure 5.1 The summary of the study

6 EXPERIMENTAL

The materials and methods used in the study are presented in the following subchapters. First the types of used CNTs are introduced together with different surfactants, matrices and other chemicals. Second the sonication processes are described following the introduction to methods used for testing and characterization of CNT dispersions and nanocomposites.

6.1 Materials

The effect of sonication on opacity of the aqueous CNT colloids used to measure the dispersion quality [Publication I], the effect of dispersion quality and post-treatment on physical properties of NBR films [Publication II], part of the polyurethane film studies [Publication V], and all cellulose experiments [Publication III - IV] were performed with NC7000 MWNTs from Nanocyl SA., Sambreville, Belgium. In polyurethane film studies [Publication V] NC 7000 was compared as a filler against two other nanotube types manufactured by university of Oxford, named here as AR110 and AR225.

Table 6.1 Carbon nanotubes used in the study.

Property	NC 7000	AR110	AR225
Average diameter	10 nm	40 - 60 nm	30 - 50 nm
Average length	1.5 μm	500 - 1000 μm	300 - 800 μm
Transitional metal oxide	$\sim 10\%$	$\sim 3\%$	5 - 6%
Elastic modulus*	200 GPa	200 GPa	200 GPa

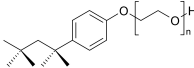
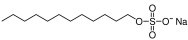
All values are based on studies performed in [Publication V].

* values were used to calculate reinforcing effect of carbon nanotubes in PU [Publication V] and NBR [Publication II] nanocomposites. Value is an estimate based on number of defects, structural disorders and inclusions of catalytic particles of used

nanotubes.

Surfactants used to disperse carbon nanotubes were selected by their popularity and varying ionic and non-ionic features.

Table 6.2 Surfactants used in the study.

Property	Triton X100	Pluronic F-127	CTAB	SDS
Molecule				
Type	non-ionic	non-ionic	cationic	anionic
CMC	0.2 - 0.9 mM	950 - 1000 ppm	0.92 mM	8.2 mM
HLB	13.5	22	10	40
Publication	I-V	I,III	I,III	I

Properties of NBR latex used in [Publication II] is listed below:

Table 6.3 Properties of Litex[®]N 2890

Property	Value	Unit	Method
Solids content	41.0	%	ISO 124
pH	7.3	-	ISO 976
Viscosity	<100	mPas	ISO 1652
Surface tension	31.9	mNm ⁻¹	DIN 1409
Elastic modulus (cured)	0.77	MPa	NA

Properties of polyurethane latex Bayhydrol[®]UH240 used in [Publication V] is listed below:

Table 6.4 Properties of Bayhydrol[®]UH240.

Property	Value	Unit
Solids content	40	%
pH	6-8	-
Elastic modulus (cured)	2.9	MPa

6.2 Mixing

In mixing nanotubes in water sonication with cylindrical probe sonicators were used. For Publications I-IV the sonicator was QSonica Q700 sonicator (Qsonica L.L.C, Newtown, USA) with a 12.7mm diameter titanium tip and 20 kHz frequency, and for Publication V Soniprep 150 plus with 9.5 mm diameter titanium tip at a frequency of 23 kHz.

In [Publication III], the nanocellulose (NFC) production was based on mechanical disintegration of bleached hardwood kraft pulp (BHKP). First, dried commercial BHKP produced from birch was soaked in water at approximately 1.7 wt. % concentration and dispersed using a high-shear Ystral dissolver for 10 min at 700 rpm. The chemical pulp suspension was predefined in a Masuko grinder (Supermasscolloider MKZA10-15J, Masuko Sangyo Co., Tokyo, Japan) at 1500 rpm and fluidized with six passes through a Microfluidizer (Microfluidics M-7115-30, Microfluidics Corp., Newton, MA, USA) using 1800 MPa pressure.

6.3 Nanocomposite manufacturing

In [Publication II and V] nanocomposites were prepared by solution casting method in glass or plastic dishes. CNT colloids with concentration between 0.5 wt% to 2 wt% were mixed with polymer solution and let dry until water was completely evaporated. After this the dishes were annealed or crosslinked in oven at approximately 100°C from 1h to 6h.

In [Publication III] rotational solution casting method was used to manufacture CNT/NFC nanocomposites. Aqueous solution with 0.25 wt% of NFC, 0.25 - 0.30 wt% of surfactant and 0.05 wt% of NC7000 were sonicated and cast in a rotating cylinder until the water was completely evaporated.

In [Publication IV] foam forming process was used to prepare conducting 3D cellulose structures. 1800 ml of NFC-CNT dispersion was poured in to 32 cm diameter cylindrical tank (Figure 6.1) with water and pulp so that the total volume of the mixture was 5.5 litres. Mechanical mixing was carried out with rotation speed of 3500 rpm for 3.5 min. Foaming produced 70% air content to the foam leading to total volume of 19 l.



Figure 6.1 (a) Laboratory scale foam forming equipment; (b) NFC-CNT dispersion, pulp, and water mixture before foaming [Publication III].

The prepared foam was then poured into mold with prepared 3D structure. After vacuum assisted foam removal the structure was dried at 70°C for 12 h until dry.

6.4 Characterization

6.4.1 Spectroscopy

For determination of opacity of the diluted CNT dispersions [Publication I-II], were performed with Shimadzu UV-1800 spectrophotometer (Shimadzu Corp., Kyoto, Japan). To determine the opacity of CNT dispersion in [Publication V] Shimadzu UV-1601 UV-VIS spectrophotometer (Shimadzu Corp., Kyoto, Japan) was used.

6.4.2 Electrical measurements

Electrical surface resistance of the NBR/CNT composites [Publication II] was measured before and after the post-treatment with an electrometer and a resistivity chamber (Keithley 6517 electrometer and 8009 Resistivity Chamber, Tektronix, Inc., Beaverton, OR, USA), and by following an ASTM D257 standard. CNT/NBR nanocomposite films were placed between electrodes and in plane current was detected at 3.0 V. The current was let to relax for 60 s after which the reading was made.

The electrical conductivity of the foam formed non-wovens [Publication IV] were measured using the four-probe measuring technique. With this method, it is possible to neglect the effect of contact resistances and thus provide more accurate conductivity measurements than using two-terminal measurement. The sheet resistances of prepared and cut foam formed non-wovens (size 30 mm x30 mm) were measured using a four-point probe setup made in-house and a multimeter (Keithley 2002, Tektronix, Inc., Beaverton, OR, USA) in four-wire mode. The probes were placed in line, with equal 3 mm spacing.

The conductivity measurements were carried out using a 1 mA current and voltage was measured. Measurements were taken before and after the remaining surfactant was removed from samples by washing them in appropriate amount of acetone in room temperature (RT).

Surface resistivity of PU/CNT composites [Publication V] was measured by Metriso 2000 resistance meter (Wolfgang WarmbiereK, Hilzingen, Germany); 100 V was applied through a surface resistance probe on a circular sample with diameter of approximately 10 cm. All measurements were performed at room temperature. The reported resistivity is an average of 5 measurements for each sample.

6.4.3 Mechanical measurements

Stress-strain measurements of NBR/CNT [Publication II] and PU/CNT [Publication V] composites were performed with tensile tester (Messphysik midi 10–20, Messphysik Materials Testing GmbH, Furstenfeld, Austria) and dumb-bell test pieces. Selected crosshead speed was 100 mm per minute. The elastic modulus was measured in the linear region between 5 and 15%

Dynamic mechanical analysis for NBR/CNT composites [Publication II] was carried out using rectangular specimen using a dynamic mechanical thermal analyzer (Eplexor 150N, Gabo Qualimeter Testanlagen GmbH, Ahleden, Germany) in the tension mode. The isochronal frequency employed was 10 Hz and the heating rate was 2 C/min with a dynamic load of 0.2% strain and static load at 0.5% strain. The amplitude sweep measurements were performed with another dynamic mechanical thermal analyzer (Eplexor-2000N, Gabo Qualimeter Testanlagen GmbH, Ahleden, Germany) in tension mode at room temperature, at a constant frequency of 10 Hz, 60% pre-strain and dynamic strain from 0.01–30%.

The mechanical testing (Testometric M500-25kN, Testometric Co Ltd, Rochdale, UK) of foam formed samples [Publication IV] was done according to the standard EN 29073-3:1992. Test methods for non-wovens, Part 3: Determination of tensile strength and elongation. From the foam formed non-wovens, ten sample pieces in total were cut (50 mm x 250 mm). Five of them were tested as such, while another set of five samples was washed in an appropriate amount of acetone in room temperature, so that the remaining surfactant Triton X-100 was removed. All of the non-woven samples were conditioned according to the standard ISO 139 before the tensile testing. The testing was performed by applying a constant rate of extension of 100 mm/min

6.4.4 Microscopy

In [Publication I] the CNT agglomerate size was evaluated by drying a droplet of the dispersions on a metal plate and characterizing them by scanning electron microscopy (FIB-SEM, Zeiss Crossbeam 540) operating at 3.00 kV.

The surface and cross-section of the films processed using surfactant Triton X-100 [Publication III] and aspect ratio of sonicated carbon nanotubes [Publication V] were studied with SEM (Zeiss ULTRAPlus scanning electron microscope). The width of nanotubes in [Publication V] and other TEM studies were performed with (Jeol JEM 2010 TEM) operating at 200 kV.

7 RESULTS AND DISCUSSION

In this chapter, the main results of this thesis are presented and discussed. First the theoretical framework of relative dispersion quality of aqueous CNT dispersions is presented, second the effect of dispersion quality and CNT characteristics on some physical properties of CNT nanocomposites is studied, and third the role of surfactants in nanocomposites is presented.

7.1 Theoretical framework for dispersion quality

CNTs can be dispersed in water by using sonication to break the agglomerates and surfactants for stabilization. An opacity of the supernatant (α) is directly related to the concentration of dispersed nanotubes and can be used to study the development of the dispersion quality [124].

Assuming that the development rate of the opacity as a function of acoustic energy (E) is proportional to the undispersed agglomerates, described by a difference between maximum achievable opacity and measured opacity ($\alpha_{max} - \alpha$), we have

$$\frac{d\alpha}{dE} = (\alpha_{max} - \alpha)f \quad (7.1)$$

where E is the effective acoustic energy divided by CNT mass, α_{max} is the maximum achievable opacity of the system and f is some shape function. By separation we arrive to

$$\frac{d\alpha}{(\alpha_{max} - \alpha)} = f dE \quad (7.2)$$

Integration, rearrangement, and then using both sides as exponents e^x leads to

$$\alpha = \alpha_{max} - C e^{-\int f dE} \quad (7.3)$$

For a system where f is a positive constant and by applying boundary conditions, $\alpha(0) = 0$ and $\lim_{E \rightarrow \infty} \alpha(E) = \alpha_{max}$, α can be expressed as a function of E

$$\alpha(E) = \alpha_{max}(1 - e^{-\alpha E}) \tag{7.4}$$

where, α is a system-specific constant related to the concentrations and properties of the chemical components in the colloid [Publication I]. α_{max} can be determined by fitting the (7.4) to experimental data and finding its boundary value at infinite energy. This value can be used to normalize the function $\alpha(E)$. In this thesis normalized value of $\alpha(E)$ is called a relative dispersion quality (RDQ) and it describes the dispersion quality of the colloid related to maximum dispersion quality of the proposed model.

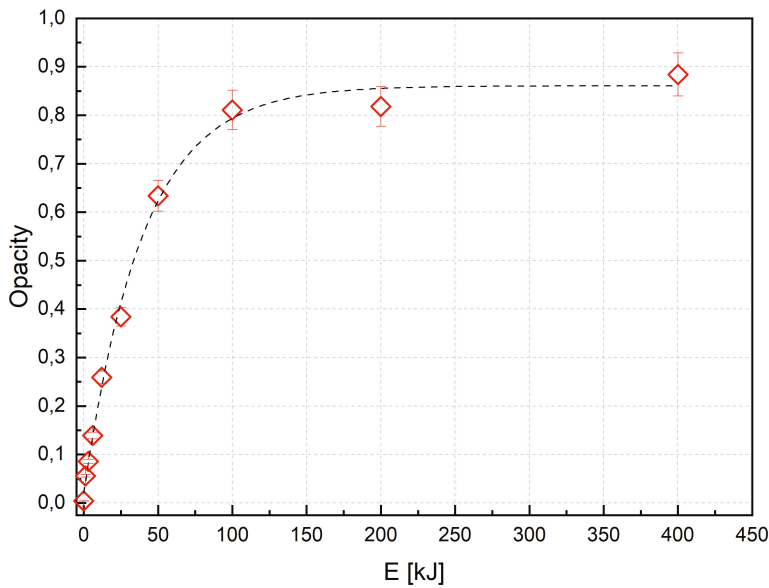


Figure 7.1 An opacity measurement of sonicated CNT dispersion @ 500 nm as a function of sonication energy together with a fitted opacity function (dashed line) before normalization (7.4).

7.2 The effect of relative dispersion quality

There are several factors affecting the performance of CNT reinforced nanocomposites including volume fraction, aspect ratio and dispersion quality of the filler

material, and a level of filler-filler and filler-matrix interactions. From theoretical perspective it is evident that improving the dispersion quality of fillers in short fibre composites, the performance of the composites is also improved due increased interfacial area between the filler and the matrix. With CNT composites the improved dispersion quality is typically achieved by overcoming the cohesive forces holding the nanotube agglomerates together by some mechanical method, and preventing their re-aggregation. Since the agglomerates are typically tightly packed, a significant shear forces are needed which can damage the individual tubes leading to decreased reinforcing effects. Therefore depending on set expected features optimizing might mean less perfect dispersion quality. Relative dispersion quality of a system is not only indicating the increase of number of dispersed particles but could also work as a measure of changes in fractal dimension of the clusters and integrity of the nanotubes.

In our studies with carbon nanotube/nitrile butadiene rubber nanocomposites [Publication II], stress-strain showed modest changes in tensile modulus as relative dispersion quality was enhancing. The highest value was achieved when 40 - 60% of the tubes were well dispersed, but the data was somewhat scattered. 40 - 60% is also the dispersion quality range where the CNT colloids showed noticeable gelation during sonication process indicating increase in filler network interaction. As the sonication continued the viscosity returned back to lower level. Ultimate tensile strength (UTS) showed similar local maximum at 40 - 60% RDQ. Both tensile modulus and UTS also improved significantly from lowest to highest values of RDQ.

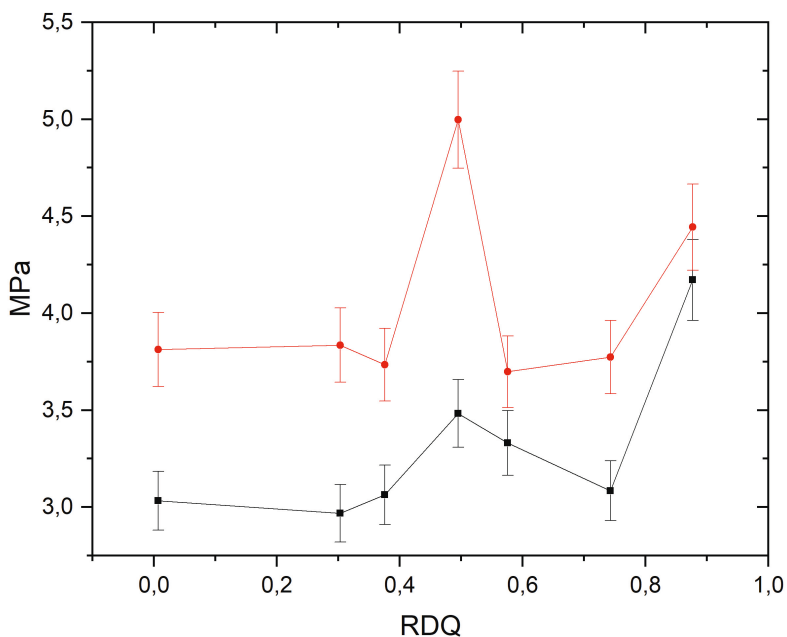


Figure 7.2 Elastic modulus (red) and ultimate tensile strength (black) of CNT/NBR nanocomposites as a function of relative dispersion quality determined by linear fitting the stress-strain from 5% to 15% strain.

Adding carbon nanotubes to rubbers typically decrease the elongation at break values [130–132]. This decrease is proportional to filler loading. One reason for this might be that reaching good dispersion quality with higher loadings is more challenging. In our experiments with reasonably high CNT loadings of 10phr, the elongation at break decreased significantly at lower RDQ values but the original elongation values were almost reached as the RDQ was closing value 1 indicating even distribution of fillers.

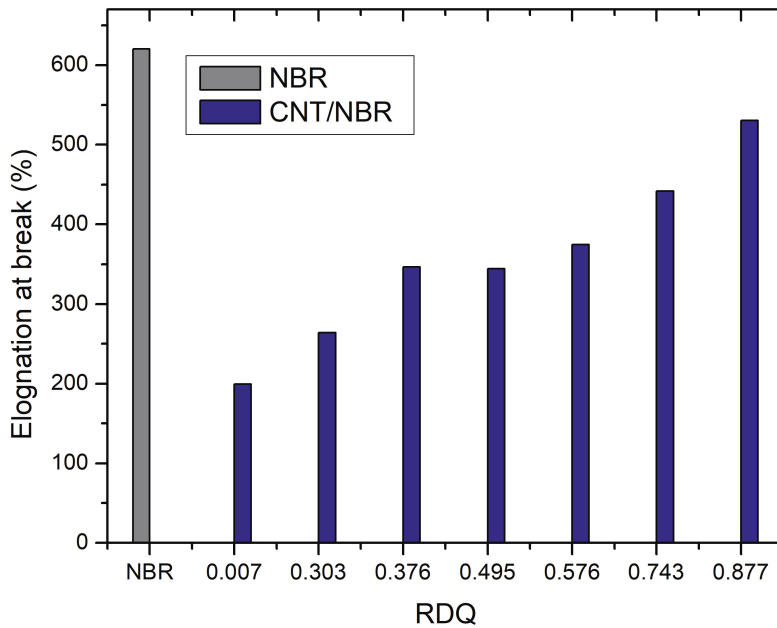


Figure 7.3 Elongation at break of NBR reference and CNT/NBR composites as a function of RDQ.

As the RDQ was increasing, the shapes of stress-strain curves changed from brittle to more ductile indicating enhanced CNT network interaction. All samples containing nanotubes showed necking which can be seen in decrease in stress before failure in stress-strain curves (Figure 7.4).

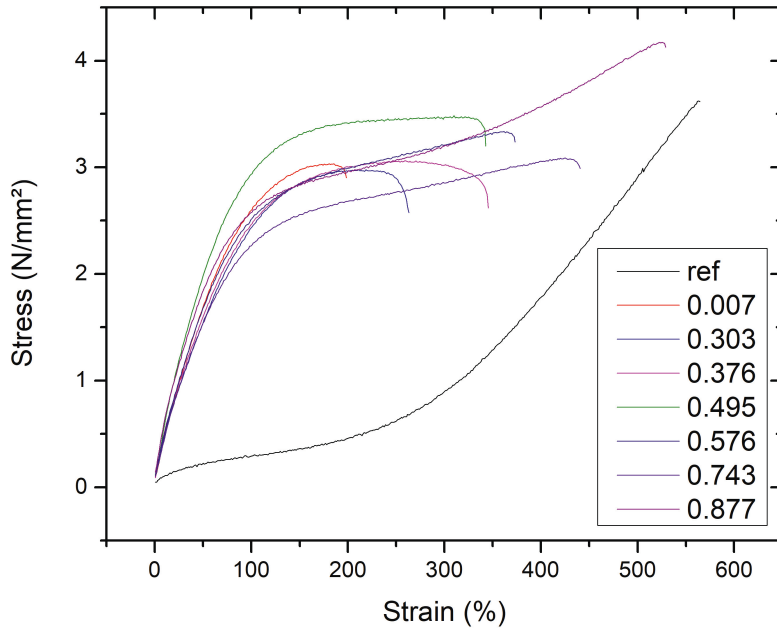


Figure 7.4 stress-strain curves of NBR reference and CNT/NBR composites with different RDQ-values.

Room temperature storage modulus (E') was determined with dynamical mechanical analysis (DMA). E' shows local peak in RDQ values 0.4 - 0.6 (Figure 7.5).

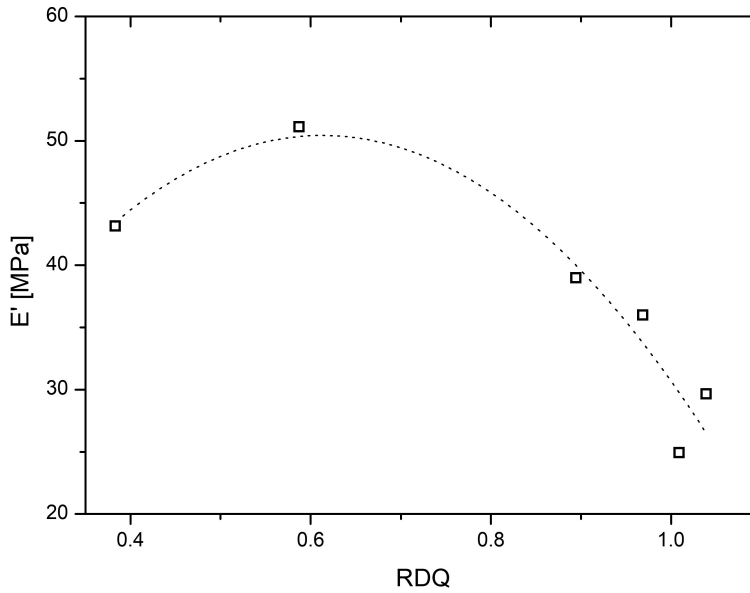


Figure 7.5 Storage modulus (E') of CNT/NBR composites as a function of RDQ with a trend line.

Strain sweeps were conducted with DMA. From figure (7.6) it can be seen that as the RDQ is enhancing the Payne effect, describing intensity of the filler-filler interaction peaks in range 0.4 - 0.6 RDQ giving further support for the conclusion that this is the optimal dispersion quality range of the system for maximal CNT network contribution for the moduli of the composite. At this this RDQ the pristine filler-filler interaction and cluster-cluster aggregation (CCA) reaches maximum values through the material. As RDQ is further enhancing the original filler-filler interaction and CCA is decreasing which can be seen in lower Payne amplitudes.

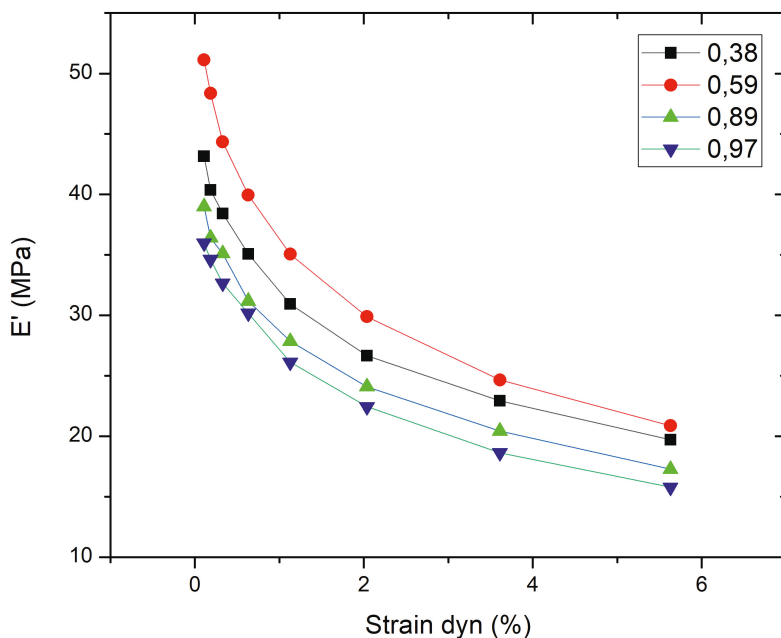


Figure 7.6 DMA strain sweeps of CNT/NBR composites with different RDQ values. Maximum Payne amplitude was received with 0.59 RDQ.

The electrical surface resistance of CNT/NBR nanocomposites was measured as a function of relative dispersion quality (Fig.7.17) [Publication II]. It was noticed that after initial drop the improvement of dispersion quality did not enhance the conductivity of the films. Initial drop might indicate that with lower dispersion qualities filler particles have more sphere-like structures with low aspect ratios which have not reached adequate percolation. The filler loading of 10% is already so high that further improvement of RDQ is not affecting the conductivity since additional conduction paths are not generated.

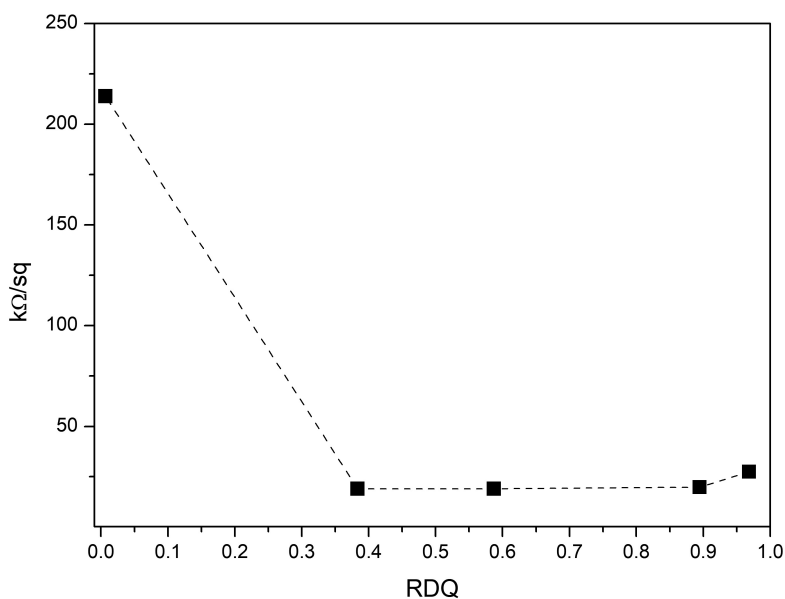


Figure 7.7 Surface resistance measurements of NBR/CNT films as a function of RDQ before the surfactant removal.

The four point conductivity measurements were performed on CNT/NFC nanocomposite films as a function of sonication energy using three different surfactants for dispersion process. The process differs from dispersing carbon nanotubes alone since also the matrix material was present in the sonication. Therefore the compatibility of surfactant needed to be optimized both for CNTs and NFC. This was done by measuring the development of electrical resistivity of the films. Using surfactant which have higher affinity towards the NFC, the CNT dispersion quality remains low indicated by lower electrical conductivity. Depending on the composition also the surfactant concentration is critical since some surfactants perform differently below and above CMC which can change during the sonication process. In (Figure 7.8) it can be seen that the development of the conductivities with non-ionic surfactants (Pluronic F-127 and Trion X-100) are outperforming the ionic surfactant (CTAB). However with Pluronic F-127 the concentration is also critical since with higher concentrations and above CMC the sonication process is causing diminishing conductivities.

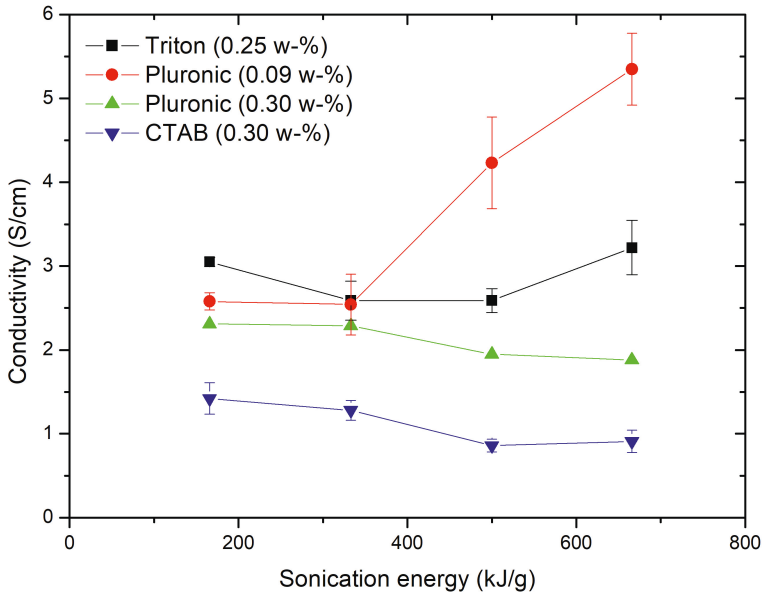


Figure 7.8 Conductivity of CNT/NFC nanocomposite films processed using surfactants Triton X-100, Pluronic F-127 and CTAB [Publication III].

7.3 The effect of surfactants

In CNT-water colloids different surfactants have different surfactant/CNT thresholds where the α_{max} is significantly lower than with higher ratios, indicating inadequate concentration of the surfactants for successful dispersion. In above this threshold, increasing the ratio is not affecting the maximum dispersion quality, but do affect on the development speed of the opacity indicated with χ in (7.4). This information can be used to optimize dispersion process for selected applications since prolonged sonication is degrading the tubes and should be avoided [Publication V].

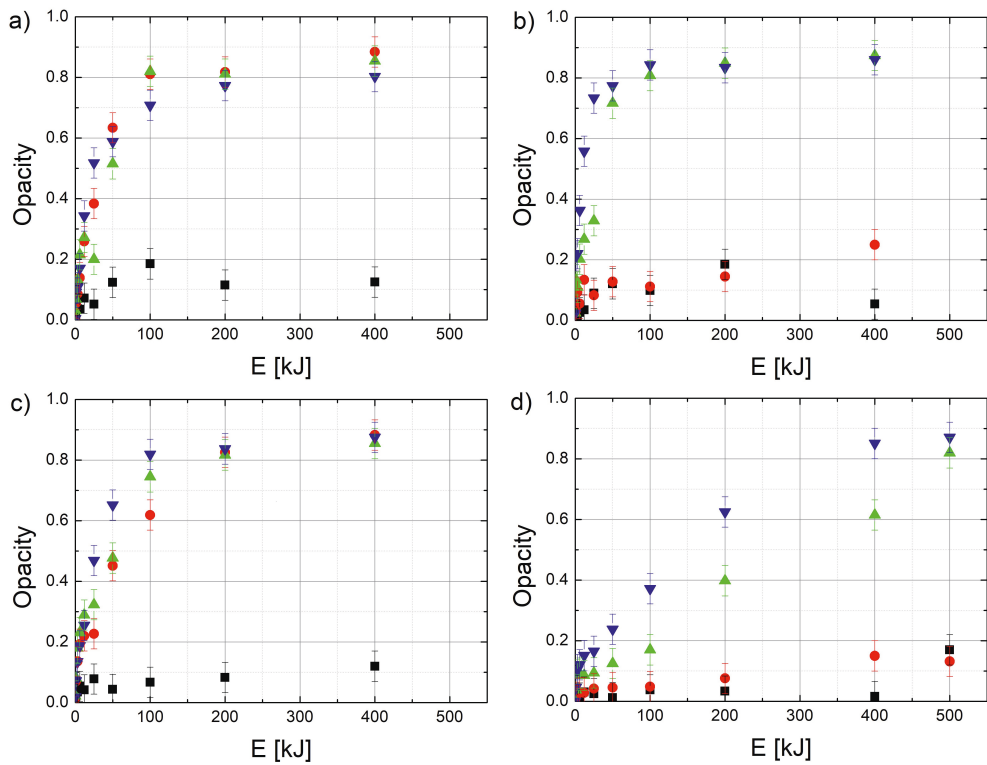


Figure 7.9 The development of opacity as a function of acoustic energy (E) with different surfactant/CNT ratios: 1:4, 1:2, 1:1 and 2:1 for a) Triton X-100, b) Pluronic F-127, c) CTAB and d) SDS. [Publication I]

After fitting Equation (7.4) to the data in (Fig.7.9) the α_{max} and χ can be found.

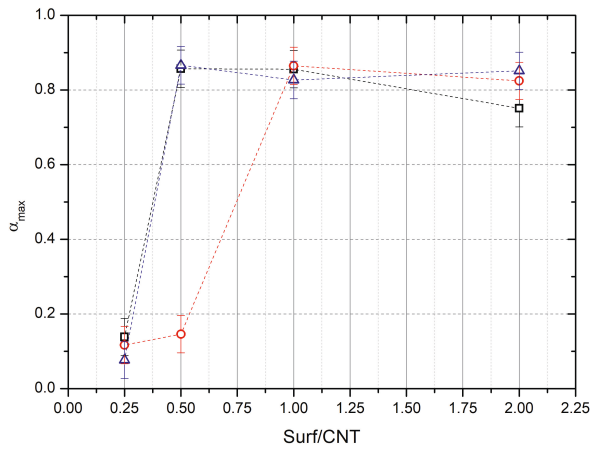


Figure 7.10 Saturation of the opacity α_{max} for three different surfactants (\square) Triton X-100, (\circ) Pluronic F-127 and (\triangle) CTAB as a function of surfactant/CNT ratio.

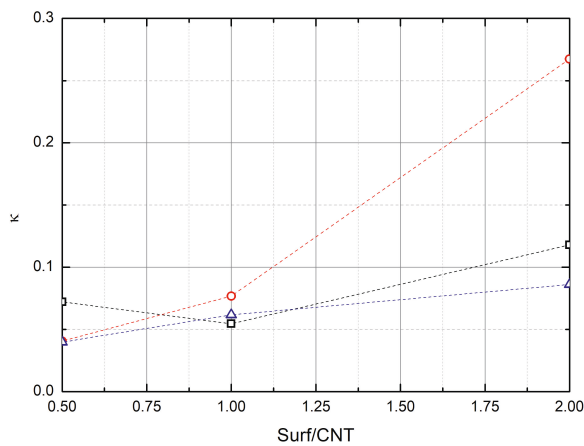


Figure 7.11 The factor κ for three different surfactants (\square) Triton X-100, (\circ) Pluronic F-127 and (\triangle) CTAB, indicating a growth speed of the opacity as a function of surfactant/CNT ratio.

Since different types of carbon nanotubes need different sonication energies and in some cases the damage and shortening is significant it is therefore suggested that in selecting of surfactants not only the compatibility of the chemicals but also the energy needed for sonication should be included in the considerations. In applications where a presence of surfactant in the matrix is diminishing the performance, it

is preferred to select a surfactant which has low surfactant/CNT threshold. On the other hand in applications where post removal of surfactant is possible higher ratios can be used in order to preserve graphitic integrity of the nanotubes by speeding up the dispersion process. The effect of post-removal of Triton X-100 from CNT/NBR nanocomposites with acetone immersion had significant effect on tensile modulus and UTS measured from stress-strain curves. After post treatment the local maximum mentioned in previous chapter in RDQ range 40 - 60% becomes more visible.

Qualitative studies of sonication induced damage to the nanotubes during aqueous sonication were performed by taking TEM images in different stages of the sonication process. After sonicating with energy of 266 kJ/g, which is enough to reach saturation in dispersion quality measurements, no significant exfoliation or cutting were noticed. Therefore changes in morphology were considered to be modest.

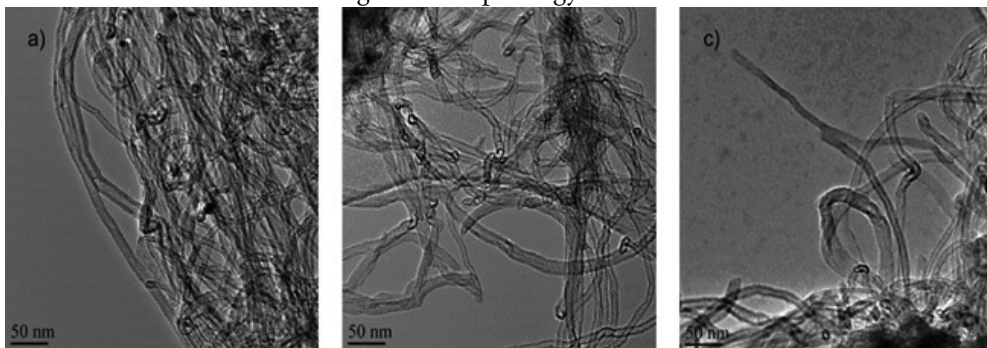


Figure 7.12 TEM images of NC7000 nanotubes (AR210) during aqueous sonication process with the energy of a) 0 kJ/g, b) 133 kJ/g and c) 266 kJ/g.

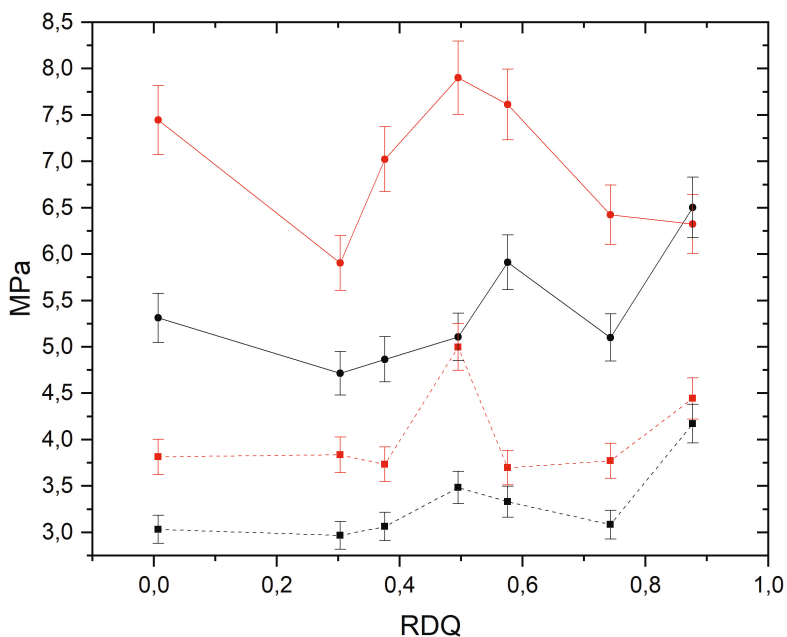


Figure 7.13 Elastic modulus before (red square with dashed line) and after post treatment (red circle with solid line), and ultimate tensile strength before (black square with dashed line) and after post treatment (black circle with solid line) of CNT/NBR nanocomposites as a function of relative dispersion quality. Modulus was determined by linear fitting the stress-strain from 5% to 15% strain [Publication II].

Removal of surfactants increased the elongation at break. The treatment also affected the NBR reference since used latex contains some surfactants which were also removed. Post treatment with highest RDQ gave higher elongation at break values than reference NBR before treatment.

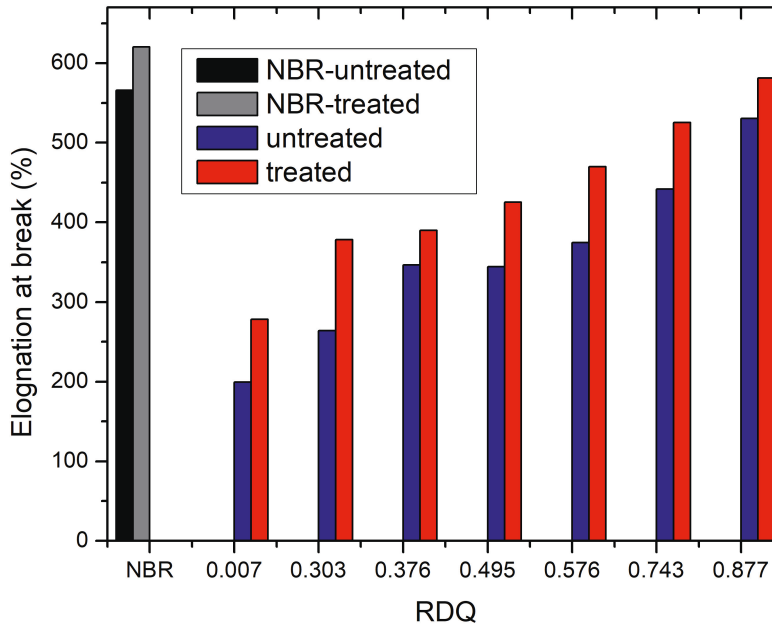


Figure 7.14 Elongation at break of NBR reference and CNT/NBR composites as a function of RDQ before and after the post treatment [Publication II].

Stress-strain curves show increased energy absorption and stiffness values. The necking phenomena was also inhibited with higher RDQ values. This indicates better adhesion between fillers and the matrix.

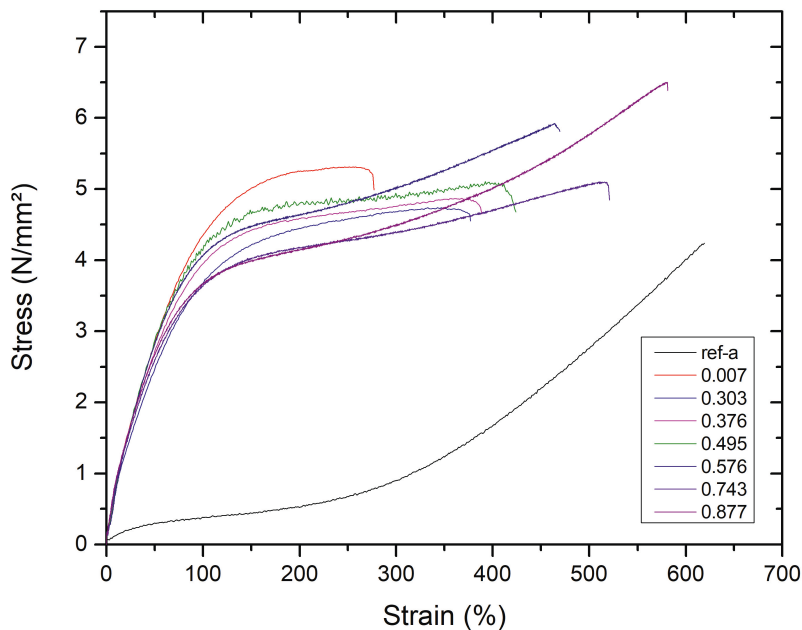


Figure 7.15 stress-strain curves of NBR reference and CNT/NBR composites with different RDQ-values after post-treatment [Publication II].

Strain sweeps were conducted with DMA after removal of surfactants. From figure (7.16) it can be seen that as the RDQ is enhancing the Payne effect, describing intensity of the filler-filler interaction peaks first in range 0.4 - 0.6 RDQ. After removal of surfactants the CNT network interaction is enhanced significantly and pristine network interaction is regained. As RDQ is further enhanced the percolating network of individual nanotubes is formed and since diminishing component of spacer molecules are removed the network interaction is increasing to same level as pristine filler-filler and CCA together.

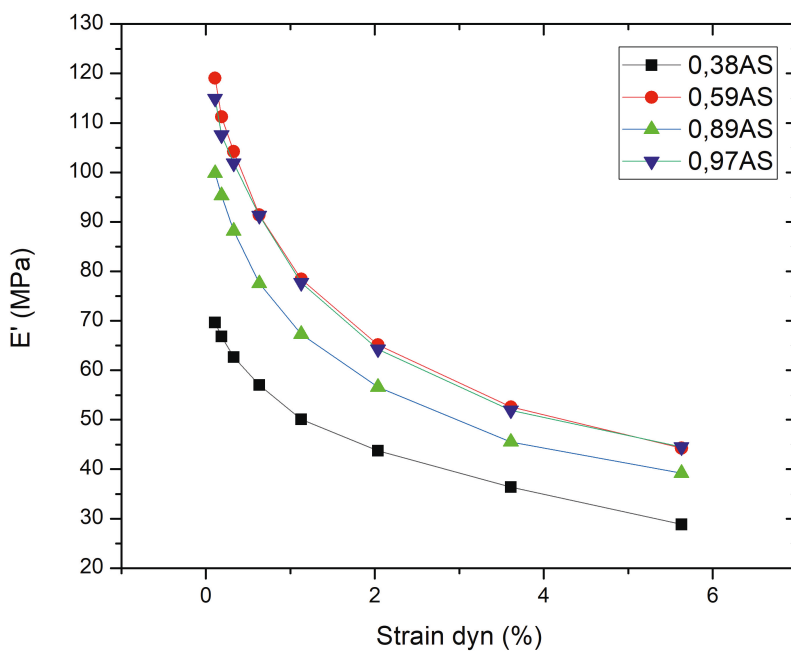


Figure 7.16 DMA strain sweeps of CNT/NBR composites with different RDQ values after surfactant removal [Publication II].

The surface resistance of CNT/NBR nanocomposites was measured after the films were immersed to acetone to remove the surfactant from the composite. It was noticed that conductivity improved in lower RDQ sample but was not affected with higher values.

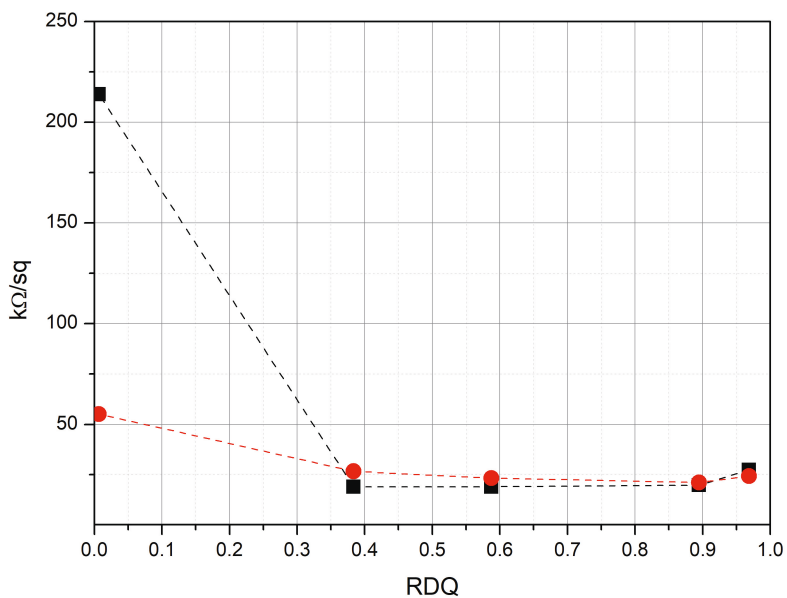


Figure 7.17 Surface resistance measurements of NBR/CNT films as a function of RDQ before the surfactant removal (black) and after (red) [Publication II].

The electrical conductivities of the CNT/NFC films were also measured after surfactant removal. Films containing Triton X-100 and Pluronic F-127 were treated with acetone and films containing CTAB with ethanol. All conductivities improved after post-treatment but the trends as a function of sonication energy remained except with Pluronic F-127 above CMC. The highest improvement was seen with Triton X-100 where the conductivity reached 8.43 S/cm at sonication energy of 666 kJ/g (Figure 7.18).

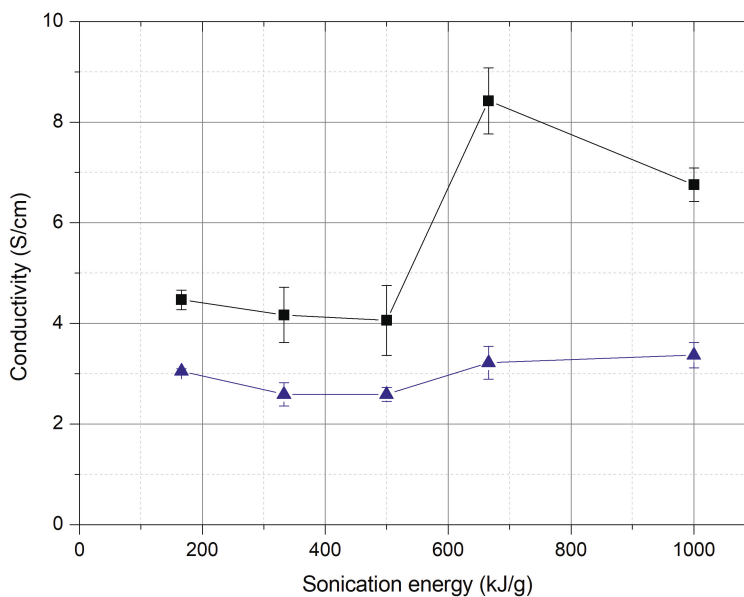


Figure 7.18 Conductivities of NFC/CNT nanocomposite films using Triton X-100, untreated films (blue) and treated films (black) [Publication III].

The developed technique to produce highly conducting CNT/NFC films was also used to coat macroscopic cellulose fibres. These cellulose based hierarchical composite materials has an even distribution of CNTs on top of the cellulose fibres as can be seen from (Figure 7.19).

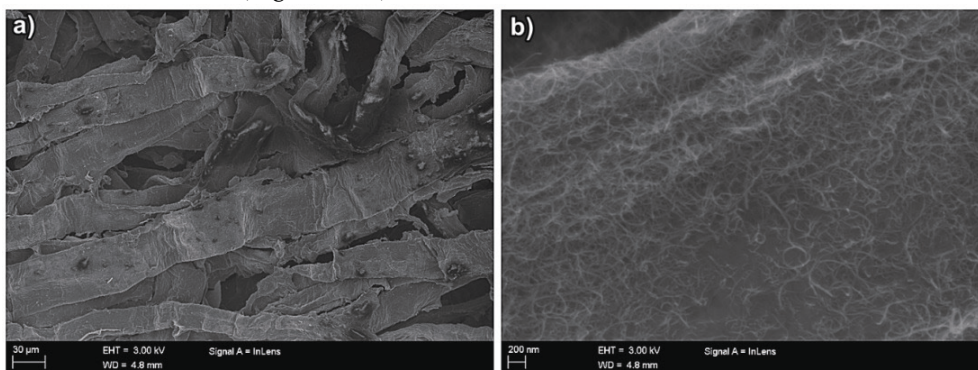


Figure 7.19 Homogenous CNT coverage over cellulose fibers and (b) carbon nanotube percolation network on the surface of cellulose fiber [Publication IV].

These hierarchical structures were used to form electrically conducting 3D ele-

ments using foam forming technology. It was presented that the elements have high enough electrical conductivity so they can be used as heating elements like can be seen from (Figure 7.20). The conductivity was 7.7 S/m, which increased to the value 8.0 S/m after surfactant removal by acetone washing.

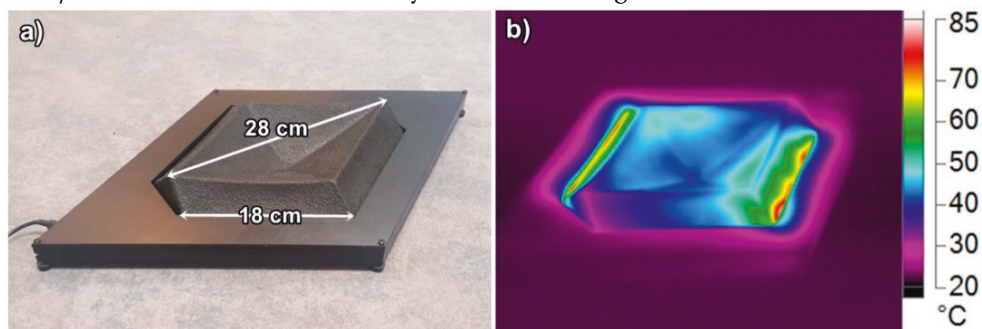


Figure 7.20 (a) Plywood mounted molded heating element with dimensions and (b) infrared camera image of heating element prototype at steady state in room temperature. [Publication IV].

7.4 The effect of aspect ratio

In PU nanocomposites the filler loading was below (1 Wt. %) and just above (2 Wt.%) the percolation threshold of 1.25 Wt.%. PU nanocomposite studies showed that elastic modulus determined from stress-strain curves follows the Halpin-Tsai model as a function of aspect ratio, but measured values remains approximately 50% lower than theoretical predictions. This can be explained to cause from poor interfacial bonding between the filler and matrix since the surfactants used in the dispersion process still remains in the matrix. The dispersion quality typically named as a reason for poor performance of the composite is not likely to cause the reduction since similar phenomena of achieving only half of the expected values was seen in CNT/NBR studies regardless of the dispersion quality before surfactant removal [Publication II].

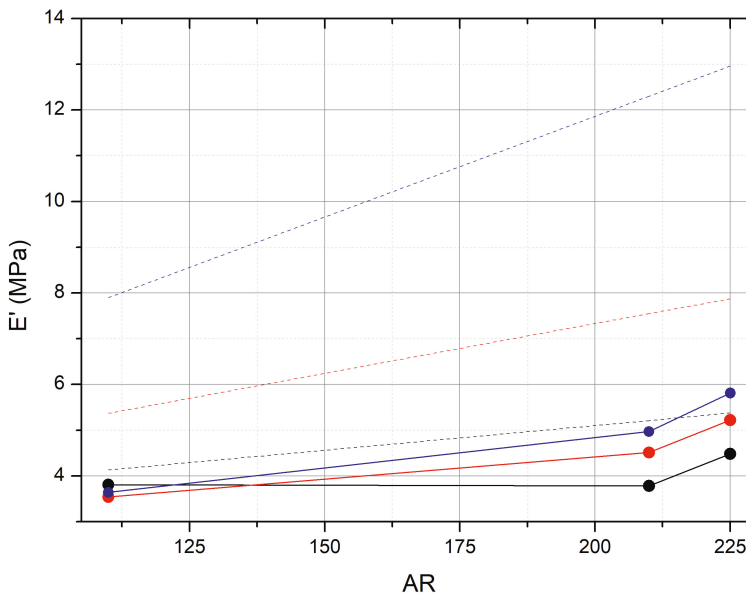


Figure 7.21 Elastic modulus of PU/CNT nanocomposites with theoretical estimates (Halpin-Tsai) as a function of aspect ratio (AR) of the filler. 0.5wt% theoretical (black dashed line), 0.5wt% measured (black circle), 1.0wt% theoretical (red dashed line), 1.0wt% measured (red circle), 2.0wt% theoretical (blue dashed line), 2.0wt% measured (blue circle).

The surface resistance of PU nanocomposites was measured with different nan-

otube concentrations and aspect ratios. A steep decrease in resistance was observed in all types of nanotubes which indicates the reaching of critical percolation threshold (Figure 7.22). It was observed that aspect ratio was not a reliable parameter in estimating the threshold values. In sample AR225 the percolation threshold was between 0.2 and 0.5 wt% whereas with AR110 it was 0.6–1 wt%. With the shorter AR210 (NC7000) the percolation threshold was much higher (1–1.5 wt%). The minimum resistance of the composites was reached with the longest nanotubes (AR225), which is approximately 1/3 of the value of AR110, and 1/10 of the AR210 network.

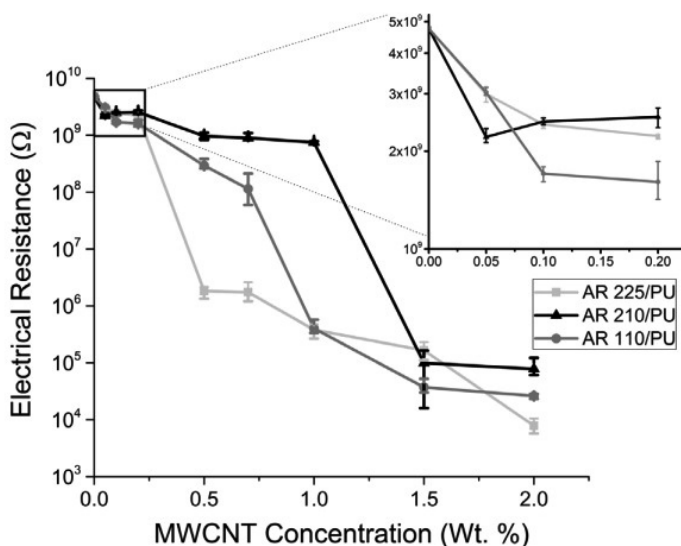


Figure 7.22 Surface resistance of CNT/PU samples with respect to concentration. The inset figure shows the region at low MWCNT concentration (up to 0.2 wt%). CNTs with longer length (AR225 and AR110) show a steep decrease in electrical resistivity, indicating ease of achieving percolation with lower concentrations. [Publication V]

This was most likely to be caused from very different morphologies since AR110 and AR225 nanotubes are stiff and linear whereas AR210 (Nanocyl NC 7000) are curly as can be seen from Figure 7.23.

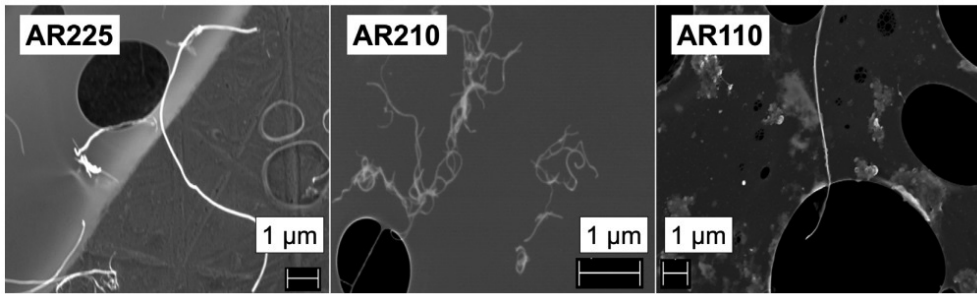


Figure 7.23 TEM images (taken at different magnification) of CNTs after sonication treatment depicting the difference in morphology; an interesting observation is significantly difference in morphology; an interesting observation is significantly different appearance of the samples AR225 and AR210, revealing the uncertain nature of the aspect ratio. AR210 are short, thin and twisted; AR225 are thick and straight [Publication V].

8 CONCLUDING REMARKS

Carbon nanotubes are excellent filler material in short fibre reinforced nanocomposites. However there are many challenges using them mainly related to difficulties in dispersing nanotubes throughout the matrix. One of the most used methods to achieve homogeneous dispersions in low viscosity liquids is sonication. The aim of this thesis was to study how the relative dispersion quality of CNT colloids is developing during sonication processes and conduct a theoretical framework for it. The effect of determined relative dispersion quality, presence of surfactants used in the dispersion process, and different characteristics of CNTs on physical properties of cellulose and elastomer composites was also studied.

The main novel scientific contribution of this thesis relays on creating a theoretical framework for development of dispersion quality in sonication assisted aqueous dispersion process of carbon nanotubes. The theory was developed from one simple relation between development rate of the opacity of the colloid and concentration of undispersed nanotubes. All the previous publications on the subject are purely empirical. Theoretical model includes constants that could be used to study mechanisms how surfactants and their concentrations affect the dispersion development. Another novelty aspects of this thesis is in studying the mechanical and electrical properties of the nanocomposites as a function of dispersion quality where composites were deliberately fabricated with poor dispersion quality, and also investigating effects of post-treatments in which components necessary for nanofluid manufacturing were being removed from the matrix.

8.1 Research question 1

In order to answer to the *research question 1*, theoretical framework for dispersion quality development during sonication was conducted. A initial assumption was

that the rate of improvement of dispersion quality as a function of used inertial sonication energy is related to a concentration of un-dispersed CNTs in larger agglomerates. This first order differential equation was solved and verified experimentally with four different surfactants. It was noticed that different surfactants were giving different values for the parameters of the equation, which could be used to classify different surfactants for dispersing CNTs using sonication.

8.2 Research question 2

In order to answer to the *research question 2*, NBR nanocomposites were manufactured with solution casting method. Different relative dispersion qualities of the aqueous CNT colloid were used and their effect on physical performance of the composites was studied. Typical assumption related to dispersion quality of CNTs is that the more homogeneous the composite is, the better the mechanical performance. It was noted that this is not true when considering elastic modulus, which peaked with relative dispersion qualities between 0.5 - 0.7. However, the elongation at break and ultimate tensile strength showed linear dependence on relative dispersion quality. With low RDQ values the reinforcement effect of nanotubes is mainly coming from reinforcement effect of the agglomerates. As the RDQ is enhancing the reinforcement is a combination of agglomerate reinforcement, filler-filler interaction, bound polymer effect and local reinforcement of individual nanotubes. Going higher with RDQ the effect of agglomerates is lost, the amount of bound polymer is decreased and a number of individual nanotubes is increased. This has lowering effect on stiffness and storage modulus of the nanocomposites but enhancing effect on elongation at break and ultimate tensile strength. Sonication is changing the fractal dimension of the filler, integrity of the graphitic structure, chemical environment and aspect ratio of the nanotubes. All of these are microscopic parameters that are included in RDQ which is a macroscopic parameter of the system and can be used to optimize the individual dispersion process.

8.3 Research question 3

In order to answer to the *research question 3*, manufactured NBR films were swelled with acetone which dissolved the surfactants from the matrix. Electrical and thermal conductivities, stress-strain and DMA measurements were performed before and after acetone treatment. While conductivities were not affected, mechanical measurements showed significant improvements in performance. This indicates improved filler-filler and matrix-filler interaction. The same acetone treatment was also made for CNT-nanocellulose films which showed significant improvements in electrical conductivities reaching highest reported values for such compositions.

8.4 Research question 4

In order to answer to the *research question 4*, polyurethane nanocomposites were manufactured with using three different nanotube types varying aspect ratio and diameter. Electrical and mechanical studies showed that longer nanotubes exhibit better electrical conductivity and that related percolation threshold is dependent on length of the nanotubes more than aspect ratio. On the other hand mechanical properties, in this case elastic modulus was found to be dependent on aspect ratio. Therefore aspect ratio should not be used as the universal parameter characterizing carbon nanotubes.

8.5 Future topics

Authors have unpublished data from sonication experiments including changes in thermal conductivity of randomly oriented CNT networks as a function of sonication energy, changes in I_G/I_D ratio from Raman-spectroscopy as a function of sonication energy and also changes in activation energy of oxidation using Kissinger method. In sonication experiments CNT dispersions experiences a gelation which probably is related to changes in morphology of the agglomerates. Combining this data with theoretical work related to reinforcing effects of fillers having various fractal dimensions would be very interesting.

REFERENCES

- [1] A. Blumstein. Polymerization of adsorbed monolayers. I. Preparation of the clay–polymer complex. *Journal of polymer science part A: general papers* 3.7 (1965), 2653–2664.
- [2] M. Bhattacharya. Polymer nanocomposites—a comparison between carbon nanotubes, graphene, and clay as nanofillers. *Materials* 9.4 (2016), 262.
- [3] K. Ghaffarzadeh. *Graphene, 2D Materials and Carbon Nanotubes: Markets, Technologies and Opportunities 2016-2026; Granular Ten-year Market Forecasts, Data-driven and Quantitative Application Assessment, More Than 40 Interview Based Company Profiles, Revenue/investment/capacity by Player, Etc.* IDTechEx, 2016.
- [4] S. Iijima. Helical microtubules of graphitic carbon. *Nature* 354.6348 (1991), 56.
- [5] X. Wang, Q. Li, J. Xie, Z. Jin, J. Wang, Y. Li, K. Jiang and S. Fan. Fabrication of ultralong and electrically uniform single-walled carbon nanotubes on clean substrates. *Nano letters* 9.9 (2009), 3137–3141.
- [6] T. Guo, P. Nikolaev, A. G. Rinzler, D. Tomanek, D. T. Colbert and R. E. Smalley. Self-assembly of tubular fullerenes. *The Journal of Physical Chemistry* 99.27 (1995), 10694–10697.
- [7] G. Z. Chen, X. Fan, A. Luget, M. S. Shaffer, D. J. Fray and A. H. Windle. Electrolytic conversion of graphite to carbon nanotubes in fused salts. *Journal of Electroanalytical Chemistry* 446.1-2 (1998), 1–6.
- [8] K. S. Kim, G. Cota-Sanchez, C. T. Kingston, M. Imris, B. Simard and G. Soucy. Large-scale production of single-walled carbon nanotubes by induction thermal plasma. *Journal of Physics D: Applied Physics* 40.8 (2007), 2375.
- [9] H. Cheng, F. Li, G. Su, H. Pan, L. He, X. Sun and M. Dresselhaus. Large-scale and low-cost synthesis of single-walled carbon nanotubes by the catalytic pyrolysis of hydrocarbons. *Applied Physics Letters* 72.25 (1998), 3282–3284.

- [10] V. N. Popov. Carbon nanotubes: properties and application. *Materials Science and Engineering: R: Reports* 43.3 (2004), 61–102.
- [11] N. Hamada, S.-i. Sawada and A. Oshiyama. New one-dimensional conductors: graphitic microtubules. *Physical review letters* 68.10 (1992), 1579.
- [12] B. Wei, R. Vajtai and P. Ajayan. Reliability and current carrying capacity of carbon nanotubes. *Applied Physics Letters* 79.8 (2001), 1172–1174.
- [13] S. Berber, Y.-K. Kwon and D. Tománek. Unusually high thermal conductivity of carbon nanotubes. *Physical review letters* 84.20 (2000), 4613.
- [14] J.-P. Salvetat, J.-M. Bonard, N. Thomson, A. Kulik, L. Forro, W. Benoit and L. Zuppiroli. Mechanical properties of carbon nanotubes. *Applied Physics A* 69.3 (1999), 255–260.
- [15] B. Peng, M. Locascio, P. Zapol, S. Li, S. L. Mielke, G. C. Schatz and H. D. Espinosa. Measurements of near-ultimate strength for multiwalled carbon nanotubes and irradiation-induced crosslinking improvements. *Nature nanotechnology* 3.10 (2008), 626.
- [16] M. R. Falvo, G. Clary, R. Taylor II, V. Chi, F. Brooks Jr, S. Washburn and R. Superfine. Bending and buckling of carbon nanotubes under large strain. *Nature* 389.6651 (1997), 582.
- [17] S. J. Tans, A. R. Verschueren and C. Dekker. Room-temperature transistor based on a single carbon nanotube. *Nature* 393.6680 (1998), 49.
- [18] T. Rueckes, K. Kim, E. Joselevich, G. Y. Tseng, C.-L. Cheung and C. M. Lieber. Carbon nanotube-based nonvolatile random access memory for molecular computing. *Science* 289.5476 (2000), 94–97.
- [19] W. A. De Heer, A. Chatelain and D. Ugarte. A carbon nanotube field-emission electron source. *Science* 270.5239 (1995), 1179–1180.
- [20] L. Dai, D. W. Chang, J.-B. Baek and W. Lu. Carbon nanomaterials for advanced energy conversion and storage. *Small* 8.8 (2012), 1130–1166.
- [21] T. Kurkina, A. Vlandas, A. Ahmad, K. Kern and K. Balasubramanian. Label-free detection of few copies of DNA with carbon nanotube impedance biosensors. *Angewandte Chemie International Edition* 50.16 (2011), 3710–3714.

- [22] D. A. Heller, H. Jin, B. M. Martinez, D. Patel, B. M. Miller, T.-K. Yeung, P. V. Jena, C. Höbartner, T. Ha, S. K. Silverman et al. Multimodal optical sensing and analyte specificity using single-walled carbon nanotubes. *Nature Nanotechnology* 4.2 (2009), 114.
- [23] J. Sandler, M. Shaffer, T. Prasse, W. Bauhofer, K. Schulte and A. Windle. Development of a dispersion process for carbon nanotubes in an epoxy matrix and the resulting electrical properties. *Polymer* 40.21 (1999), 5967–5971.
- [24] F. H. Gojny, J. Nastalczyk, Z. Roslaniec and K. Schulte. Surface modified multi-walled carbon nanotubes in CNT/epoxy-composites. *Chemical physics letters* 370.5-6 (2003), 820–824.
- [25] T. McNally, P. Pötschke, P. Halley, M. Murphy, D. Martin, S. E. Bell, G. P. Brennan, D. Bein, P. Lemoine and J. P. Quinn. Polyethylene multiwalled carbon nanotube composites. *Polymer* 46.19 (2005), 8222–8232.
- [26] M. S. Shaffer and A. H. Windle. Fabrication and characterization of carbon nanotube/poly (vinyl alcohol) composites. *Advanced materials* 11.11 (1999), 937–941.
- [27] F. Li, H. Cheng, S. Bai, G. Su and M. Dresselhaus. Tensile strength of single-walled carbon nanotubes directly measured from their macroscopic ropes. *Applied physics letters* 77.20 (2000), 3161–3163.
- [28] J. Sandler, S. Pegel, M. Cadek, F. Gojny, M. Van Es, J. Lohmar, W. Blau, K. Schulte, A. Windle and M. Shaffer. A comparative study of melt spun polyamide-12 fibres reinforced with carbon nanotubes and nanofibres. *Polymer* 45.6 (2004), 2001–2015.
- [29] H. Lorenz, J. Fritzsche, A. Das, K. Stöckelhuber, R. Jurk, G. Heinrich and M. Klüppel. Advanced elastomer nano-composites based on CNT-hybrid filler systems. *Composites Science and Technology* 69.13 (2009), 2135–2143.
- [30] H. Ismail, A. Ramly and N. Othman. Effects of silica/multiwall carbon nanotube hybrid fillers on the properties of natural rubber nanocomposites. *Journal of Applied Polymer Science* 128.4 (2013), 2433–2438.
- [31] G. Sui, W. Zhong, X. Yang and S. Zhao. Processing and material characteristics of a carbon-nanotube-reinforced natural rubber. *Macromolecular Materials and Engineering* 292.9 (2007), 1020–1026.

- [32] G. Sui, W. Zhong, X. Yang, Y. Yu and S. Zhao. Preparation and properties of natural rubber composites reinforced with pretreated carbon nanotubes. *Polymers for Advanced Technologies* 19.11 (2008), 1543–1549.
- [33] A. A. Abdullateef, S. P. Thomas, M. A. Al-Harthi, S. De, S. Bandyopadhyay, A. Basfar and M. A. Atieh. Natural rubber nanocomposites with functionalized carbon nanotubes: mechanical, dynamic mechanical, and morphology studies. *Journal of Applied Polymer Science* 125.S1 (2012), E76–E84.
- [34] Z. Peng, C. Feng, Y. Luo, Y. Li and L. Kong. Self-assembled natural rubber/multi-walled carbon nanotube composites using latex compounding techniques. *Carbon* 48.15 (2010), 4497–4503.
- [35] Y.-S. Park, M.-Y. Huh, S.-J. Kang, S.-I. Yun and K.-H. Ahn. Effect of CNT diameter on physical properties of styrene-butadiene rubber nanocomposites. *Carbon letters* 10.4 (2009), 320–324.
- [36] A. Das, G. R. Kasaliwal, R. Jurk, R. Boldt, D. Fischer, K. W. Stöckelhuber and G. Heinrich. Rubber composites based on graphene nanoplatelets, expanded graphite, carbon nanotubes and their combination: A comparative study. *Composites Science and Technology* 72.16 (2012), 1961–1967.
- [37] L. D. Perez, M. A. Zuluaga, T. Kyu, J. E. Mark and B. L. Lopez. Preparation, characterization, and physical properties of multiwall carbon nanotube/elastomer composites. *Polymer Engineering & Science* 49.5 (2009), 866–874.
- [38] S. Schopp, R. Thomann, K.-F. Ratzsch, S. Kerling, V. Altstädt and R. Mülhaupt. Functionalized Graphene and Carbon Materials as Components of Styrene-Butadiene Rubber Nanocomposites Prepared by Aqueous Dispersion Blending. *Macromolecular Materials and Engineering* 299.3 (2014), 319–329.
- [39] H. Jiang, Q. Ni, H. Wang and J. Liu. Fabrication and characterization of NBR/MWCNT composites by latex technology. *Polymer Composites* 33.9 (2012), 1586–1592.
- [40] A. Boonbumrung, P. Sea-Oui and C. Sirisinha. Dispersion enhancement of multi-walled carbon nanotube (MWCNT) in nitrile rubber (NBR). *Advanced Materials Research*. Vol. 747. Trans Tech Publ. 2013, 59–62.

- [41] M. M. Möwes, F. Fleck and M. Klüppel. Effect of filler surface activity and morphology on mechanical and dielectric properties of NBR/Graphene nanocomposites. *Rubber Chemistry and Technology* 87.1 (2014), 70–85.
- [42] E. Guth. Theory of filler reinforcement. *Journal of applied physics* 16.1 (1945), 20–25.
- [43] M. M. Shokrieh and H. Moshrefzadeh-Sani. On the constant parameters of Halpin-Tsai equation. *Polymer* 106 (2016), 14–20.
- [44] W. Bauhofer and J. Z. Kovacs. A review and analysis of electrical percolation in carbon nanotube polymer composites. *Composites Science and Technology* 69.10 (2009), 1486–1498.
- [45] J. Aguilar, J. Bautista-Quijano and F. Avilés. Influence of carbon nanotube clustering on the electrical conductivity of polymer composite films. *Express Polym. Lett* 4.5 (2010), 292–299.
- [46] S. Bhattacharyya, C. Sinturel, O. Bahloul, M.-L. Saboungi, S. Thomas and J.-P. Salvetat. Improving reinforcement of natural rubber by networking of activated carbon nanotubes. *Carbon* 46.7 (2008), 1037–1045.
- [47] Z.-M. Dang, K. Shehzad, J.-W. Zha, A. Mujahid, T. Hussain, J. Nie and C.-Y. Shi. Complementary percolation characteristics of carbon fillers based electrically percolative thermoplastic elastomer composites. *Composites science and technology* 72.1 (2011), 28–35.
- [48] J. Yu, K. Lu, E. Sourty, N. Grossiord, C. E. Koning and J. Loos. Characterization of conductive multiwall carbon nanotube/polystyrene composites prepared by latex technology. *Carbon* 45.15 (2007), 2897–2903.
- [49] A. Das, K. Stöckelhuber, R. Jurk, M. Saphiannikova, J. Fritzsche, H. Lorenz, M. Klüppel and G. Heinrich. Modified and unmodified multiwalled carbon nanotubes in high performance solution-styrene-butadiene and butadiene rubber blends. *Polymer* 49.24 (2008), 5276–5283.
- [50] D. Klemm, B. Heublein, H.-P. Fink and A. Bohn. Cellulose: fascinating biopolymer and sustainable raw material. *Angewandte Chemie International Edition* 44.22 (2005), 3358–3393.

- [51] L. Hu, G. Zheng, J. Yao, N. Liu, B. Weil, M. Eskilsson, E. Karabulut, Z. Ruan, S. Fan, J. T. Bloking et al. Transparent and conductive paper from nanocellulose fibers. *Energy & Environmental Science* 6.2 (2013), 513–518.
- [52] A. Hebeish, S. Farag, S. Sharaf and T. I. Shaheen. Development of cellulose nanowhisker-polyacrylamide copolymer as a highly functional precursor in the synthesis of nanometal particles for conductive textiles. *Cellulose* 21.4 (2014), 3055–3071.
- [53] A. Mihranyan, M. Esmaceli, A. Razaq, D. Alexeichik and T. Lindström. Influence of the nanocellulose raw material characteristics on the electrochemical and mechanical properties of conductive paper electrodes. *Journal of Materials Science* 47.10 (2012), 4463–4472.
- [54] D. Müller, J. Mandelli, J. Marins, B. Soares, L. Porto, C. Rambo and G. Barra. Electrically conducting nanocomposites: preparation and properties of polyaniline (PAni)-coated bacterial cellulose nanofibers (BC). *Cellulose* 19.5 (2012), 1645–1654.
- [55] J. Fan, W. Shao, G. Xu, X. T. Cui and X. Luo. Preparation and electrochemical catalytic application of nanocrystalline cellulose doped poly (3, 4-ethylenedioxythiophene) conducting polymer nanocomposites. *RSC Advances* 4.46 (2014), 24328–24333.
- [56] L. Jabbour, C. Gerbaldi, D. Chaussy, E. Zeno, S. Bodoardo and D. Beneventi. Microfibrillated cellulose–graphite nanocomposites for highly flexible paper-like Li-ion battery electrodes. *Journal of Materials Chemistry* 20.35 (2010), 7344–7347.
- [57] Z. Weng, Y. Su, D.-W. Wang, F. Li, J. Du and H.-M. Cheng. Graphene–cellulose paper flexible supercapacitors. *Advanced Energy Materials* 1.5 (2011), 917–922.
- [58] M. M. Hamed, A. Hajian, A. B. Fall, K. Hakansson, M. Salajkova, F. Lundell, L. Wagberg and L. A. Berglund. Highly conducting, strong nanocomposites based on nanocellulose-assisted aqueous dispersions of single-wall carbon nanotubes. *ACS nano* 8.3 (2014), 2467–2476.
- [59] V. Kuzmenko, O. Naboka, M. Haque, H. Staaf, G. Göransson, P. Gatenholm and P. Enoksson. Sustainable carbon nanofibers/nanotubes composites from cellulose as electrodes for supercapacitors. *Energy* 90 (2015), 1490–1496.

- [60] C. Basavaraja, E. A. Jo, B. S. Kim and D. S. Huh. Electromagnetic interference shielding of cellulose triacetate/multiwalled carbon nanotube composite films. *Polymer Composites* 32.3 (2011), 438–444.
- [61] B. Fugetsu, E. Sano, M. Sunada, Y. Sambongi, T. Shibuya, X. Wang and T. Hiraki. Electrical conductivity and electromagnetic interference shielding efficiency of carbon nanotube/cellulose composite paper. *Carbon* 46.9 (2008), 1256–1258.
- [62] S. Yun and J. Kim. Multi-walled carbon nanotubes–cellulose paper for a chemical vapor sensor. *Sensors and Actuators B: Chemical* 150.1 (2010), 308–313.
- [63] H. Qi, J. Liu, J. Pionteck, P. Pötschke and E. Mäder. Carbon nanotube–cellulose composite aerogels for vapour sensing. *Sensors and Actuators B: Chemical* 213 (2015), 20–26.
- [64] H. Qi, E. Mäder and J. Liu. Unique water sensors based on carbon nanotube–cellulose composites. *Sensors and Actuators B: Chemical* 185 (2013), 225–230.
- [65] M. Wang, I. V. Anoshkin, A. G. Nasibulin, J. T. Korhonen, J. Seitsonen, J. Pere, E. I. Kauppinen, R. H. Ras and O. Ikkala. Modifying native nanocellulose aerogels with carbon nanotubes for mechanoresponsive conductivity and pressure sensing. *Advanced materials* 25.17 (2013), 2428–2432.
- [66] T.-W. Lee, S.-E. Lee and Y. G. Jeong. Carbon nanotube/cellulose papers with high performance in electric heating and electromagnetic interference shielding. *Composites Science and Technology* 131 (2016), 77–87.
- [67] R. E. Anderson, J. Guan, M. Ricard, G. Dubey, J. Su, G. Lopinski, G. Dorris, O. Bourne and B. Simard. Multifunctional single-walled carbon nanotube–cellulose composite paper. *Journal of Materials Chemistry* 20.12 (2010), 2400–2407.
- [68] T. Zhou, D. Chen, J. Jiu, T. Nge, T. Sugahara, S. Nagao, H. Koga, M. Nogi, K. Suganuma, X. Wang et al. Electrically conductive bacterial cellulose composite membranes produced by the incorporation of graphite nanoplatelets in pristine bacterial cellulose membranes. *Express Polymer Letters* 7.9 (2013).
- [69] S. H. Yoon, H.-J. Jin, M.-C. Kook and Y. R. Pyun. Electrically conductive bacterial cellulose by incorporation of carbon nanotubes. *Biomacromolecules* 7.4 (2006), 1280–1284.

- [70] J. Choi, S. Park, J. Cheng, M. Park and J. Hyun. Amphiphilic comb-like polymer for harvest of conductive nano-cellulose. *Colloids and Surfaces B: Biointerfaces* 89 (2012), 161–166.
- [71] T. Oya and T. Ogino. Production of electrically conductive paper by adding carbon nanotubes. *Carbon* 1.46 (2008), 169–171.
- [72] W.-I. Park, H.-S. Kim, S.-M. Kwon, Y.-H. Hong and H.-J. Jin. Synthesis of bacterial celluloses in multiwalled carbon nanotube-dispersed medium. *Carbohydrate polymers* 77.3 (2009), 457–463.
- [73] L. Hu, J. W. Choi, Y. Yang, S. Jeong, F. La Mantia, L.-F. Cui and Y. Cui. Highly conductive paper for energy-storage devices. *Proceedings of the National Academy of Sciences* 106.51 (2009), 21490–21494.
- [74] D.-Q. Yang, J.-F. Rochette and E. Sacher. Functionalization of multiwalled carbon nanotubes by mild aqueous sonication. *The Journal of Physical Chemistry B* 109.16 (2005), 7788–7794.
- [75] Y. Y. Huang and E. M. Terentjev. Dispersion of carbon nanotubes: mixing, sonication, stabilization, and composite properties. *Polymers* 4.1 (2012), 275–295.
- [76] K. Lu, R. Lago, Y. Chen, M. Green, P. Harris and S. Tsang. Mechanical damage of carbon nanotubes by ultrasound. *Carbon* 34.6 (1996).
- [77] R. Andrews, D. Jacques, M. Minot and T. Rantell. Fabrication of carbon multiwall nanotube/polymer composites by shear mixing. *Macromolecular Materials and Engineering* 287.6 (2002), 395–403.
- [78] P. Pötschke, A. R. Bhattacharyya and A. Janke. Morphology and electrical resistivity of melt mixed blends of polyethylene and carbon nanotube filled polycarbonate. *Polymer* 44.26 (2003), 8061–8069.
- [79] F. Gojny, M. Wichmann, U. Köpke, B. Fiedler and K. Schulte. Carbon nanotube-reinforced epoxy-composites: enhanced stiffness and fracture toughness at low nanotube content. *Composites science and technology* 64.15 (2004), 2363–2371.
- [80] E. T. Thostenson and T.-W. Chou. Processing-structure-multi-functional property relationship in carbon nanotube/epoxy composites. *Carbon* 44.14 (2006), 3022–3029.

- [81] Y. Huang and E. Terentjev. Dispersion and rheology of carbon nanotubes in polymers. *International Journal of Material Forming* 1.2 (2008), 63–74.
- [82] T. Yamamoto, Y. Miyauchi, J. Motoyanagi, T. Fukushima, T. Aida, M. Kato and S. Maruyama. Improved bath sonication method for dispersion of individual single-walled carbon nanotubes using new triphenylene-based surfactant. *Japanese Journal of Applied Physics* 47.4R (2008), 2000.
- [83] L. Jiang, L. Gao and J. Sun. Production of aqueous colloidal dispersions of carbon nanotubes. *Journal of colloid and interface science* 260.1 (2003), 89–94.
- [84] H.-C. Wu, X. Chang, L. Liu, F. Zhao and Y. Zhao. Chemistry of carbon nanotubes in biomedical applications. *Journal of Materials Chemistry* 20.6 (2010), 1036–1052.
- [85] N. Nakashima, H. Kobae, T. Sagara and H. Murakami. Formation of Single-Walled Carbon Nanotube Thin Films on Electrodes Monitored by an Electrochemical Quartz Crystal Microbalance. *ChemPhysChem* 3.5 (2002), 456–458.
- [86] C. E. Brennen. *Cavitation and bubble dynamics*. Cambridge University Press, 2014.
- [87] J. Stegen. Mechanics of carbon nanotube scission under sonication. *The Journal of Chemical Physics* 140.24 (2014), 244908.
- [88] W. T. Richards and A. L. Loomis. The chemical effects of high frequency sound waves I. A preliminary survey. *Journal of the American Chemical Society* 49.12 (1927), 3086–3100.
- [89] Y. Iida, K. Yasui, T. Tuziuti and M. Sivakumar. Sonochemistry and its dosimetry. *Microchemical Journal* 80.2 (2005), 159–164.
- [90] P. Riesz, D. Berdahl and C. Christman. Free radical generation by ultrasound in aqueous and nonaqueous solutions. *Environmental Health Perspectives* 64 (1985), 233–252.
- [91] S. Koda, T. Kimura, T. Kondo and H. Mitome. A standard method to calibrate sonochemical efficiency of an individual reaction system. *Ultrasonics sonochemistry* 10.3 (2003), 149–156.
- [92] A. Keck, E. Gilbert and R. Köster. Influence of particles on sonochemical reactions in aqueous solutions. *Ultrasonics* 40.1-8 (2002), 661–665.

- [93] J.-M. Bonard, T. Stora, J.-P. Salvetat, F. Maier, T. Stöckli, C. Duschl, L. Forró, W. A. de Heer and A. Châtelain. Purification and size-selection of carbon nanotubes. *Advanced Materials* 9.10 (1997), 827–831.
- [94] T. J. McDonald, C. Engtrakul, M. Jones, G. Rumbles and M. J. Heben. Kinetics of PL quenching during single-walled carbon nanotube rebundling and diameter-dependent surfactant interactions. *The Journal of Physical Chemistry B* 110.50 (2006), 25339–25346.
- [95] M. Bystrzejewski, A. Huczko, H. Lange, T. Gemming, B. Büchner and M. Rümeli. Dispersion and diameter separation of multi-wall carbon nanotubes in aqueous solutions. *Journal of Colloid and Interface Science* 345.2 (2010), 138–142.
- [96] Y. Geng, M. Y. Liu, J. Li, X. M. Shi and J. K. Kim. Effects of surfactant treatment on mechanical and electrical properties of CNT/epoxy nanocomposites. *Composites Part A: Applied Science and Manufacturing* 39.12 (2008), 1876–1883.
- [97] J. Rausch, R.-C. Zhuang and E. Mäder. Surfactant assisted dispersion of functionalized multi-walled carbon nanotubes in aqueous media. *Composites Part A: Applied Science and Manufacturing* 41.9 (2010), 1038–1046.
- [98] S. Javadian, A. Motae, M. Sharifi, H. Aghdastinat and F. Taghavi. Dispersion stability of multi-walled carbon nanotubes in cationic surfactant mixtures. *Colloids and Surfaces A: Physicochemical and Engineering Aspects* 531 (2017), 141–149.
- [99] M. Islam, E. Rojas, D. Bergey, A. Johnson and A. Yodh. High weight fraction surfactant solubilization of single-wall carbon nanotubes in water. *Nano letters* 3.2 (2003), 269–273.
- [100] B. Vigolo, A. Penicaud, C. Coulon, C. Sauder, R. Paillet, C. Journet, P. Bernier and P. Poulin. Macroscopic fibers and ribbons of oriented carbon nanotubes. *Science* 290.5495 (2000), 1331–1334.
- [101] M. J. O’connell, S. M. Bachilo, C. B. Huffman, V. C. Moore, M. S. Strano, E. H. Haroz, K. L. Rialon, P. J. Boul, W. H. Noon, C. Kittrell et al. Band gap fluorescence from individual single-walled carbon nanotubes. *Science* 297.5581 (2002), 593–596.

- [102] P. Poulin, B. Vigolo and P. Launois. Films and fibers of oriented single wall nanotubes. *Carbon* 40.10 (2002), 1741–1749.
- [103] V. C. Moore, M. S. Strano, E. H. Haroz, R. H. Hauge, R. E. Smalley, J. Schmidt and Y. Talmon. Individually suspended single-walled carbon nanotubes in various surfactants. *Nano letters* 3.10 (2003), 1379–1382.
- [104] K. Yurekli, C. A. Mitchell and R. Krishnamoorti. Small-angle neutron scattering from surfactant-assisted aqueous dispersions of carbon nanotubes. *Journal of the American Chemical Society* 126.32 (2004), 9902–9903.
- [105] T. Chatterjee, K. Yurekli, V. G. Hadjiev and R. Krishnamoorti. Single-Walled Carbon Nanotube Dispersions in Poly (Ethylene Oxide). *Advanced Functional Materials* 15.11 (2005), 1832–1838. URL: <http://dx.doi.org/10.1002/adfm.200500290>.
- [106] T. Hertel, A. Hagen, V. Talalaev, K. Arnold, F. Hennrich, M. Kappes, S. Rosenthal, J. McBride, H. Ulbricht and E. Flahaut. Spectroscopy of single- and double-wall carbon nanotubes in different environments. *Nano letters* 5.3 (2005), 511–514. URL: <http://dx.doi.org/10.1021/nl050069a>.
- [107] N. Grossiord, J. Loos, L. Van Laake, M. Maugey, C. Zakri, C. E. Koning and A. J. Hart. High-Conductivity Polymer Nanocomposites Obtained by Tailoring the Characteristics of Carbon Nanotube Fillers. *Advanced Functional Materials* 18.20 (2008), 3226–3234. URL: <http://dx.doi.org/10.1002/adfm.200800528>.
- [108] A. J. Blanch, C. E. Lenehan and J. S. Quinton. Optimizing surfactant concentrations for dispersion of single-walled carbon nanotubes in aqueous solution. *The Journal of Physical Chemistry B* 114.30 (2010), 9805–9811. URL: <http://dx.doi.org/10.1021/jp104113d>.
- [109] M. D. Clark, S. Subramanian and R. Krishnamoorti. Understanding surfactant aided aqueous dispersion of multi-walled carbon nanotubes. *Journal of colloid and interface science* 354.1 (2011), 144–151. URL: <http://dx.doi.org/10.1016/j.jcis.2010.10.027>.
- [110] A. Ryabenko, L. Fokeeva and T. Dorofeeva. Spectroscopic study of suspensions of single-wall carbon nanotubes in polyaniline solutions in N-methylpyrrolidone in UV—Vis—NIR regions. *Russian chemical bulletin* 53.12 (2004), 2695–2699.

- [111] M.-J. Jiang, Z.-M. Dang, S.-H. Yao and J. Bai. Effects of surface modification of carbon nanotubes on the microstructure and electrical properties of carbon nanotubes/rubber nanocomposites. *Chemical physics letters* 457.4 (2008), 352–356. URL: <http://dx.doi.org/10.1016/j.cplett.2008.04.022>.
- [112] R. Rastogi, R. Kaushal, S. Tripathi, A. L. Sharma, I. Kaur and L. M. Bhargava. Comparative study of carbon nanotube dispersion using surfactants. *Journal of colloid and interface science* 328.2 (2008), 421–428. URL: <http://dx.doi.org/10.1016/j.jcis.2008.09.015>.
- [113] Y. Bai, D. Lin, F. Wu, Z. Wang and B. Xing. Adsorption of Triton X-series surfactants and its role in stabilizing multi-walled carbon nanotube suspensions. *Chemosphere* 79.4 (2010), 362–367. URL: <http://dx.doi.org/10.1016/j.chemosphere.2010.02.023>.
- [114] I. Madni, C.-Y. Hwang, S.-D. Park, Y.-H. Choa and H.-T. Kim. Mixed surfactant system for stable suspension of multiwalled carbon nanotubes. *Colloids and Surfaces A: Physicochemical and Engineering Aspects* 358.1 (2010), 101–107. URL: <http://dx.doi.org/10.1016/j.colsurfa.2010.01.030>.
- [115] Y. Bai, I. S. Park, S. J. Lee, T. S. Bae, F. Watari, M. Uo and M. H. Lee. Aqueous dispersion of surfactant-modified multiwalled carbon nanotubes and their application as an antibacterial agent. *Carbon* 49.11 (2011), 3663–3671. URL: <http://dx.doi.org/10.1016/j.carbon.2011.05.002>.
- [116] K. Yang and B. Xing. Adsorption of organic compounds by carbon nanomaterials in aqueous phase: Polanyi theory and its application. *Chemical reviews* 110.10 (2010), 5989–6008. URL: <http://dx.doi.org/10.1021/cr100059s>.
- [117] H. Wang. Dispersing carbon nanotubes using surfactants. *Current Opinion in Colloid & Interface Science* 14.5 (2009), 364–371.
- [118] W. Wenseleers, I. I. Vlasov, E. Goovaerts, E. D. Obraztsova, A. S. Lobach and A. Bouwen. Efficient Isolation and Solubilization of Pristine Single-Walled Nanotubes in Bile Salt Micelles. *Advanced Functional Materials* 14.11 (2004), 1105–1112. URL: <http://dx.doi.org/10.1002/adfm.200400130>.
- [119] J. Yu, N. Grossiord, C. E. Koning and J. Loos. Controlling the dispersion of multi-wall carbon nanotubes in aqueous surfactant solution. *Carbon* 45.3 (2007), 618–623. URL: <http://dx.doi.org/10.1016/j.carbon.2006.10.010>.

- [120] S. Utsumi, M. Kanamaru, H. Honda, H. Kanoh, H. Tanaka, T. Ohkubo, H. Sakai, M. Abe and K. Kaneko. RBM band shift-evidenced dispersion mechanism of single-wall carbon nanotube bundles with NaDDBS. *Journal of colloid and interface science* 308.1 (2007), 276–284. URL: <http://dx.doi.org/10.1016/j.jcis.2006.12.041>.
- [121] Z. Sun, V. Nicolosi, D. Rickard, S. D. Bergin, D. Aherne and J. N. Coleman. Quantitative evaluation of surfactant-stabilized single-walled carbon nanotubes: dispersion quality and its correlation with zeta potential. *The Journal of Physical Chemistry C* 112.29 (2008), 10692–10699. URL: <http://dx.doi.org/10.1021/jp8021634>.
- [122] L. Maillaud, C. Zakri, I. Ly, A. Pénicaud and P. Poulin. Conductivity of transparent electrodes made from interacting nanotubes. *Applied Physics Letters* 103.26 (2013), 263106. URL: <http://dx.doi.org/10.1063/1.4858215>.
- [123] P. Angelikopoulos, A. Gromov, A. Leen, O. Nerushev, H. Bock and E. E. Campbell. Dispersing individual single-wall carbon nanotubes in aqueous surfactant solutions below the cmc. *The Journal of Physical Chemistry C* 114.1 (2009), 2–9. URL: <http://dx.doi.org/10.1021/jp905925r>.
- [124] N. Grossiord, O. Regev, J. Loos, J. Meuldijk and C. E. Koning. Time-dependent study of the exfoliation process of carbon nanotubes in aqueous dispersions by using UV-Visible spectroscopy. *Analytical chemistry* 77.16 (2005), 5135–5139.
- [125] L. Vaisman, G. Marom and H. D. Wagner. Dispersions of surface-modified carbon nanotubes in water-soluble and water-insoluble polymers. *Advanced Functional Materials* 16.3 (2006), 357–363.
- [126] A. M. Shetty, G. M. Wilkins, J. Nanda and M. J. Solomon. Multiangle depolarized dynamic light scattering of short functionalized single-walled carbon nanotubes. *The Journal of Physical Chemistry C* 113.17 (2009), 7129–7133.
- [127] P. K. Rai, A. N. G. Parra-Vasquez, J. Chattopadhyay, R. A. Pinnick, F. Liang, A. K. Sadana, R. H. Hauge, W. E. Billups and M. Pasquali. Dispersions of functionalized single-walled carbon nanotubes in strong acids: Solubility and rheology. *Journal of nanoscience and nanotechnology* 7.10 (2007), 3378–3385.

- [128] A. Ryabenko, T. Dorofeeva and G. Zvereva. UV–VIS–NIR spectroscopy study of sensitivity of single-wall carbon nanotubes to chemical processing and Van-der-Waals SWNT/SWNT interaction. Verification of the SWNT content measurements by absorption spectroscopy. *Carbon* 42.8-9 (2004), 1523–1535.
- [129] Y. Tan and D. E. Resasco. Dispersion of single-walled carbon nanotubes of narrow diameter distribution. *The Journal of Physical Chemistry B* 109.30 (2005), 14454–14460.
- [130] M. A. Tarawneh, S. H. Ahmad, S. Yahya, R. Rasid and S. Y. E. Noum. Mechanical properties of thermoplastic natural rubber reinforced with multi-walled carbon nanotubes. *Journal of Reinforced Plastics and Composites* 30.4 (2011), 363–368.
- [131] D. Ponnamma, R. Ramachandran, S. Hussain, R. Rajaraman, G. Amarendra, K. Varughese and S. Thomas. Free-volume correlation with mechanical and dielectric properties of natural rubber/multi walled carbon nanotubes composites. *Composites Part A: Applied Science and Manufacturing* 77 (2015), 164–171.
- [132] Y. Nakaramontri, C. Kummerlöwe, C. Nakason and N. Vennemann. The effect of surface functionalization of carbon nanotubes on properties of natural rubber/carbon nanotube composites. *Polymer Composites* 36.11 (2015), 2113–2122.
- [133] P. Keinänen, S. Siljander, M. Koivula, J. Sethi, E. Sarlin, J. Vuorinen and M. Kanerva. Optimized dispersion quality of aqueous carbon nanotube colloids as a function of sonochemical yield and surfactant/CNT ratio. *Heliyon* 4.9 (2018), e00787.
- [134] P. Keinänen, A. Das and J. Vuorinen. Further Enhancement of Mechanical Properties of Conducting Rubber Composites Based on Multiwalled Carbon Nanotubes and Nitrile Rubber by Solvent Treatment. *Materials* 11.10 (2018), 1806.
- [135] S. Siljander, P. Keinänen, A. Rätty, K. R. Ramakrishnan, S. Tuukkanen, V. Kunnari, A. Harlin, J. Vuorinen and M. Kanerva. Effect of surfactant type and sonication energy on the electrical conductivity properties of nanocellulose-CNT nanocomposite films. *International journal of molecular sciences* 19.6 (2018), 1819.

- [136] S. Siljander, P. Keinänen, A. Ivanova, J. Lehmonen, S. Tuukkanen, M. Kanerva and T. Björkqvist. Conductive cellulose based foam formed 3D shapes—From innovation to designed prototype. Vol. 12. 3. Multidisciplinary Digital Publishing Institute, 2019, 430.
- [137] J. Sethi, E. Sarlin, S. S. Meysami, R. Suihkonen, A. R. S. S. Kumar, M. Honkanen, P. Keinänen, N. Grobert and J. Vuorinen. The effect of multi-wall carbon nanotube morphology on electrical and mechanical properties of polyurethane nanocomposites. Vol. 102. Elsevier, 2017, 305–313.

PUBLICATIONS

PUBLICATION

I

Optimized dispersion quality of aqueous carbon nanotube colloids as a function of sonochemical yield and surfactant/CNT ratio

P. Keinänen, S. Siljander, M. Koivula, J. Sethi, E. Sarlin, J. Vuorinen and M. Kanerva

Heliyon 4.9 (2018), e00787

Publication reprinted with the permission of the copyright holders

Received:

29 March 2018

Revised:

6 July 2018

Accepted:

11 September 2018

Cite as: Pasi Keinänen, Sanna Siljander, Mikko Koivula, Jatin Sethi, Essi Sarlin, Jyrki Vuorinen, Mikko Kanerva. Optimized dispersion quality of aqueous carbon nanotube colloids as a function of sonochemical yield and surfactant/CNT ratio.

Heliyon 4 (2018) e00787.

doi: 10.1016/j.heliyon.2018.e00787



Optimized dispersion quality of aqueous carbon nanotube colloids as a function of sonochemical yield and surfactant/CNT ratio

Pasi Keinänen^{a,*}, Sanna Siljander^a, Mikko Koivula^a, Jatin Sethi^b, Essi Sarlin^a, Jyrki Vuorinen^a, Mikko Kanerva^a

^a Tampere University of Technology, Laboratory of Materials Science, P.O. Box 527, FIN-33101, Tampere, Finland

^b University of Oulu, Fiber and Particle engineering research unit, P.O. Box 4300, FIN-90014, Oulu, Finland

* Corresponding author.

E-mail address: pasi.keinanen@tut.fi (P. Keinänen).

Abstract

In this paper, we propose and verify a theoretical model of the development of dispersion quality of aqueous carbon nanotube (CNT) colloid as a function of sonochemical yield of the sonication process. Four different surfactants; Triton X-100, Pluronic F-127, CTAB and SDS were studied. From these four SDS had the lowest dispersion performance which was surprising. Optical dispersion quality results fits well with proposed theoretical model.

Keywords: Physical chemistry, Materials science

1. Introduction

There is one significant feature requiring attention when it comes to CNT-nanocomposites and colloids; a dispersion quality. Dispersion quality, i.e. dispersed nanotubes divided by the total number of nanotubes, has a huge impact on the effective surface area of the interaction between the matrix and the filler. In

order to optimize the performance one needs to know how to control the dispersion quality during each step of the manufacturing process.

CNTs forming large agglomerates creates challenges to process and stabilize colloids made of them. To optimize a dispersion process, enough energy density needs to be generated to overcome internal forces holding the aggregates together. Typical methods are shear-mixing [1] and sonication [2]. Of these two methods, sonication is superior especially for low viscosity systems where conventional mixing methods cannot create the required high strains rates. The dispersion process using sonication is based on inertial cavitation where imploding microscopic cavities generate intensive streams of molecules with high energy densities inside the liquid. Cavities are known to preferably exist at the boundaries of different materials [3] which makes sonication a very effective and precise method for dispersing nanotubes. Prolonged sonication however can cause damages to the tubes and must be avoided [4].

After the CNTs have been detached from aggregates, there is a possibility of re-agglomeration. To stabilize the system in water based dispersions, different types of surfactants such as ionic (anionic and cationic), non-ionic, polymer based and their combinations have been used comprising current state-of-the-art [5,6,7,8, 9,10,11,12,13,14,15,16,17,18,19,20,21,22,23,24,25,26,27,28]. The basic idea is to enable surfactant molecules to be adsorbed on the surface of CNTs via hydrophobic interactions, π - π bonds, hydrogen bonds or electrostatic interactions [29,30].

The nanotube dispersing efficiency of surfactants is linked to the length of an alkyl chain of the surfactant, presence of benzene ring, and the functional (terminal) group [10], concentration [22] and charge [31]. An optimum surfactant-CNT weight ratio has been reported to vary, ranging from 1:1 to 1:10 [10,32]. It has been reported that an efficient CNT dispersion is possible only when the surfactant concentration is above the CMC value [27,33,34,35]. It has also been reported that dispersing agents can form stable dispersions below and equal to their CMC limit [5,7,12,36]. Moreover, it has been noted that the best result can be reached with a concentration of 0.5 CMC, and that any further increases in the concentration of the surfactant has only a minor effect [36]. Even with a absence of consensus using too high surfactant concentration may affect the properties of CNT network in the end product, using too low surfactant concentration can cause re-aggregation in colloid since a sufficient amount is needed to cover all CNT surfaces [32].

During the sonication, there is a dynamic equilibrium of concentrations between individual, surfactant coated nanotubes and nanotube agglomerates. As more energy is brought into the system, more nanotubes are being detached from the agglomerates and a dispersion quality is approaching unity. There are number of methods available for studying the quality of CNT-dispersions and they include; atomic force microscopy (AFM) [10], transmission electron microscopy (TEM) [32], Raman

spectroscopy [37] and UV-Vis spectroscopy [38]. Of these methods, UV-Vis spectroscopy has been shown to represent the most accessible and versatile method to determine the dispersion quality of CNT dispersions especially for liquid systems. In the method, the light passing through a sample of colloid experiences scattering and absorbance. Both of these phenomena scale linearly with the concentration of colloidal particles and, therefore, the opacity α of the dispersion can be used to measure the number of nanotubes (individual tubes or dispersed small aggregates) in the supernatant [23]. At a fixed wavelength, UV-Vis spectroscopy can be used to determine the onset point of α as a function of the applied acoustic sonication energy. At this point, the system is close to its optimal dispersion state and further sonication would only damage the nanotubes without improving the quality of the dispersion.

In the previous studies the parameters to describe sonication have been total energy and time [38,39]. These parameters work well with specific processes but are insufficient for comparing different studies since different sonication systems have different yields of transforming electrical energy to acoustic energy and individual systems also produce different amounts of inertial cavitation (vs. non-inertial). Inertial cavitation is mainly responsible of exfoliation of nanotubes whereas non-inertial cavitation is related to surface damages of the tubes [40]. In order to generalize all types of sonication systems parameter of sonochemical yield should be used; like first proposed by Koda et al. [41].

This article introduces theoretical framework for controlling the dispersion quality of aqueous carbon nanotube colloids during a sonication process. This framework is indifferent towards the sonication system, used energies and times.

2. Theory

We propose that for an ultrasound system, where the re-agglomeration of carbon nanotubes is inhibited by using surfactants the rate of opacity increase is related to effective acoustic energy in a following way:

$$\frac{d\alpha}{dE} = (\alpha_{max} - \alpha)f \quad (1)$$

where E is the effective acoustic energy divided by CNT mass, α_{max} is the maximum achievable opacity of the system and f is a shape function. By separation we arrive to

$$\frac{d\alpha}{(\alpha_{max} - \alpha)} = f dE \quad (2)$$

Integration, rearrangement, and then using both sides as exponents e^x leads to

$$\alpha = \alpha_{max} - C e^{-\int f dE} \quad (3)$$

For a system where f is a positive constant, and by applying boundary conditions, $\alpha(0) = 0$ and $\lim_{E \rightarrow \infty} \alpha(E) = \alpha_{max}$, α can be expressed as

$$\alpha(E) = \alpha_{max}(1 - e^{-\kappa E}) \quad (4)$$

where, κ is a system-specific constant related to the types and quantities of the chemical components in the colloid.

In order to generalize (4) for all types of sonication systems, sonochemical yield is used instead of energy. In our experiments we used the concentration of iodine-ions I_3^- divided by CNT mass, $C_{I_3^-}$ as a parameter [42].

It is known that sonolysis of water produces hydrogen peroxide H_2O_2 via hydroxyl and hydrogen radicals and it causes oxidation of $2I^-$ to I_2 from dissolved potassium iodide. I_2 then reacts with I^- to produce I_3^- , which has a peak absorbance at 355 nm and which can be detected by using UV-vis spectroscopy. The method, also known as Weessler reaction, has been proposed to be used as a standard method for the calibration of sonication systems [41]. The chain of chemical reactions is induced only by inertial cavitation, which is mainly responsible of the de-agglomeration of CNT aggregates. Therefore, Weessler reaction can be used to measure and compare effective dispersive processes of different sonication systems.

Thus, using $C_{I_3^-}$ with Equation (4), it leads to

$$\alpha(C_{I_3^-}) = \alpha_{max}(1 - e^{-\kappa C_{I_3^-}}) \quad (5)$$

where the value of $C_{I_3^-}$ is determined based on an experimental graph of electrical energy E_e versus concentration of iodine-ions.

For determination of sonochemical yield of I_3^- versus electrical energy consumed by the sonicator concentrations of I_3^- were analyzed using the Beer-Lambert law

$$\alpha = \epsilon bc \quad (6)$$

where α is the absorbance, ϵ is the molar attenuation coefficient of I_3^- , b is the length of the optical path (in cm), and c is the concentration of I_3^- . Linear fitting was used to interpolate I_3^- production as a function of electrical energy and slope of the fitting was used to calculate values for the sonochemical yield.

3. Materials & methods

3.1. Materials

In this study, we used Nanocyl7000 multiwall carbon nanotubes (Nanocyl SA., Sambreville, Belgium) and four different surfactants: octyl phenol ethoxylate (Triton

X-100), polyoxyethylene-polyoxypropylene block co-polymer (Pluronic F-127), sodium dodecyl sulfate (SDS) and cetyltrimethylammonium bromide (CTAB), all from Sigma Aldrich (Merck KGaA, Darmstadt, Germany). For the Weissler reaction potassium iodide (KI) (Merck KGaA, Darmstadt, Germany) was used.

3.2. Weissler reaction

For determination of sonochemical yield of I_3^- versus electrical energy consumed by the sonicator, 200 ml of 0.1M KI solution was sonicated using different total energies and corresponding concentrations of I_3^- were detected by measuring I_3^- specific absorbance with Shimadzu UV-1800 spectrophotometer (Shimadzu Corp., Kyoto, Japan).

3.3. Dispersion of carbon nanotubes

160 samples with 0.40 ± 0.01 g of Nanocyl NC 7000 multiwall carbon nanotubes, four different surfactants (Triton X100, Pluronic F-127, CTAB, and SDS) with four different surfactant masses (0.1 ± 0.01 g, 0.2 ± 0.01 g, 0.4 ± 0.01 g and 0.8 ± 0.01 g) and deionized water were weighed in 100 ml glass beakers so that all samples weighted 80 ± 0.1 g. Dispersions were sonicated using 10 different electrical energies with QSonica Q700 sonicator (Qsonica L.L.C, Newtown, USA). A 12.7 mm diameter titanium probe was used and the vibration amplitude of a sonotrode was set to 60 μm . To guarantee identical sample preparation throughout the series, the tip was always placed in the same position inside the beaker ($15 \text{ mm} \pm 2 \text{ mm}$ from the bottom) and an external cooling bath with c. 200 W cooling capacity was used to limit the temperature variations during the sonication. The applied acoustic energy was varied by controlling the sonication time and it was monitored by an internal calorimeter of the QSonica Q700 sonicator. A power reading given by the sonicator remained between 100–120 W for all the sonications. An opacity at 500 nm, directly related to the concentration of carbon nanotubes in the dispersed state, was used to measure the quality of the sonicated dispersions. A portion of each dispersion was collected, let settle for five days, and its supernatant was diluted with to 1:300 with deionized water to get the solutions transparent. The opacity of the diluted dispersions were measured by using Shimadzu UV-1800 spectrophotometer and plastic cuvettes with 1 cm optical path length.

3.4. Imaging

The CNT agglomerate size was evaluated by drying a droplet of the dispersions on a metal plate and characterizing them by scanning electron microscopy (FIB-SEM, Zeiss Crossbeam 540).

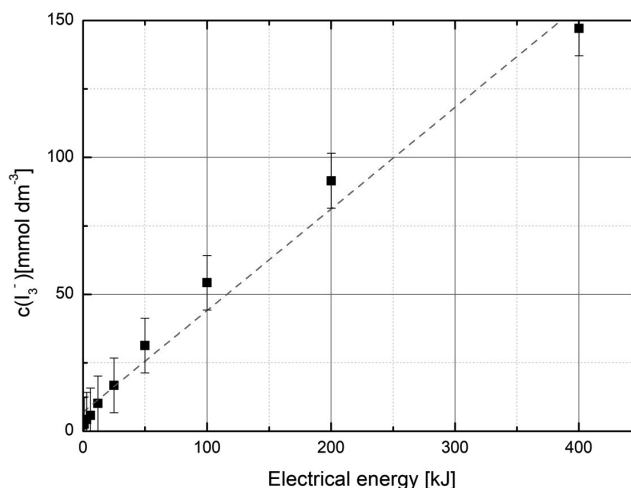


Figure 1. Concentration of I_3^- as a function of electrical energy E_{el} used by the sonicator. The sonochemical yield/energy for this particular sonication system was $0.371 \text{ mmol dm}^{-3} \text{ kJ}^{-1}$. An error from sample preparation and measurements were estimated to be $\pm 10 \text{ mmol dm}^{-3}$.

4. Results

4.1. Weissler reaction

Figure 1 shows the development of I_3^- concentration as a function of electrical energy consumed by the sonicator. It can be observed that the production rate was higher in the beginning of the sonication. This is caused by the dissolved gases, which accelerate the hydrogen peroxide production by participating in the chemical reactions (oxygen) and by lowering the inertial cavitation threshold [43]. After dissolved gases have fully diffused and consumed by the process, the rate of I_3^- conversion slightly slows down. Linear fitting still gives a good approximation for $C(I_3^-)$ versus E_e and was used in all future calculations.

4.2. Dispersion of CNTs

As the applied sonication energy gets higher, the supernatant of the dispersion becomes darker indicating an increase in the concentration of CNTs in dispersed state (Figure 2). The dark appearance was found to be stable up to several weeks.

Figure 3 shows that the opacity at 500 nm follows the proposed dependence on sonochemical yield (5). It can be seen that Triton X-100 and CTAB can disperse CNTs close to the maximum dispersion quality at a lower surfactant/CNT mass ratios compared to Pluronic F-127 and SDS. It is also evident that the acoustic energy required to disperse CNTs with SDS is significantly higher compared to others,

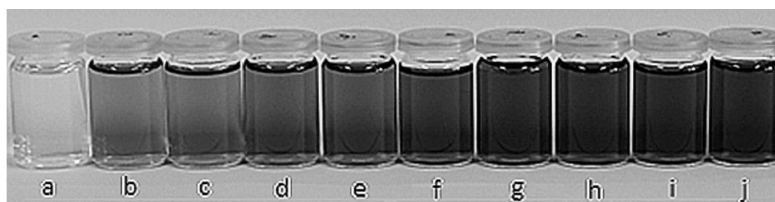


Figure 2. Series of diluted supernatants of CNT-dispersions corresponding different acoustic energies of sonication. Evolution of the dispersion quality can be seen from samples a to j. As solutions get darker, more individual nanotubes are being dispersed in to the liquid.

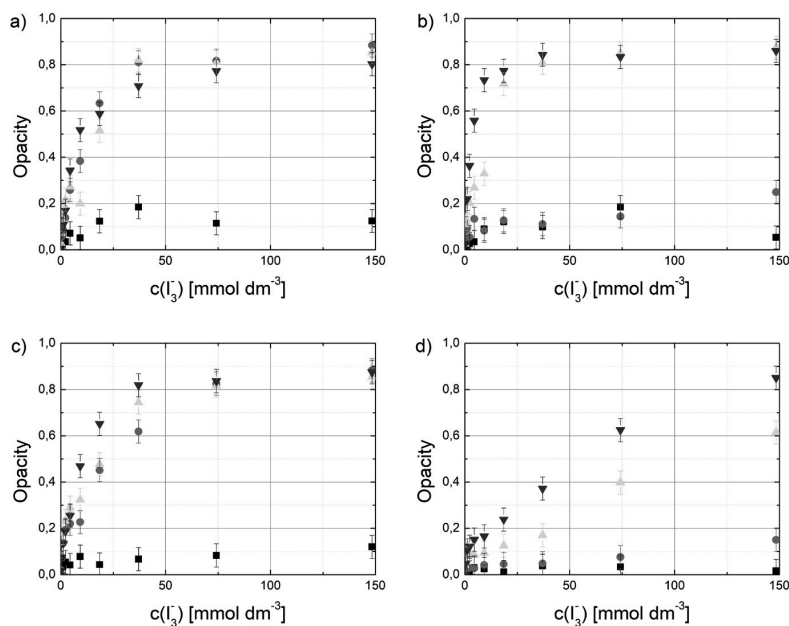


Figure 3. The development of opacity as a function of $C(I_3)$ with different surfactant/CNT ratios: ■ 1:4, ● 1:2, ▲ 1:1 and ▼ 2:1 for a) Triton X-100, b) Pluronic F-127, c) CTAB and d) SDS.

and that the rate of development of dispersion quality is respectively lower. This is somewhat surprising since SDS is widely used in many of the reported studies and yet it seems to be more difficult to use in order to optimize the dispersion quality.

In Figure 4, a fitted opacity function (5) gives a theoretical asymptote for the maximum opacity, α_{max} , with a theoretical infinite yield. Possible deviations from (5) with higher yields are due to the fracture (damage) of CNTs as the sonication progresses causing additional opacity, which is not related to the surfactant-assisted exfoliation of the aggregates.

In Figure 5 it can be seen that investigating dispersion quality with dried samples is rather challenging. One can say that larger agglomerates do disappear as a function

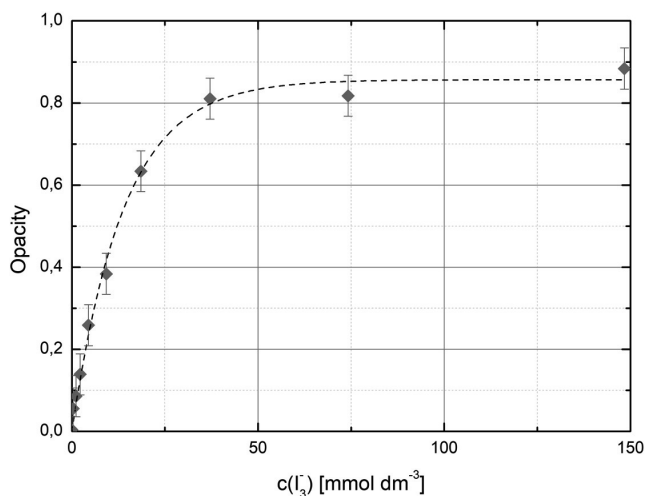


Figure 4. Measured opacity of sonicated 1:2 Triton X-100/CNT dispersion as a function of sonochemical yield of the sonicator together with a fitted opacity function (5).

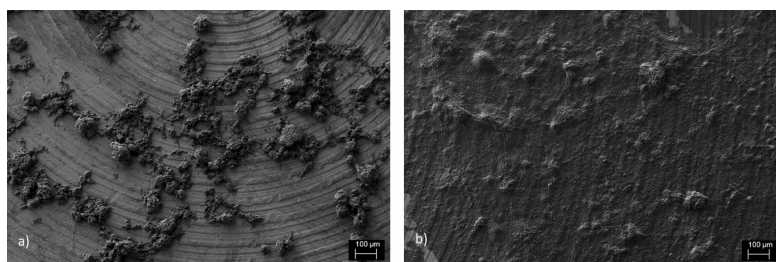


Figure 5. FIB images of dried 1:2 Triton X-100/CNT dispersions. a) Non-sonicated and b) sonicated with maximum opacity. It can be seen that most of the large agglomerates have been dispersed and the metal plate is coated with individual CNTs. Still some larger particles exist.

of sonochemical yield, but calculating a number describing the dispersion quality is basically impossible. Dried sample for FIB microscopy is not an accurate 2D presentation of the 3D situation. During the drying process the surface tension of water affects how 2D-structure is being formed. Therefore SEM or FIB microscopy is not optimal for studying dispersion quality of water based CNT colloids.

Variation of maximum absorbance can be seen for different surfactant/CNT ratios depending on the surfactant type (Figure 6). It is noticeable that there is a sharp change in the development of the maximum opacity as the surfactant/CNT ratio increases. Below this threshold value of surfactant/CNT ratio, the highest reachable opacity (indicating the maximum dispersion quality) is to be low. On the other hand, when the ratio matches the threshold value, the maximum opacity gets also rapidly reached and further increase in the ratio does not improve the dispersion. For applications where surfactant assisted dispersions are necessary, the determination

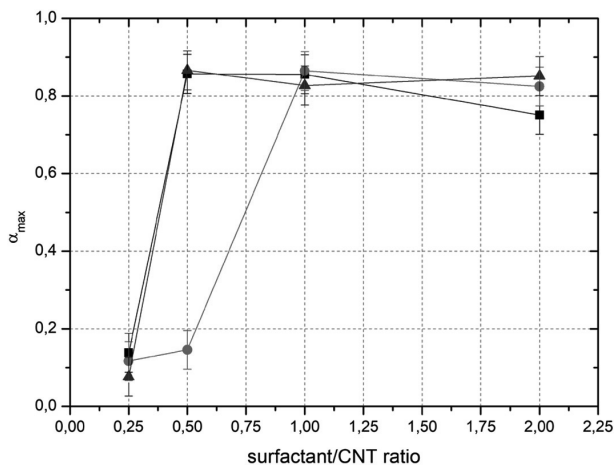


Figure 6. Measured maximum opacities as a function of surfactant/CNT ratio for three different surfactants; ■ Triton X-100, ● Pluronic F-127 and ▲ CTAB.

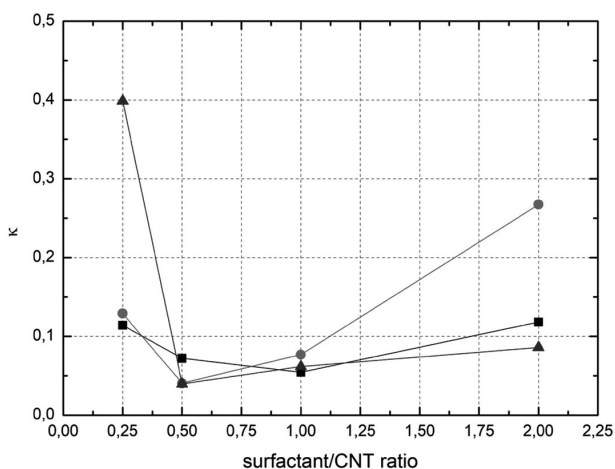


Figure 7. The factor κ , indicating a growth speed of the opacity as a function of surfactant/CNT for ■ Triton X-100, ● Pluronic F-127 and ▲ CTAB.

of an optimum surfactant ratio is critical since excess surfactant remaining, for example in a nanocomposite matrix, will diminish the physical properties. SDS is not included in Figure 6 since the applied acoustic energy range was not high enough to reach the saturation in the opacity. SDS was the only surfactant which did not reach saturation point of the opacity with used energies even with highest concentrations. All sonications except the lowest concentration of SDS were above critical micelle concentration.

The factor κ in Equation (5), indicating the rate of opacity increase as a function of acoustic energy, is implicitly dependent on the surfactant/CNT ratio (Figure 7).

κ can be observed to have a different local minimum for different surfactants, which is most likely related to the adsorption mechanism of the surfactant on the CNT surface. Depending on surfactant concentration, the assembly on the CNT surface is different. The tendency to improve the dispersion along with the increase in the acoustic energy is weaker the stronger is the surfactant layers internal binding on the initial agglomerates. Also, the response in the acoustic energy transfer by the surfactant layer can hinder the CNT agglomerate dispersion yet it is challenging to theoretically verify the difference in this response between different surfactants.

5. Conclusions

A theoretical equation for a development of the dispersion quality of aqueous CNT colloid as a function of sonochemical yield was proposed. Sonication experiments with four different surfactant types and different surfactant/CNT ratios and inertial cavitation activities were performed. The inertial cavitation activity was determined using the Weisser reaction. It was shown that the proposed equation fits well with the performed measurements and that the maximum opacities, received via fitting the equations, follows an S-curve as a function of surfactant/CNT ratio. The revealed sonochemical yield-dispersion (SCY-D) relation indicates that there is a threshold for the minimum surfactant/CNT ratio to achieve the optimal dispersion quality for a CNT-surfactant system. Here, we determined the lower and upper values of the threshold region of surfactant/CNT ratios for three different surfactants, namely Triton X-100, Pluronic F-127, and CTAB.

Declarations

Author contribution statement

Pasi Keinänen – Conceived and designed the experiments; Performed the experiments; Analyzed and interpreted the data; Contributed reagents, materials, analysis tools or data; Wrote the paper.

Sanna Siljander – Conceived and designed the experiments; Performed the experiments; Wrote the paper.

Mikko Koivula, Essi Sarlin – Performed the experiments.

Jatin Sethi, Jyrki Vuorinen, Mikko Kanerva: Analyzed and interpreted the data.

Funding statement

This research did not receive any specific grant from funding agencies in the public, commercial, or not-for-profit sectors.

Competing interest statement

The authors declare no conflict of interest.

Additional information

No additional information is available for this paper.

References

- [1] R. Andrews, D. Jacques, M. Minot, T. Rantell, Fabrication of carbon multiwall nanotube/polymer composites by shear mixing, *Macromol. Mater. Eng.* 287 (6) (2002) 395–403.
- [2] Y. Huang, E. Terentjev, Dispersion and rheology of carbon nanotubes in polymers, *Int. J. Mater. Forming* 1 (2) (2008) 63–74.
- [3] I. Lavilla, C. Bendicho, Fundamentals of ultrasound-assisted extraction, in: *Water Extraction of Bioactive Compounds*, Elsevier, 2018, pp. 291–316.
- [4] D.-Q. Yang, J.-F. Rochette, E. Sacher, Functionalization of multiwalled carbon nanotubes by mild aqueous sonication, *J. Phys. Chem. B* 109 (16) (2005) 7788–7794.
- [5] J.-M. Bonard, T. Stora, J.-P. Salvetat, F. Maier, T. Stöckli, C. Duschl, L. Forró, W.A. de Heer, A. Châtelain, Purification and size-selection of carbon nanotubes, *Adv. Mater.* 9 (10) (1997) 827–831.
- [6] L. Vaisman, G. Marom, H.D. Wagner, Dispersions of surface-modified carbon nanotubes in water-soluble and water-insoluble polymers, *Adv. Funct. Mater.* 16 (3) (2006) 357–363.
- [7] Y. Geng, M.Y. Liu, J. Li, X.M. Shi, J.K. Kim, Effects of surfactant treatment on mechanical and electrical properties of CNT/epoxy nanocomposites, *Composites, Part A, Appl. Sci. Manuf.* 39 (12) (2008) 1876–1883.
- [8] J. Rausch, R.-C. Zhuang, E. Mäder, Surfactant assisted dispersion of functionalized multi-walled carbon nanotubes in aqueous media, *Composites, Part A, Appl. Sci. Manuf.* 41 (9) (2010) 1038–1046.

- [9] S. Javadian, A. Motae, M. Sharifi, H. Aghdastinat, F. Taghavi, Dispersion stability of multi-walled carbon nanotubes in cationic surfactant mixtures, *Colloids Surf. A, Physicochem. Eng. Asp.* 531 (2017) 141–149.
- [10] M. Islam, E. Rojas, D. Bergey, A. Johnson, A. Yodh, High weight fraction surfactant solubilization of single-wall carbon nanotubes in water, *Nano Lett.* 3 (2) (2003) 269–273.
- [11] T.J. McDonald, C. Engtrakul, M. Jones, G. Rumbles, M.J. Heben, Kinetics of PL quenching during single-walled carbon nanotube rebundling and diameter-dependent surfactant interactions, *J. Phys. Chem. B* 110 (50) (2006) 25339–25346.
- [12] M. Bystrzejewski, A. Huczko, H. Lange, T. Gemming, B. Büchner, M. Rummeli, Dispersion and diameter separation of multi-wall carbon nanotubes in aqueous solutions, *J. Colloid Interface Sci.* 345 (2) (2010) 138–142.
- [13] B. Vigolo, A. Penicaud, C. Coulon, C. Sauder, R. Paillet, C. Journet, P. Bernier, P. Poulin, Macroscopic fibers and ribbons of oriented carbon nanotubes, *Science* 290 (5495) (2000) 1331–1334.
- [14] M.J. O'connell, S.M. Bachilo, C.B. Huffman, V.C. Moore, M.S. Strano, E.H. Haroz, K.L. Rialon, P.J. Boul, W.H. Noon, C. Kittrell, Band gap fluorescence from individual single-walled carbon nanotubes, *Science* 297 (5581) (2002) 593–596.
- [15] P. Poulin, B. Vigolo, P. Launois, Films and fibers of oriented single wall nanotubes, *Carbon* 40 (10) (2002) 1741–1749.
- [16] L. Jiang, L. Gao, J. Sun, Production of aqueous colloidal dispersions of carbon nanotubes, *J. Colloid Interface Sci.* 260 (1) (2003) 89–94.
- [17] V.C. Moore, M.S. Strano, E.H. Haroz, R.H. Hauge, R.E. Smalley, J. Schmidt, Y. Talmon, Individually suspended single-walled carbon nanotubes in various surfactants, *Nano Lett.* 3 (10) (2003) 1379–1382.
- [18] K. Yurekli, C.A. Mitchell, R. Krishnamoorti, Small-angle neutron scattering from surfactant-assisted aqueous dispersions of carbon nanotubes, *J. Am. Chem. Soc.* 126 (32) (2004) 9902–9903.
- [19] T. Chatterjee, K. Yurekli, V.G. Hadjiev, R. Krishnamoorti, Single-walled carbon nanotube dispersions in poly (ethylene oxide), *Adv. Funct. Mater.* 15 (11) (2005) 1832–1838.
- [20] T. Hertel, A. Hagen, V. Talalaev, K. Arnold, F. Hennrich, M. Kappes, S. Rosenthal, J. McBride, H. Ulbricht, E. Flahaut, Spectroscopy of single-

- and double-wall carbon nanotubes in different environments, *Nano Lett.* 5 (3) (2005) 511–514.
- [21] N. Grossiord, J. Loos, L. Van Laake, M. Maugey, C. Zakri, C.E. Koning, A.J. Hart, High-conductivity polymer nanocomposites obtained by tailoring the characteristics of carbon nanotube fillers, *Adv. Funct. Mater.* 18 (20) (2008) 3226–3234.
- [22] A.J. Blanch, C.E. Lenehan, J.S. Quinton, Optimizing surfactant concentrations for dispersion of single-walled carbon nanotubes in aqueous solution, *J. Phys. Chem. B* 114 (30) (2010) 9805–9811.
- [23] M.D. Clark, S. Subramanian, R. Krishnamoorti, Understanding surfactant aided aqueous dispersion of multi-walled carbon nanotubes, *J. Colloid Interface Sci.* 354 (1) (2011) 144–151.
- [24] A. Ryabenko, L. Fokeeva, T. Dorofeeva, Spectroscopic study of suspensions of single-wall carbon nanotubes in polyaniline solutions in *N*-methylpyrrolidone in UV–Vis–NIR regions, *Russ. Chem. Bull.* 53 (12) (2004) 2695–2699.
- [25] M.-J. Jiang, Z.-M. Dang, S.-H. Yao, J. Bai, Effects of surface modification of carbon nanotubes on the microstructure and electrical properties of carbon nanotubes/rubber nanocomposites, *Chem. Phys. Lett.* 457 (4) (2008) 352–356.
- [26] R. Rastogi, R. Kaushal, S. Tripathi, A.L. Sharma, I. Kaur, L.M. Bharadwaj, Comparative study of carbon nanotube dispersion using surfactants, *J. Colloid Interface Sci.* 328 (2) (2008) 421–428.
- [27] Y. Bai, D. Lin, F. Wu, Z. Wang, B. Xing, Adsorption of triton x-series surfactants and its role in stabilizing multi-walled carbon nanotube suspensions, *Chemosphere* 79 (4) (2010) 362–367.
- [28] I. Madni, C.-Y. Hwang, S.-D. Park, Y.-H. Choa, H.-T. Kim, Mixed surfactant system for stable suspension of multiwalled carbon nanotubes, *Colloids Surf. A, Physicochem. Eng. Asp.* 358 (1) (2010) 101–107.
- [29] Y. Bai, I.S. Park, S.J. Lee, T.S. Bae, F. Watari, M. Uo, M.H. Lee, Aqueous dispersion of surfactant-modified multiwalled carbon nanotubes and their application as an antibacterial agent, *Carbon* 49 (11) (2011) 3663–3671.
- [30] K. Yang, B. Xing, Adsorption of organic compounds by carbon nanomaterials in aqueous phase: Polanyi theory and its application, *Chem. Rev.* 110 (10) (2010) 5989–6008.
- [31] W. Wenseleers, I.I. Vlasov, E. Goovaerts, E.D. Obraztsova, A.S. Lobach, A. Bouwen, Efficient isolation and solubilization of pristine single-walled nanotubes in bile salt micelles, *Adv. Funct. Mater.* 14 (11) (2004) 1105–1112.

- [32] J. Yu, N. Grossiord, C.E. Koning, J. Loos, Controlling the dispersion of multi-wall carbon nanotubes in aqueous surfactant solution, *Carbon* 45 (3) (2007) 618–623.
- [33] S. Utsumi, M. Kanamaru, H. Honda, H. Kanoh, H. Tanaka, T. Ohkubo, H. Sakai, M. Abe, K. Kaneko, RBM band shift-evidenced dispersion mechanism of single-wall carbon nanotube bundles with NaDDBs, *J. Colloid Interface Sci.* 308 (1) (2007) 276–284.
- [34] Z. Sun, V. Nicolosi, D. Rickard, S.D. Bergin, D. Aherne, J.N. Coleman, Quantitative evaluation of surfactant-stabilized single-walled carbon nanotubes: dispersion quality and its correlation with zeta potential, *J. Phys. Chem. C* 112 (29) (2008) 10692–10699.
- [35] L. Maillaud, C. Zakri, I. Ly, A. Pénicaud, P. Poulin, Conductivity of transparent electrodes made from interacting nanotubes, *Appl. Phys. Lett.* 103 (26) (2013) 263106.
- [36] P. Angelikopoulos, A. Gromov, A. Leen, O. Nerushev, H. Bock, E.E. Campbell, Dispersing individual single-wall carbon nanotubes in aqueous surfactant solutions below the cmc, *J. Phys. Chem. C* 114 (1) (2009) 2–9.
- [37] K. Shen, S. Curran, H. Xu, S. Rogelj, Y. Jiang, J. Dewald, T. Pietrass, Single-walled carbon nanotube purification, pelletization, and surfactant-assisted dispersion: a combined TEM and resonant micro-Raman spectroscopy study, *J. Phys. Chem. B* 109 (10) (2005) 4455–4463.
- [38] N. Grossiord, O. Regev, J. Loos, J. Meuldijk, C.E. Koning, Time-dependent study of the exfoliation process of carbon nanotubes in aqueous dispersions by using UV-visible spectroscopy, *Anal. Chem.* 77 (16) (2005) 5135–5139.
- [39] P. Alafogianni, K. Dassios, S. Farmaki, S. Antiohos, T. Matikas, N.-M. Barkoula, On the efficiency of UV-vis spectroscopy in assessing the dispersion quality in sonicated aqueous suspensions of carbon nanotubes, *Colloids Surf. A, Physicochem. Eng. Asp.* 495 (2016) 118–124.
- [40] A. Sesis, M. Hodnett, G. Memoli, A.J. Wain, I. Jurewicz, A.B. Dalton, J.D. Carey, G. Hinds, Influence of acoustic cavitation on the controlled ultrasonic dispersion of carbon nanotubes, *J. Phys. Chem. B* 117 (48) (2013) 15141–15150.
- [41] S. Koda, T. Kimura, T. Kondo, H. Mitome, A standard method to calibrate sonochemical efficiency of an individual reaction system, *Ultrason. Sonochem.* 10 (3) (2003) 149–156.

- [42] A. Weissler, H.W. Cooper, S. Snyder, Chemical effect of ultrasonic waves: oxidation of potassium iodide solution by carbon tetrachloride, *J. Am. Chem. Soc.* 72 (4) (1950) 1769–1775.
- [43] C. Petrier, M.-F. Lamy, A. Francony, A. Benahcene, B. David, V. Renaudin, N. Gondrexon, Sonochemical degradation of phenol in dilute aqueous solutions: comparison of the reaction rates at 20 and 487 kHz, *J. Phys. Chem.* 98 (41) (1994) 10514–10520.

PUBLICATION

II

**Further Enhancement of Mechanical Properties of Conducting Rubber
Composites Based on Multiwalled Carbon Nanotubes and Nitrile Rubber by
Solvent Treatment**

P. Keinänen, A. Das and J. Vuorinen

Materials 11.10 (2018), 1806

Publication reprinted with the permission of the copyright holders

Article

Further Enhancement of Mechanical Properties of Conducting Rubber Composites Based on Multiwalled Carbon Nanotubes and Nitrile Rubber by Solvent Treatment

Pasi Keinänen ^{1,*} , Amit Das ^{1,2}  and Jyrki Vuorinen ¹ 

¹ Tampere University of Technology, Laboratory of Materials Science P.O. Box 527, FI-33101 Tampere, Finland; das@ipfdd.de (A.D.); jyrki.vuorinen@tut.fi (J.V.)

² Leibniz Institute of Polymer Research Dresden, P.O. Box 120 411, D-01005 Dresden, Germany

* Correspondence: pasi.keinanen@tut.fi; Tel.: +358-404-404-355

Received: 3 September 2018; Accepted: 21 September 2018; Published: 23 September 2018



Abstract: Post-treatment removal of dispersion agents from carbon nanotube/rubber composites can greatly enhance the mechanical properties by increasing the filler–matrix interaction. In this study, multiwall carbon nanotubes (MWNT) were dispersed in water by sonication and nonionic surfactant, octyl-phenol-ethoxylate was used as a dispersion agent. The dispersed MWNTs were incorporated in thermo-reactive acrylonitrile butadiene rubber (NBR) latex and nanocomposite films were prepared by solution casting. As a post-treatment, the surfactant was removed with acetone and films were dried in air. Dispersion quality of the colloid before casting was determined, and mechanical, electrical and thermal properties of the composites before and after the acetone post-treatment were studied. It was found that removal of dispersion agent increased the storage modulus of films between 160–300% in all samples. Relative enhancement was greater in samples with better dispersion quality, whereas thermal conductivity changed more in samples with smaller dispersion quality values. Electrical properties were not notably affected.

Keywords: CNT; NBR; nanocomposite; dispersion; post-treatment

1. Introduction

Elastomers are being reinforced with several different types of fillers to improve their mechanical, electrical and thermal properties. Typical fillers include sub-micron carbonaceous particles or silica depending on the application. There are many factors influencing the enhancements in composite properties including size distribution of the particles, aspect ratio, dispersion quality and adhesion to the matrix.

In last two decades, there has been a great effort to introduce novel nanosized particles in to elastomer matrices. These include nano-silica [1], organo-clays [2] and carbon with different morphologies like carbon nanotubes, graphene, etc. In theoretical speculations, one of the most promising nanosized fillers are carbon nanotubes (CNT) [3] due to their geometrical structure and intrinsic mechanical and electrical properties. Despite the high expectations, there have been many challenges in realizing their potential as filler in soft rubber matrix including achieving proper dispersion, mixing technology, no standard specification about the quality and type of the tubes.

Compared to many other fillers, carbon nanotubes forming large agglomerates are more challenging to use. To optimize the dispersion process, enough energy density needs to be generated to overcome internal forces holding the aggregates together. Typical methods include shear-mixing [4,5], and sonication [5,6]. From these, the sonication is superior especially in low viscosity systems

where conventional mixing methods cannot create required high strain rates. The dispersion process using sonication is based on inertial cavitation where imploding microscopic cavities are generating intensive streams of molecules, which again creates high strain rates and energy densities inside the liquid, enough to break nanotube agglomerates in to smaller aggregates and detach individual tubes. These cavities are also known to preferably exist on boarder lines of different materials, which make sonication a very effective and precise method for dispersing nanosize particles [7]. It is important to optimize the sonication process since prolonged sonication however can cause damage and alter the properties of the tubes [8,9]

After the nanotubes have been detached from aggregates, there is a high possibility of re-agglomeration. To stabilize the system different types of surfactants are being used including sodium dodecyl sulfate (SDS) [10], sodium dodecylbenzene sulfonate (SDBS) [11] and octyl phenol ethoxylate (TritonX-100) [10]. Molecules act as buffers between separated nanotubes preventing their re-agglomeration since van der Waals forces, responsible for the phenomena, is decreasing very rapidly as a function of distance. Surfactants are therefore essential in stabilizing and improving a dispersion quality of the colloids, a factor greatly affecting the properties of many applications. However, they can also inhibit the physical interactions between fillers and the matrix in processed nanocomposites.

Reinforcing the matrix is directly related to good adhesion and to the percolating contact area of the individual nanotubes and therefore wrapping the tubes with surfactants constrains the enhancements. Different procedures have been presented to remove the excess surfactant after nanocomposite structures were manufactured including: nitric acid [12], Fenton reaction [13], photocatalysis [13], organic solvents [14] and water rinsing [15]. Most of the studies were performed on transparent conducting thermoplastic films or on cellulose structures and very little information is found regarding elastomer composites.

In this paper, we demonstrate a simple method to enhance physical properties of NBR/CNT nanocomposite films by removing the surfactant from the matrix with acetone. It was found that removal of dispersion agent increased the storage modulus of films over 150% in all samples. Relative enhancement was greater in samples with better dispersion quality. In addition, thermal conductivity increased by over 100% with lower dispersion quality samples. Electrical properties were not notably affected.

2. Materials and Methods

2.1. Materials

Aqueous dispersion of thermoreactive butadiene acrylonitrile copolymer (Litex®N2890, Synthomer plc, London, UK) was used to cast a matrix (Table 1), multiwall carbon nanotube powder (NC7000™, Nanocyl SA., Sambreville, Belgium) was used as a filler (Table 2) and octyl phenol ethoxylate (Triton X-100, Merck KGaA, Darmstadt, Germany) was used as a dispersion agent.

Table 1. Physical properties of Litex®N2890 LATEX.

Property	Value	Unit	Method
Solids content	41.0	%	ISO 124
pH	7.3	-	ISO 976
Viscosity	<100	mPas	ISO 1652
Surface tension	31.9	mNm ⁻¹	DIN 1409

Table 2. Physical properties of NC7000TM carbon nanotubes.

Property	Value	Unit	Method
Average diameter	10	nm	TEM
Average length	1.5	μm	TEM
Carbon purity	90	%	TGA
Transitional metal oxide	<1	%	ICP-MS
Surface area	250–300	m ² g ⁻¹	BET

2.2. Dispersion of Carbon Nanotubes

Fifteen samples with 0.40 ± 0.02 g of NC7000TM multiwall carbon nanotubes, 0.40 ± 0.02 g of Triton X-100 and 79.20 ± 0.01 of deionized water was weighed in 100 mL glass beakers and sonicated using different acoustic energies. A concentration of carbon nanotubes was selected to be low enough to avoid dramatic increase in viscosity as CNTs start to disperse. Increase in viscosity would otherwise increase the acoustic resistance which could diminish the dispersive power of the process. For sonication, a tip sonicator (QSonica Q700, QSonica L.L.C, Newton, CT, USA) with 12.7 mm diameter titanium probe and vibration amplitude of 120 μm was used. To guarantee identical sample preparation, the tip was always placed in the same position inside the beaker ($15 \text{ mm} \pm 2 \text{ mm}$ from the bottom) and external cooling bath with c. 200 W cooling capacity was used to limit the temperature variations during the sonication. Acoustic energy was monitored by internal calorimeter of the QSonica Q700 device and varied by controlling the sonication time. An acoustic power reading given by the sonicator remained between 110–140 W in all sonications.

2.3. UV-VIS Measurements

An opacity at 500 nm, directly related to a concentration of carbon nanotubes in dispersed state, was used to measure the quality of the sonicated MWNT-dispersions in water [16]. A portion of each dispersion was collected, settled for five days and its supernatant diluted with deionized water with the ratio of 1:300 to get the solutions transparent. The absorbance of the diluted dispersions was measured with spectrophotometer (Shimadzu UV-1800, Shimadzu Corp., Kyoto, Japan) using quartz cuvettes.

2.4. Casting of NBR/CNT Nanocomposites

After the dispersion quality as a function of sonication energy for MWNT dispersion was determined, selected colloids were prepared for casting. Five samples of 61.5 ± 0.1 g of CNT-solution with different dispersion qualities were mixed with 6.0 ± 0.1 g of NBR copolymer latex and left to dry for 72 h in flat 120×120 mm size acrylic molds. After drying, the films were cross-linked by heat in an oven for 3 h 100°C . A CNT concentration in all samples was the same, 12.5 ± 0.3 phr and average thickness of the films was 200 ± 20 μm. The concentration was chosen to be higher than a percolation threshold of NC7000TM carbon nanotubes [17]. To remove surfactants as a post-treatment from the selected samples, films were immersed in acetone for 60 min and dried in room temperature.

Another similar set of films were fabricated for stress–strain measurements by repeating the solution casting steps three times increasing the film thickness to 600 ± 50 μm.

2.5. Surface Resistance Measurements

Electrical surface resistance of the NBR/CNT composites was measured before and after the post-treatment with an electrometer and a resistivity chamber (Keithley 6517 electrometer and 8009 Resistivity Chamber, Tektronix, Inc., Beaverton, OR, USA), and by following an ASTM D257 standard. CNT/NBR nanocomposite films were placed between electrodes and in plane current was detected at 3.0 V. The current was let to relax for 60 s after which the reading was made.

2.6. Thermal Conductivity Measurements

Through plane thermal diffusivity of the films before and after the post-treatment was determined with a laser flash analysis (LFA) method (Netzsch Hyperflash LFA 467, Erich NETZSCH GmbH & Co. Holding KG, Selb, Germany) following ASTM E1461 standard. In addition, 10 mm × 10 mm piece of the sample film was placed in a sample holder, sprayed with graphite paint and a through plane heat signal was detected at room temperature. The specific heat of the samples for LFA was determined in room temperature with a differential scanning calorimeter (DSC) (DSC 204 F1 Phoenix, Erich NETZSCH GmbH & Co. Holding KG, Selb, Germany) using standard ISO 11357 Part 4. In addition, 10 ± 0.1 mg of the film material was weighed in a crucible and heated from −60 °C to 60 °C with 10 °C/min heating rate and using N₂ as purge gas. Reference material for specific heat capacity measurements was single crystal sapphire. Heat exchange and temperature was monitored from which specific heat was calculated. A volume density of the samples was calculated from the volume and weight of the samples.

2.7. Stress–Strain Measurements

Stress–strain studies were performed with tensile tester (Messphysik midi 10–20, Messphysik Materials Testing GmbH, Furstenfeld, Austria) and dumb-bell test pieces. Selected crosshead speed was 100 mm per minute.

2.8. Dynamical Mechanical Analysis

Dynamic mechanical analysis was carried out using rectangular specimen using a dynamic mechanical thermal analyzer (Eplexor 150N, Gabo Qualimeter Testanlagen GmbH, Ahleden, Germany) in the tension mode. The isochronal frequency employed was 10 Hz and the heating rate was 2 °C/min with a dynamic load of 0.2% strain and static load at 0.5% strain. The amplitude sweep measurements were performed with another dynamic mechanical thermal analyzer (Eplexor-2000N, Gabo Qualimeter Testanlagen GmbH, Ahleden, Germany) in tension mode at room temperature, at a constant frequency of 10 Hz, 60% pre-strain and dynamic strain from 0.01–30%.

3. Results and Discussion

3.1. UV-VIS Measurements

Figure 1 shows that the opacity at 500 nm as a function of sonication energy follows a logistic curve (dashed line) deduced in the author's earlier work [18]. Since opacity is related to dispersion quality, one can use it to optimize the sonication energy to prevent oversonication and damaging the tubes. For casting, five samples were selected representing different dispersion qualities and sonication energies from 0 to 0.4 MJ/g. In order to simplify future data analysis, a concept of relative dispersion quality (RDQ) was used referring to measured opacity of an individual sample divided by saturated opacity achievable by the system with infinite sonication energy.

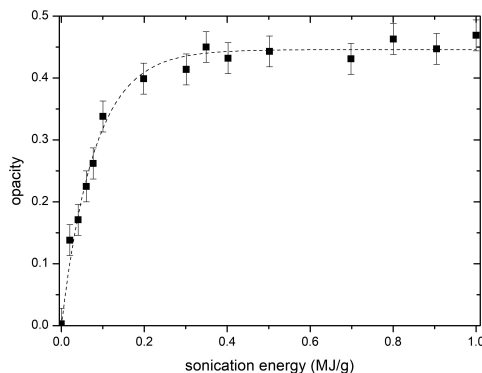


Figure 1. Opacity of 300 times diluted CNT colloid supernatant as a function of sonication energy per CNT mass with fitted logistic function.

3.2. Acetone Immersion

In order to remove free and bound surfactant from the films, they were immersed in acetone for 60 min. After drying, it was noticed that mass change was greater than the mass of added surfactant (Triton X-100). This was concluded to be caused by removal of surfactants of the pristine latex.

The masses of the films in Table 3 are not equal even the casting was done with equal masses. The reason is that, during the removal of films from the molds, part of the material was lost and only undamaged parts were processed further.

Table 3. Mass changes of films after acetone treatment.

RDQ	Mass of the Film (g)	Mass Difference From Acetone Treatment (g)
0.0	1.36	0.48
0.4	2.06	0.60
0.6	1.82	0.51
0.9	1.70	0.51
1.0	1.89	0.53

3.3. Surface Resistance Measurements

After an initial drop, the surface resistance of the rubber sample did not notably change as a function of dispersion quality or post treatment (Figure 2). The resistance values are remaining in the range of 20 kΩ/sq to 30 kΩ/sq. The loading of the tubes in all samples is at 12.5 phr, so the concentration of carbon nanotubes is significantly above the critical percolating concentration. For this reason, the conductivity of the samples did not alter that much with different dispersion qualities after acetone treatment. Even at lower dispersion quality, the distribution of the CNTs took place in such a way that the nanotubes could form a percolating network. Surfactant absorbed on CNTs did not significantly increase the contact resistance of the percolating network.

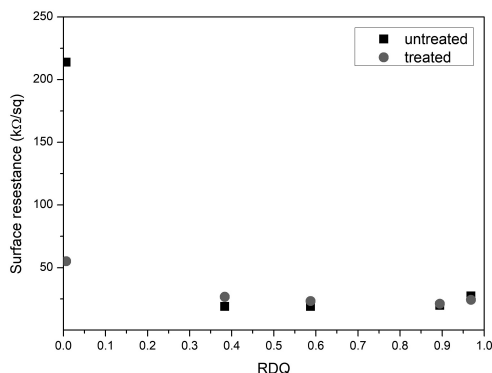


Figure 2. Surface resistance of untreated and post treated samples with different relative dispersion qualities.

3.4. Thermal Conductivity Measurements

Thermal diffusivity was determined as an average from 15 individual flashes. Thermal conductivity κ of the sample was calculated using relation, $\kappa = a\rho c_p$, where a is the thermal diffusivity, ρ is volume density and c_p is the specific heat determined with DSC (0.75 ± 0.05 kJ/°C kg).

Thermal conductivity peaked with relative dispersion quality close to 0.6 (Figure 3). In this value, the sonication process experienced some type of gelation point where loose CNT agglomerates start to percolate throughout the dispersion. At this point, the physical interaction of CNT network is at the highest level, which also leads to an increase in thermal conductivity. Acetone post-treatment enhanced the thermal conductivity with smaller dispersion quality values but was marginal with higher values.

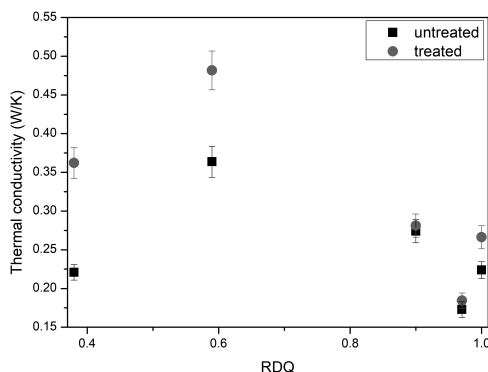


Figure 3. Thermal through-plane conductivity of untreated and post treated samples with different relative dispersion qualities.

3.5. Stress–Strain

The mechanical properties of the rubber composites were evaluated that were prepared with the pre-dispersed CNT solution. It can be found that the NBR behaves like a well crosslinked rubber matrix with elongation at break around 600%. This rubber sample (without any filler) was also treated with solvent and, after the treatment, the stress–strain properties were not altered that much. After incorporation of CNT, the mechanical properties were improved to a considerable extent. It can be found that the modulus of the composites was gradually increased with the increase of the sonication dosage i.e., better relative dispersion quality. To understand the effect more elaborately, the stress–strain

diagram from one of the representative samples is shown in Figure 4. It is clear that a small amount of nanotubes reinforces the rubber matrix as the curves becoming steeper. Here, it is interesting to note that, after solvent treatment, the stress is more at a given strain. This could be explained by the way that the small molecules of surfactant (what was used to disperse the tubes in aqueous medium) are leached away during the solvent treatment process. Thus, this result indicates that a vulcanized rubber sample could be made more mechanically robust by suitable solvent treatment.

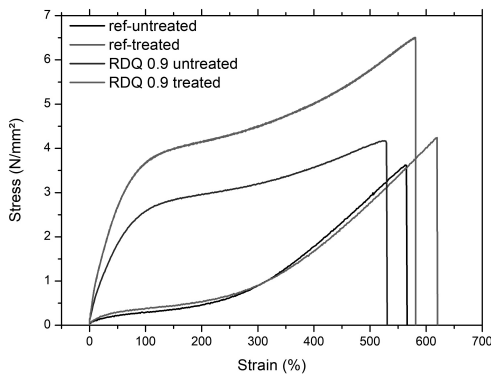


Figure 4. Comparison between untreated and treated nanocomposites with high relative dispersion quality vs. untreated and treated reference material.

From Figure 5, it can be seen that, as RDQ is increasing, the ultimate strength is also increasing. Before acetone treatment, the ultimate strength of the nanocomposite is below the untreated value of the pristine NBR film (lower dashed line), and after acetone treatment all ultimate strength values of nanocomposites are above the treated values of NBR (upper dashed line). One note again is to be made close to RDQ of 0.6 where the local peak is to be seen similar to thermal conductivity measurements.

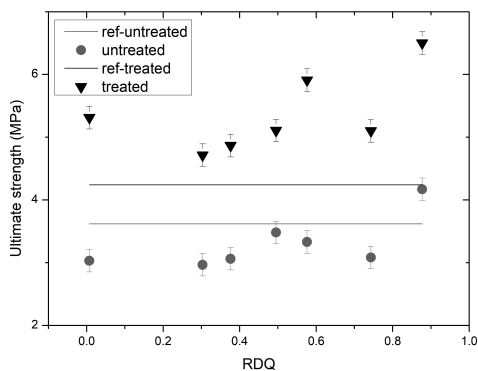


Figure 5. A development of ultimate strength of CNT/NBR nanocomposites as a function of relative dispersion quality. Dashed lines are representing unfilled NBR elastomer films.

Reference material is also being affected by the acetone treatment. This is due to the fact that the used Litex latex is also containing some surfactants that presumably are dissolved into acetone, improving the mechanical interaction of the rubber molecules.

Figure 6 shows the development of elongation at the break of the films. As expected, the filled elastomers are more brittle compared to pristine rubber. However, in filled and treated elastomers, elongation at break is growing linearly as a function of RDQ and comes very close to unfilled NBR and over the untreated values of pristine film. It is therefore possible to manufacture stiffer elastomer composite that have the same properties of maximum elongation.

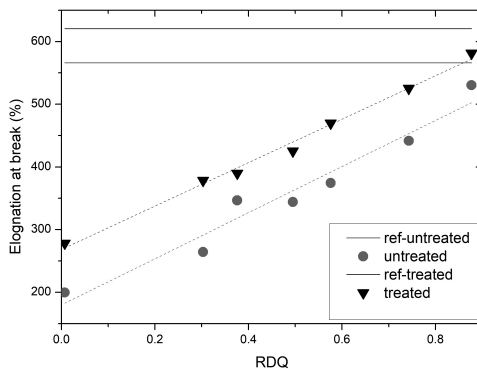


Figure 6. A development of elongation at break of CNT/NBR nanocomposites as a function of relative dispersion quality together with fitted dashed lines. Elongation at break is growing at slope $367\% \times \text{RDQ}$ in untreated composites and $346\% \times \text{RDQ}$ in treated composites. Solid lines are representing unfilled NBR elastomer films.

3.6. Dynamical Mechanical Analysis

The rubber composites were further investigated by strain sweep analysis to understand filler–filler interaction, which is generally called Payne effect. For filler containing cross linked rubber, the dynamic mechanic properties is largely dependent on the dynamic strain and this property is well known as the Payne effect. At higher dynamic strain, the filler–filler networks, developed inside the rubber matrix, is broken and a gradual fall of the storage modulus is noticed. However, a gum rubber without any filler does not respond with strain.

In the present case, the storage modulus (E') of the sample is plotted against dynamic strain (Figure 7). It can be seen that acetone post treatment enhanced the filler–filler interaction more than 300% in samples with higher RDQ. However, it can be seen that, with the increase of the filler dispersion, the dependencies of the storage modulus as a function of dynamic strain is not increasing linearly, but have again two local maximums at 0.6 with untreated and 0.7 RDQ with treated samples. (Figure 8). With higher sonication energy, the tubes are dissociated into finer particles and the native interaction of the CNT aggregates is lost. With RDQ close to 0.6, there seems to be an optimum where the pristine interaction from original aggregates is still present, and the aspect ratio of the particle is improved by the dispersion process. These two factors both have reinforcing effects on the composite. The relative improvement as a function of RDQ can be seen in Figure 9. It also very interesting to observe that, after solvent treatment, the dependency is more prominent, indicating more filler–filler interaction within the dispersed tubes. It can be envisaged that the surfactant molecules were initially deposited in between the tubes and were acting as plasticizers. After removing the surfactant, the two adjacent tubes are again coming closer and strong filler–filler interactions are realized. This trend also was observed with all other samples that are not shown here.

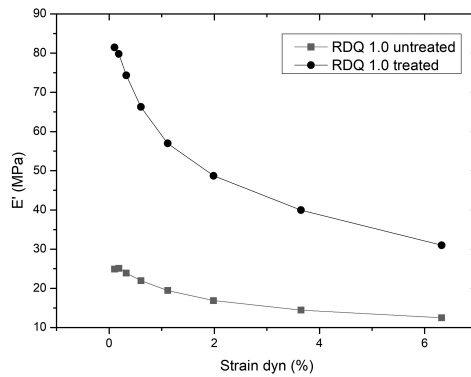


Figure 7. Payne effect of a CNT/NBR nanocomposites before and after the post-treatment.

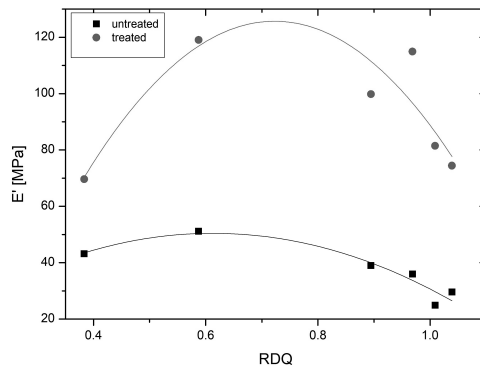


Figure 8. A development of storage modulus of CNT/NBR nanocomposites as a function of relative dispersion quality for untreated and treated films.

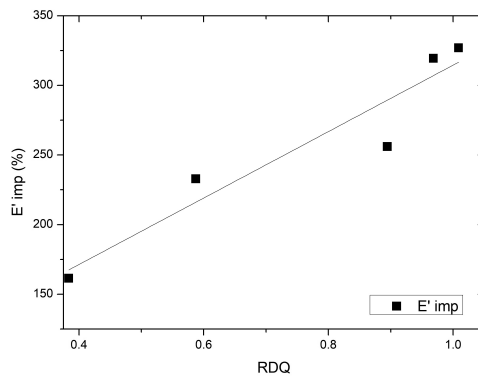


Figure 9. A development of relative improvement due to the post treatment of the storage modulus of CNT/NBR nanocomposites as a function of relative dispersion quality.

Dynamic mechanical properties of the samples were analyzed, a plot of storage modulus as a function of temperature was analyzed and the storage modulus values are tabulated, which were obtained at room temperature (rubbery plateau region). It can be seen that the storage modulus (above glass transition temperature) is increasing with the increase of dispersion quality of the CNTs (Figure 10). It should be noted here that the amount of the tubes is constant for all composites. In this

case, higher storage modulus is associated with the reinforcing of the tubes to the soft elastomers. When the agglomerated structure of the tubes is dissociated under sonication conditions into fine individual tubes, the effective aspect ratio of the tubes is greatly enhanced and directly reflected in the reinforcing effect.

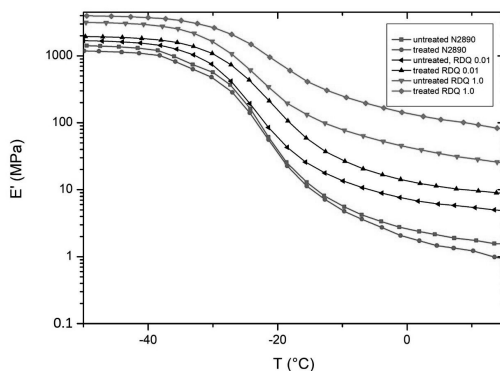


Figure 10. A development of storage modulus of CNT/NBR nanocomposites as a function of relative dispersion quality for untreated and treated films.

The Guth and Smallwood (GS) model was used to understand the reinforcing activity of CNT. Here, the shape factor f can be considered as the ratio of length to thickness of the tubes in order to explain stiffening caused by chain-like structure or non-spherical particles (Equation (1)):

$$\frac{E_c}{E_m} = 1 + 0.67f\varphi + 1.62f^2\varphi^2, \quad (1)$$

where E_c is Young's modulus of the composites, E_m is the Young's modulus of the gum sample (without any filler) and φ is the volume fraction of the filler in the elastomeric composites. In the present case, the Young's modulus is replaced by the storage modulus at a very low strain, $E'(0)$, obtained from strain sweep analysis (Figure 7). In Equation (1), the φ is not constant but is dependent on size and shape of the particulate aggregates as stated by Sambrook [19]. A tightly bound interphasial volume between filler and the matrix is behaving more like a filler affecting the effective volume fraction of the filler-like domains. Using this approach and assuming no major decrease of the aspect ratio of the CNTs, the development of the effective volume fraction φ is shown in (Figure 11).

Calculating with Equation (1), the effective volume fractions are shown in (Figure 11). After an initial increase, φ starts to decrease as RDQ is increasing. It is interesting that again there is a peak close to RDQ value of 0.6 indicating strong total interaction. Acetone treatment is clearly enhancing the φ values of the model. An explanation to this could be that, as the interaction between filler and matrix is increased by removing the surfactant, an interphasial layer outside of the filler–matrix interface is gaining more filler-like characteristics, therefore changing the effective volume fraction and overall stiffness of the composite. This interphase is also dependent on the morphology of the filler particles. When filler morphology starts to get a more cylindrical shape by better dispersion quality, the overall interphasial volume is decreasing, since geometrical hindrance of the bound rubber is lost. This leads to decrease in the effective filler volume fraction and total reinforcement as can be seen in Figure 8.

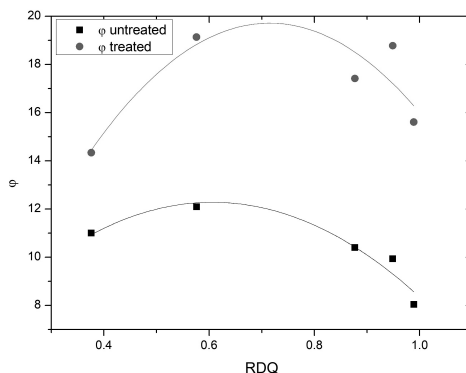


Figure 11. Shape factors, f , calculated using Equation (1), as a function of RDQ.

4. Conclusions

Surfactants are perfect tools in non-covalent exohedral functionalization of carbon nanotubes. They leave the nanotubes undamaged during the mixing process and enable stable and high quality dispersion to be made. However, surfactants inhibit the realization of physical properties in nanocomposites by disturbing the interaction in filler networks and between fillers and matrix.

In this study, we have shown that simple acetone immersion after vulcanization removes residual surfactants from NBR/CNT nanocomposite films and improves their physical properties. Room temperature pre-strain storage modulus of the films increased more than 300% in some samples and storage modulus below glass transition, T_g increased over 30%. We also saw that post treatment is affected more in samples with better dispersion quality. This is expected since better dispersion quality is related to increased concentration of adsorbed surfactant on a CNT surface. Removing surfactant enables better physical interaction between individual nanotubes and between tubes and the matrix. In our samples, the relative enhancements in mechanical performance of the nanocomposite films were significantly higher with post treatment than by using the CNTs as filler in the first place.

Author Contributions: Conceptualization, P.K., A.D. and J.V.; Methodology, P.K., A.D. and J.V.; Formal Analysis, P.K., A.D. and J.V.; Writing—Original Draft Preparation, P.K.; Writing—Review and Editing, P.K.; Visualization, P.K.; Supervision, A.D. and J.V.

Acknowledgments: We would like to acknowledge Research and Development Consulting Oy, Tampere, Finland for providing essential chemicals and valuable information for the research.

Conflicts of Interest: The authors declare no conflict of interest.

References

1. McCarthy, D.; Mark, J.; Schaefer, D. Synthesis, structure, and properties of hybrid organic–inorganic composites based on polysiloxanes. I. Poly (dimethylsiloxane) elastomers containing silica. *J. Polym. Sci. Part B Polym. Phys.* **1998**, *36*, 1167–1189. [CrossRef]
2. Joly, S.; Garnaud, G.; Ollitrault, R.; Bokobza, L.; Mark, J. Organically modified layered silicates as reinforcing fillers for natural rubber. *Chem. Mater.* **2002**, *14*, 4202–4208. [CrossRef]
3. Frogley, M.D.; Ravich, D.; Wagner, H.D. Mechanical properties of carbon nanoparticle-reinforced elastomers. *Compos. Sci. Technol.* **2003**, *63*, 1647–1654. [CrossRef]
4. Andrews, R.; Jacques, D.; Minot, M.; Rantell, T. Fabrication of carbon multiwall nanotube/polymer composites by shear mixing. *Macromol. Mater. Eng.* **2002**, *287*, 395–403. [CrossRef]
5. Huang, Y.Y.; Terentjev, E.M. Dispersion of carbon nanotubes: Mixing, sonication, stabilization, and composite properties. *Polymers* **2012**, *4*, 275–295. [CrossRef]

6. Sethi, J.; Sarlin, E.; Meysami, S.S.; Suihkonen, R.; Kumar, A.R.S.S.; Honkanen, M.; Keinänen, P.; Grobert, N.; Vuorinen, J. The effect of multi-wall carbon nanotube morphology on electrical and mechanical properties of polyurethane nanocomposites. *Compos. Part A Appl. Sci. Manuf.* **2017**, *102*, 305–313. [CrossRef]
7. Lavilla, I.; Bendicho, C. Fundamentals of Ultrasound-Assisted Extraction. In *Water Extraction of Bioactive Compounds*; Elsevier: New York, NY, USA, 2018; pp. 291–316.
8. Yang, D.Q.; Rochette, J.F.; Sacher, E. Functionalization of multiwalled carbon nanotubes by mild aqueous sonication. *J. Phys. Chem. B* **2005**, *109*, 7788–7794. [CrossRef] [PubMed]
9. Shahshahan, M.; Keinänen, P.; Vuorinen, J. The effect of ultrasonic dispersion on the surface chemistry of carbon nanotubes in the Jeffamine D-230 polyetheramine medium. *IEEE Trans. Nanotechnol.* **2017**, *16*, 741–744. [CrossRef]
10. Liu, J.; Rinzler, A.G.; Dai, H.; Hafner, J.H.; Bradley, R.K.; Boul, P.J.; Lu, A.; Iverson, T.; Shelimov, K.; Huffman, C.B.; et al. Fullerene pipes. *Science* **1998**, *280*, 1253–1256. [CrossRef] [PubMed]
11. Islam, M.; Rojas, E.; Bergey, D.; Johnson, A.; Yodh, A. High weight fraction surfactant solubilization of single-wall carbon nanotubes in water. *Nano Lett.* **2003**, *3*, 269–273. [CrossRef]
12. Geng, H.Z.; Kim, K.K.; So, K.P.; Lee, Y.S.; Chang, Y.; Lee, Y.H. Effect of acid treatment on carbon nanotube-based flexible transparent conducting films. *J. Am. Chem. Soc.* **2007**, *129*, 7758–7759. [CrossRef] [PubMed]
13. Wang, J.; Sun, J.; Gao, L.; Wang, Y.; Zhang, J.; Kajiura, H.; Li, Y.; Noda, K. Removal of the residual surfactants in transparent and conductive single-walled carbon nanotube films. *J. Phys. Chem. C* **2009**, *113*, 17685–17690. [CrossRef]
14. Siljander, S.; Keinänen, P.; Rätty, A.; Ramakrishnan, K.R.; Tuukkanen, S.; Kunnari, V.; Harlin, A.; Vuorinen, J.; Kanerva, M. Effect of Surfactant Type and Sonication Energy on the Electrical Conductivity Properties of Nanocellulose-CNT Nanocomposite Films. *Int. J. Mol. Sci.* **2018**, *19*, 1819. [CrossRef] [PubMed]
15. Wu, Z.; Chen, Z.; Du, X.; Logan, J.M.; Sippel, J.; Nikolou, M.; Kamaras, K.; Reynolds, J.R.; Tanner, D.B.; Hebard, A.F.; et al. Transparent, conductive carbon nanotube films. *Science* **2004**, *305*, 1273–1276. [CrossRef] [PubMed]
16. Clark, M.D.; Subramanian, S.; Krishnamoorti, R. Understanding surfactant aided aqueous dispersion of multi-walled carbon nanotubes. *J. Colloid Interface Sci.* **2011**, *354*, 144–151. [CrossRef] [PubMed]
17. Das, A.; Kasaliwal, G.R.; Jurk, R.; Boldt, R.; Fischer, D.; Stöckelhuber, K.W.; Heinrich, G. Rubber composites based on graphene nanoplatelets, expanded graphite, carbon nanotubes and their combination: A comparative study. *Compos. Sci. Technol.* **2012**, *72*, 1961–1967. [CrossRef]
18. Keinänen, P.; Siljander, S.; Koivula, M.; Sethi, J.; Sarlin, E.; Vuorinen, J.; Kanerva, M. Optimized dispersion quality of aqueous carbon nanotube colloids as a function of sonochemical yield and surfactant/CNT ratio. *Heliyon* **2018**, *4*, 1–15. [CrossRef] [PubMed]
19. Sambrook, R. Influence of Temperature on the Tensile Strength of Carbon Filled Vulcanizates. *Rubber Chem. Technol.* **1971**, *44*, 728–743. [CrossRef]



PUBLICATION

III

Effect of surfactant type and sonication energy on the electrical conductivity properties of nanocellulose-CNT nanocomposite films

S. Siljander, P. Keinänen, A. Rätty, K. R. Ramakrishnan, S. Tuukkanen, V. Kunnari, A. Harlin, J. Vuorinen and M. Kanerva

International journal of molecular sciences 19.6 (2018), 1819

Publication reprinted with the permission of the copyright holders



Article

Effect of Surfactant Type and Sonication Energy on the Electrical Conductivity Properties of Nanocellulose-CNT Nanocomposite Films

Sanna Siljander ^{1,*}, Pasi Keinänen ¹, Anna Rätty ¹, Karthik Ram Ramakrishnan ¹, Sampo Tuukkanen ², Vesa Kunnari ³, Ali Harlin ³, Jyrki Vuorinen ¹ and Mikko Kanerva ¹

¹ Laboratory of Materials Science, Tampere University of Technology, FI-33720 Tampere, Finland; pasi.keinanen@tut.fi (P.K.); anna.ratty@tut.fi (A.R.); karthik.ramakrishnan@tut.fi (K.R.R.); jyrki.vuorinen@tut.fi (J.V.); mikko.kanerva@tut.fi (M.K.)

² BioMediTech, Tampere University of Technology, FI-33720 Tampere, Finland; sampo.tuukkanen@tut.fi

³ VTT Research Center, FI-02044 Espoo, Finland; vesa.kunnari@vtt.fi (V.K.); ali.harlin@vtt.fi (A.H.)

* Correspondence: sanna.siljander@tut.fi; Tel.: +358-50-3-555-777

Received: 15 May 2018; Accepted: 15 June 2018; Published: 20 June 2018



Abstract: We present a detailed study on the influence of sonication energy and surfactant type on the electrical conductivity of nanocellulose-carbon nanotube (NFC-CNT) nanocomposite films. The study was made using a minimum amount of processing steps, chemicals and materials, to optimize the conductivity properties of free-standing flexible nanocomposite films. In general, the NFC-CNT film preparation process is sensitive concerning the dispersing phase of CNTs into a solution with NFC. In our study, we used sonication to carry out the dispersing phase of processing in the presence of surfactant. In the final phase, the films were prepared from the dispersion using centrifugal cast molding. The solid films were analyzed regarding their electrical conductivity using a four-probe measuring technique. We also characterized how conductivity properties were enhanced when surfactant was removed from nanocomposite films; to our knowledge this has not been reported previously. The results of our study indicated that the optimization of the surfactant type clearly affected the formation of freestanding films. The effect of sonication energy was significant in terms of conductivity. Using a relatively low 16 wt. % concentration of multiwall carbon nanotubes we achieved the highest conductivity value of 8.4 S/cm for nanocellulose-CNT films ever published in the current literature. This was achieved by optimizing the surfactant type and sonication energy per dry mass. Additionally, to further increase the conductivity, we defined a preparation step to remove the used surfactant from the final nanocomposite structure.

Keywords: nanocellulose; carbon nanotubes; nanocomposite; conductivity; surfactant

1. Introduction

Conductive composite materials with micrometer and nanoscale fillers, like metallic powders, carbon black, graphite and carbon fibers, are used in many applications, such as antistatic films and electromagnetic interference (EMI) shielding. Electrical conductivity of 0.01 S/cm or higher is required for the composite to be considered conductive, while materials with lower conductivity can be used as antistatic and semiconducting materials. One of the drawbacks with most fillers is that the filler content ratio needs to be as high as 50 wt. % to achieve the percolation threshold (i.e., the critical concentration of filler that corresponds to the sharp rise of conductivity). However, this high filler content ratio might lead to a decrease in the resultant composite's mechanical properties [1,2]. Nanomaterials, such as carbon nanotubes (CNTs) and graphene, play a role in the development of future composite materials.

For example, CNTs and graphene have been used to toughen matrix polymers [3], to adjust barrier properties of nanocomposite films [4], and to form hierarchical reinforcements [5]. It is possible to attain the percolation threshold in the insulating polymer matrix at a low CNT concentration due to their excellent electrical, mechanical and thermal properties.

Individual CNTs are part of a group of the strongest and most conductive nanomaterials known [6]. Additionally, CNTs can carry higher current density than any other known material, with its highest measured value being 109 A/cm^2 [7,8]. However, to obtain an ideal conductive network, the carbon nanotubes have to be well separated and homogenous dispersion should be maintained in the final product. Without efficient dispersion, filler aggregates act as defect sites, which leads to lower mechanical performance [9,10]. As the most abundant polymer on earth, cellulose is a promising and well-known material that can be used as a matrix in nanocomposites.

Cellulose is environmentally conscious, low-cost, strong, dimension-stable, non-melting, non-toxic and is a non-metal matrix. The interest towards nanoscale cellulose has increased during the past few years because of its inherent properties, including its good mechanical properties, which are better than those of the respective source biomass material [11]. Cellulose-based micro-/nanofibrils (MFC/NFC) can be extracted from various types of plant fibers using mechanical forces, chemical treatments, enzymes or combinations of these. The most typical approach, however, is to apply wood pulp and mechanical methods such as homogenization, microfluidization, microgrinding and cryocrushing. Finally, after fibrillation, the width of NFC is typically between 5 and 20 nm, with a length of several micrometers. Nanocellulose (NFC) has hydroxyl groups in its structure and is therefore associated with high aspect ratio and strong hydrogen bonds formed between nanocellulose fibers [12]. These bonds enhance mechanical properties and enable the formation of free standing films. A combination of CNTs and cellulose I provides a conductive nanocomposite network. CNT-cellulose composites have been reported to be used as supercapacitor electrodes [13,14], electromagnetic interference shielding devices [15], chemical vapor sensors [16], water sensors [17,18], and pressure sensors [19].

There are different manufacturing methods for the fabrication of CNT-cellulose nanocomposites, but all the methods typically include (1) a phase of dispersing CNTs into a solution, and (2) an impregnation phase into the cellulose substrates (e.g., paper, filter paper) [15,16,20–23]. Alternatively, the dispersion can be used as a wet component with bacterial cellulose [24,25], with cellulose I and regenerated cellulose fibers [13,18,26] or in an aerogel form [17]. The processing of nanocellulose in an aqueous medium is the most common way due to its tendency to react with water, and strong affinity to itself and hydroxyl group containing materials [12]. Chen et al. [27] showed that NFCs and CNTs can form a three-dimensional conductive network structure in a gel-film morphology to achieve high electrical conductivity.

The properties of the nanocellulose-CNT composites are affected by the quality of CNT dispersion, amount of structural and oxidative defects in the graphitic structure of the CNTs, the aspect ratio of the CNTs after the disaggregate treatment, the strength of the matrix, and the interactions between the CNTs and the cellulose matrix. [28] The key challenge in numerous industrial applications is to achieve uniform and stable CNT dispersion. The homogenization phase is vital to maximize the excellent mechanical, electrical and thermal properties of the CNTs and the eco-friendly, strong and low-cost nanocellulose matrix. This is particularly important in the case of submicron- or nanometer-sized particles. In these scales, the surface chemistry plays an important role, managing the particle dispersion within the final product [29]. CNT dispersions are challenging because as the surface area of particles increases, the attractive forces between the aggregates [29] and the high aspect ratio enable the entanglement and bundling of CNTs [30]. There are two phenomena that affect CNT dispersions: nanotube morphology and the forces between the tubes. Entanglement of CNTs occurs due to tube morphology, as well as molecular forces, high aspect ratio, and high flexibility. Dispersing these entangled aggregates is difficult without damaging the nanotubes. Both CNT and aggregate size are expected to play a crucial role in the achieved level of electrical conductivity [31].

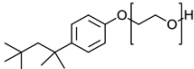
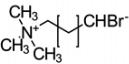
Two typical dispersion methods for CNTs include high shear mixing and pure sonication [13,15,16,19–21,24,32]. Sonication is based on ultrasonic waves that generate microscopic bubbles

or inertial cavitation, which produces a shearing action. This results in liquid and suspended particles becoming intensely agitated. Another common technique is to use a centrifuge in one of the processing steps to extract the unwanted agglomerates from the supernatant, but this additional phase takes time and effort and affects the concentration of dispersed particles in the dispersion. In general, sonication is superior to shear mixing, especially for low-viscosity systems [33], where conventional mixing does not create high enough strain rates to disintegrate the CNT aggregates.

Another issue in the manufacturing of films using NFC is the shrinkage and distortion of the structure because of faster evaporation rate on surface than the mass transport of moisture within the material. When strong enough gradient occurs, film distortions emerge because of local stresses [34,35].

One widely used method for CNT dispersion is the non-covalent method. In this method, chemical moieties are adsorbed onto the surface of CNTs, the CNTs are non-covalently dispersed in a water medium, and the resultant mixture is sonicated in the presence of the moieties, namely surfactants. Surfactants are a group of organic compounds that have a hydrophilic head and a hydrophobic tail, and they are commonly used as detergents, wetting agents, emulsifiers, foaming agents and dispersants. The advantage of the non-covalent method lies in the fact that it does not deteriorate the electronic structure of the CNTs' graphitic shells, maintaining their high electrical conductivity. Good dispersion can be achieved by having a mixture of both nanocellulose and carbon nanotubes with the help of surfactants, as the surfactants lower the interfacial free energy between the particles. Table 1 lists information about surfactants and their properties used in this study.

Table 1. Surfactants used in this study.

Product Name	Triton™ x-100	Pluronic® F-127	CTAB
Type	Non-ionic	Non-ionic Polymeric	Cationic
Name	Octylphenol Ethoxylate	Poloxamer	Hexadecyltri-methylammonium bromide
Chemical Structure		$H(OCH_2CH_2)_x(OCH_2CH(CH_3))_y(OCH_2CH_2)_zOH$	
Critical Micelle Concentration	0.2–0.9 mM (20–25) °C	950–1000 ppm (25 °C)	0.92 mM (20–25) °C
HLB value	13.5	22	10

In the current literature, there are several different types of surfactants used for dispersing nanocellulose and carbon nanotubes. Choosing a surfactant type for effective dispersion of nanotubes through surfactant adsorption is complicated, as the results in the published literature often give contradictory results. For example, some researchers [29] have suggested that ionic surfactants are preferable for creating aqueous dispersions. However, the non-ionic surfactant Triton X-100 was shown to be a better surfactant than the anionic surfactant SDS, which was attributed to the π - π stacking ability of the former. The quality of the NFC-CNT dispersion is dependent on the nature of the surfactant, the concentration and the type of interactions between the surfactant and dispersing particles [36]. It has been stated that, for dispersing CNTs it is preferable for the surfactant to have a relatively high HLB (hydrophilic-lipophilic balance) value [29]. This assumption was proven false in our previous study [37]. Not only are the surfactant's nature and energy carried into the dispersed system, but the concentration of the surfactant also has a crucial role in the dispersion process [38]. Too high a surfactant concentration may negatively affect conductivity properties by blocking off the charge transport through the CNT network [39]. In addition, a low surfactant concentration can cause re-aggregation, because a sufficient amount is required to cover CNT surfaces to prevent re-aggregation [39,40]. It has been shown that an efficient CNT dispersion is only possible when the surfactant concentration is above the critical micelle concentration (CMC) value [41–44]. In some cases, the surfactant concentration is reported to be higher than the (CMC), but no micelle structures are

observed in the dispersion. Presumably, most of the surfactant has been adsorbed onto the surface of the CNTs [40]. In other cases, surfactants can prefer surfactant-surfactant interactions over spreading on the CNT surface [45]. It has also been reported that dispersing agents can form stable dispersions below and equal to their CMC limit [46–49]. Moreover, it has been noted that commonly, the best results can be reached with a concentration of 0.5 CMC and that any further increase in the concentration of surfactant has only a minor effect [48].

The ISO 14887:2000(E) standard can be used to determine prospective dispersing agents for both cellulose and carbon. We can categorize nanocellulose and CNTs as solids. In that case, when using water as liquid, the category of suitable dispersing agent would be a poly ethylene-oxide (PEO)/alcohol for CNT and PEO/poly propylene oxide (PPO) copolymer for nanocellulose. The standard also provides information about commercial surfactants that fall into the mentioned categories. PEO/PPO copolymer is a suitable surfactant for nanocellulose. The standard denotes that a commercial equivalent is Pluronic®. In the case of CNTs, one example of alkyl phenoxy PEO ethanol dispersing agent is Triton™.

The typical approach to the manufacturing of conductive cellulose-CNT films has been to increase CNT weight percentage without optimizing the dispersion procedure or the used surfactants. Also, the effect of the particular ratios of the cellulose, CNT and surfactant toward each other has not been fully investigated. Even though ultrasonication is widely used for the dispersion and stabilization of CNTs, there is not a standard procedure for the sonication process, and different research groups have applied different sonication treatments to their samples. Sonication can cause chemical functionalization but it can also cause defects and breakage of CNTs [1,50–52]. This will further affect the performance of CNT-based materials and their applications. It has been found in the current literature that sonication parameters such as sonicator type, sonication time and temperature control vary significantly, with reported sonication times ranging from 2 min with tip sonication to 20 h for bath sonication. Dassios et al. [53] attempted to optimize the sonication parameters for the dispersion of MWCNTs in an aqueous solution. Two critical questions concerning the homogeneity of aqueous suspensions of carbon nanotubes by ultrasonic processing were identified; namely, the dependence of dispersion quality on the duration and intensity of sonication and the identification of the appropriate conditions for retaining the highly desirable initial aspect ratio of the free-standing tubes in the dispersed state. Fuge et al. [54] studied the effect of different ultrasonication parameters (time, amplitude) on undoped and nitrogen-doped MWCNTs in aqueous dispersions and found a nearly linear decrease of the arithmetic mean average in MWCNT length with increasing ultrasonication time.

The aim of this study was to optimize the conductivity of NFC-CNT nanocomposite films using a minimum amount of processing steps (e.g., without centrifugal processing of dispersion or pressing of the film), materials and chemicals. In this paper, NFC and multiwall carbon nanotubes (MWCNT) were used to prepare composite films and study the effect of the sonication energy and surfactant type on the electrical conductivity of the nanocomposite. In addition, we investigated the removal of the surfactant from the nanocomposites and the subsequent effect on the electrical conductivity. To our knowledge this is a novel approach and has not been reported previously. The conductivity properties of the nanocomposites were studied as a function of the used sonication energy amount, as well as with and without the presence of surfactant.

2. Results

The impact of sonication energy on electrical conductivity was one of the processing parameters with the highest interest in this study. This was due to the lack of previous research in the current literature. Also, our results show that the surfactant type and sonication energy play a major role in achieving excellent conductivity. In addition to the previously mentioned parameters, removal of surfactant can enhance conductivity values toward levels never seen or reported.

Overall, the shelf-life of the sonicated dispersion samples was significantly long, since samples remained unchanged before the film preparation. Also, sedimentation was not detected, based on the fact that conductivity values were at the same level when measured from both sides of the

nanocomposite films. The appearance of the sonicated dispersion samples was identical; however, the consistency and visually inspected viscosity varied with increasing sonication energy. This was observed with Triton X-100 and Pluronic F-127 samples but not in cetyl trimethylammonium bromide (CTAB) surfactant-containing dispersions.

2.1. Conductivity of NFC-CNT Nanocomposite Films

Electrical conductivity of the even and uniform centrifugally cast films was measured using the four-probe measuring technique. With this method, it is possible to minimize the contact resistances and thus provide more accurate conductivity measurements than for the commonly used two-terminal measurement. The sheet resistances of prepared and cut nanocomposite films (size 30 mm × 30 mm) were measured using a four-point probe setup made in-house and a multimeter (Keithley 2002, Tektronix, Inc., Beaverton, OR, USA) in four-wire mode. The probes were placed in line, with equal 3 mm spacing. The four-probe setup is described elsewhere in detail [55]. The conductivity measurements were carried out using a 1 mA current and voltage was measured. Measurements were taken before and after removal of surfactant.

The selection of the most functional surfactant was an important aspect in this study. This selection was determined based on the sheet resistance measurements. The effect of different surfactants and sonication energy on conductivity is shown in Figure 1. From the conductivity diagrams, the effect of surfactant type can be visually observed and estimated.

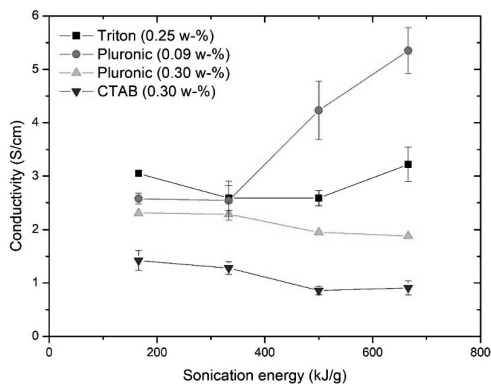


Figure 1. Conductivity of nanocomposite films processed using surfactants Triton X-100, Pluronic F-127 and cetyl trimethylammonium bromide. Concentration in weight percentages.

According to the standard, our assumption was that non-ionic surfactants would be the most promising surfactants. This was clearly the case, since the films made with surfactants Triton X-100 and Pluronic F-127 outperformed the films made with ionic surfactant CTAB.

Visual observations made with CTAB aqueous dispersion samples after sonication indicated that these samples did not gelate even with a higher amount of sonication energy per dry mass (666 kJ/g). This suggests that the dispersion process may not have been entirely successful, since samples had different consistencies and visually separate particles. The ionic surfactant (CTAB) was used to manufacture films at a 1 to 1 ratio of dry mass content of NFC and CNT. The conductivity of films processed using CTAB decreased as the sonication increased from almost 1.5 S/cm to less than 0.90 S/cm. The conductivity diagram of these films was different in its nature; the highest values were measured with the lowest amount of sonication energy.

Based on the standard Pluronic F-127, surfactant should be compatible with cellulosic materials. The first set of Pluronic F-127 nanocomposite films were done with a 1 to 1 ratio to dry mass content (0.30 wt. %). Results show that conductivity is decreasing as a function of sonication energy. Based on

this finding, another set of films was manufactured using a surfactant concentration below the CMC limit (0.09 wt. %). Conductivity results for this set of samples show higher conductivity values than films manufactured using a surfactant concentration higher than the CMC value (0.30 wt. %). Using Pluronic F-127 surfactant, the highest conductivity for nanocomposite films was achieved using a sonication energy of 666 kJ/g. When comparing values of films below and above CMC value the difference is sensational 5.36 S/cm (0.09 wt. %) versus 1.88 S/cm (0.30 wt. %).

For Triton, the highest conductivity value of 3.37 S/cm was achieved with 666 kJ/g sonication energy. It should be noted that almost the same conductivity result (3.02 S/cm) was achieved using just 166 kJ/g of sonication energy.

2.2. Effect of Surfactant Removal

Conductivity measurements were also carried out after the removal of the surfactant used in the dispersing phase. Triton X-100 and Pluronic F-127 films were acetone treated and CTAB films were treated with ethanol. It can be clearly seen in Figure 2 that removal of surfactant has a strong effect. Removal of surfactant from films made with CTAB increased the conductivity significantly; the maximum conductivity was 3.02 S/cm for 166 kJ/g sonication energy. However, the films expressed a decrease in conductivity at sonication energy similar to the films with the surfactants present. For Pluronic F-127 films (Figure 2c) made below the CMC limit of the surfactant, the removal of surfactant did not have a significant effect on the conductivity. Even though there was no clear trend, the film with surfactant had somewhat higher conductivity than the one where surfactant was not present. For Pluronic F-127 (0.30 wt. %), the shape of the diagram differed from other previous sets. The films initially exhibited a decrease in conductivity as a function of increasing sonication energy, and the highest values were measured for the samples sonicated at the least energy, but also for the highest amount of sonication energy. For the samples with high conductivity, the removal of the non-ionic surfactant increased the conductivity. The highest value obtained from these measurements was 2.88 S/cm for a sonication energy of 166 kJ/g. A dramatic increase was observed in conductivity values of films manufactured with surfactant Triton X-100 (Figure 2a): the conductivity increases from approximately 3.0 S/cm to a value of 8.42 S/cm when the non-ionic surfactant was removed (sample was sonicated at 666 kJ/g). It should be noted that the films containing the surfactant did not exhibit as strong a sensitivity to increasing sonication energy (as those without surfactant).

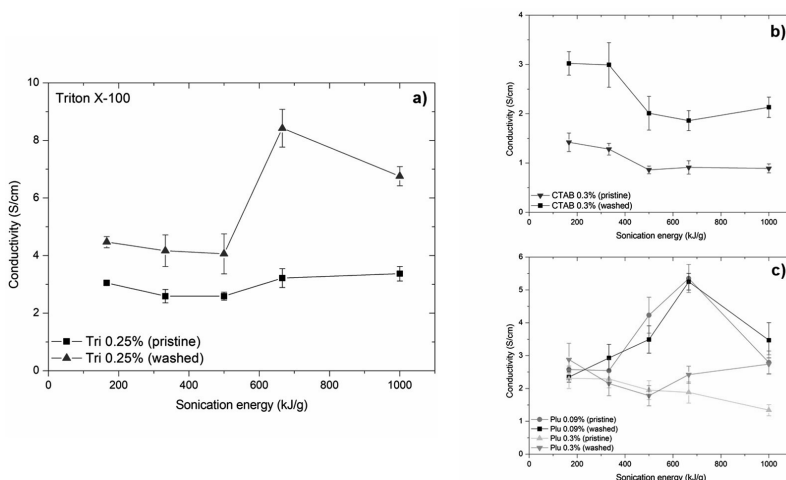


Figure 2. Conductivity of nanocomposite films before and after (a) Triton X-100 surfactant removal, (b) CTAB surfactant removal, and (c) Pluronic surfactant removal.

It is well known that surfactants can plasticize the structure of composites and interfere with conductivity properties by situating themselves at the interface between the conductive particles and matrix. This phenomenon was demonstrated when the properties of the nanocomposite films were compared in this study. Firstly, there was a clear increase in the conductivity of the films processed using the Triton X-100 and CTAB surfactants due to the removal of the surfactant. The diagrams (pristine vs. washed) were similar in their trend, and a clear increase in terms of conductivity was observed. When using the surfactant Pluronic F-127 for processing, a clear conclusion could not be made because the conductivity diagrams did not show a corresponding, monotonic trend due to surfactant removal. However, the results showed that, when the surfactant is present in the film structure, the effect of interference by Pluronic F-127 (concentration below CMC) on the electrical conductivity is at its minimum.

2.3. Comparison to Previous Results

When comparing our nanocomposite film's conductivity results to previous studies, we found that our results were superior to reported values. In Figure 3 are illustrated electrical conductivity results from studies that have used native NFC and manufactured homogenous nanocomposites from it. For non-ionic surfactants, the highest conductivity value found was 0.022 S/cm at a 10 wt. % CNT loading [17]. In our study, the highest value was 8.42 S/cm after removing Triton X-100 and, likewise, 5.35 S/cm with Pluronic F-127 still present in the film.

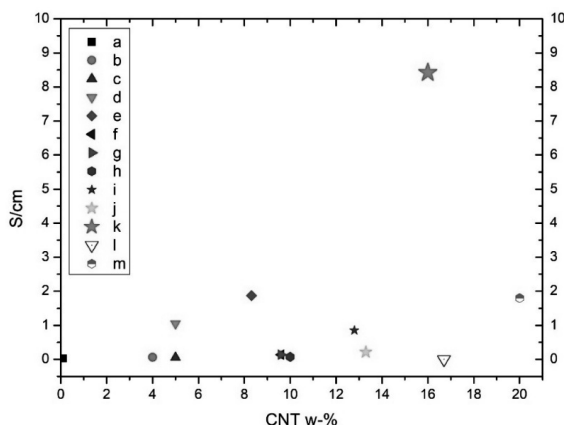


Figure 3. Comparison of obtained electrical conductivity of NFC-CNT nanocomposite films from the current literature. Pink star (letter k) refers to our data (Triton X-100), while other letters refer to a [9], b [56], c [57], d [58], e [22], f [9], g [24], h [57], i [59], j [15], l [32] and m [27].

Huang et al. [57] reported the results of a multiphase process which was used to accomplish a conductivity of 0.072 S/cm using MWCNT-doping at 10 wt. % and 0.056 S/cm with 5 wt. % doping with cotton linters and CTAB as a surfactant. CTAB surfactant was also used with bacterial nanocellulose and CNTs, where the conductivity was 0.027 S/cm (MWCNT 0.1 wt. %) [9]. Also, Yoon et al. [24] used bacterial cellulose as a matrix and obtained conductivity of 0.14 S/cm with 9.6 wt. % MWCNT loading. Electrical conductivity of TEMPO-oxidized cellulose films with 16.7 wt. % concentration of MWCNTs was 0.001 S/cm, which is lower than the conductive material limit [32]. For chitosan-cellulose-CNT membranes, Xiao et al. [56] accomplished conductivity of 0.062 S/cm with a 4 wt. % content of MWCNTs. By using comparable materials, but by applying a filtering method, Yamakawa et al. [58] obtained a 1.05 S/cm electrical conductivity with a 5 wt. % MWCNT loading and

Chen et al. 1.8 S/cm with 20 wt. % MWCNT. They were able to increase the conductivity to a value of 5.02 S/cm using a chemical alkali treatment.

In addition, studies about manufacturing conductive cellulose composites via coating cellulosic filter paper with a CNT dispersion have revealed rather good results, but the consistency of the materials is not homogeneous—not exactly an integral composite. Lee et al. [15] achieved conductivity of 1.11 S/cm using 13.3 wt. % MWCNT. Mondal et al. [59] reported conductivity values after using a dipping method, and they reached 0.85 S/cm with a 12.8 wt. % carbon nanofiber (CNF) content. Fugetsu et al. [22] manufactured conductive cellulose-based composites using a traditional paper making process with 8.32 wt. % CNT concentration and, finally, a conductivity of 1.87 S/cm was obtained.

2.4. Characterization of Nanocomposite Structure

The surface and cross-section of the films processed using surfactant Triton X-100 was studied with SEM. Images were taken with Zeiss ULTRAPlus scanning electron microscope (SEM). The effect of sonication as well as the removal of surfactant were studied with the SEM images shown in Figure 4. Two samples were specifically chosen for this inspection: 166 kJ/g and 666 kJ/g sonication energy films containing surfactant (Figure 4a,c) and after removal of surfactant Triton X-100 by washing them in acetone (Figure 4b,d).

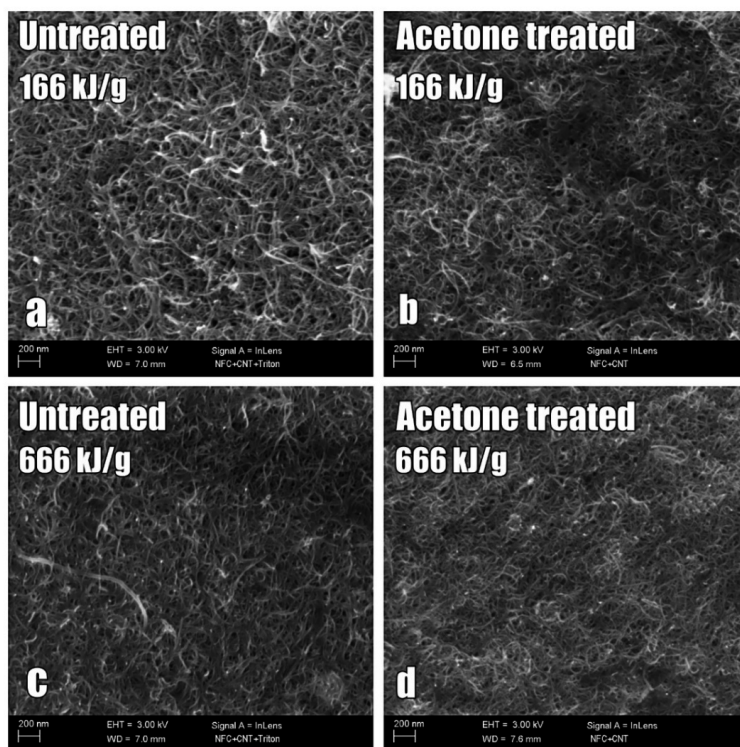


Figure 4. SEM imaging of NFC-CNT nanocomposite films surface (166 and 666 kJ/g) containing surfactant (a,c) and after removal of surfactant Triton X-100 by washing them in acetone (b,d).

In the top left (Figure 4a) image, some clusters of CNTs are present in the 166 kJ/g sonication energy sample, but not in the higher sonication energy 666 kJ/g sample. Both films have abundant

amount of CNTs in the surface. Here, the 166 kJ/g film has a more porous structure than the 666 kJ/g film. In addition, the CNTs form a more consistent network in the 666 kJ/g film after washing the surfactant away (Figure 4d).

The SEM images of the sonicated samples in Figure 4 showed that there were clusters present in the 166 kJ/g sonicated film, while the higher sonicated energy sample did not have similar kinds of clusters. This indicates that, for lower sonication energies, non-dispersed particles remain in the films. This is not preferred, since the purpose is to achieve good dispersion of all the particles in the dispersion and in the films manufactured. This is an indication that the sonication process and amount of energy used affect the extent of the dispersion of particles.

The through-thickness structure of the films was also generally studied using polished cross-sections of the films embedded in epoxy. The cross-section in Figure 5 shows the CNT ends (bright contrast spots) and their even distribution in the film (500 kJ/g), (Triton system) through the thickness. A slightly layered structure can be observed and concluded as a result of dispersion flow during the casting.

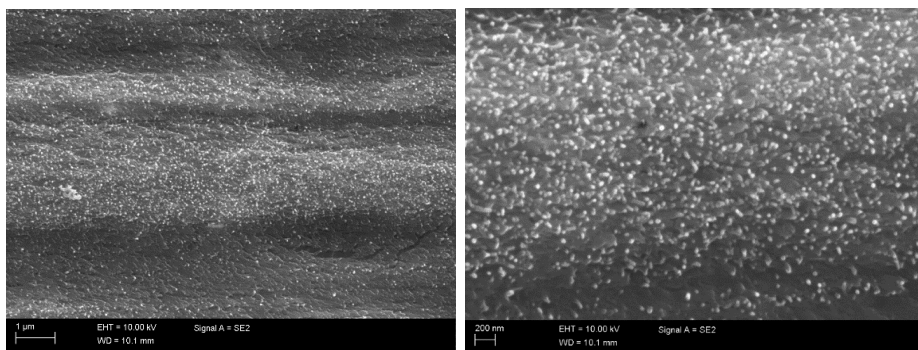


Figure 5. SEM imaging of the nanocomposite film (Triton X-100, 500 kJ/g) cross-section when embedded in epoxy: **Left** side: overall structure; **Right** side: magnification in the center of the film.

3. Discussion

Ultrasonication is a widely used process to manufacture aqueous CNT dispersions. However, how much it changes the properties of dispersed particles and the medium is often overlooked. It is known that sonication can, for example, generate hydrogen peroxide from water, degrade carbon nanotubes and ultimately destroy them. Therefore, it is important that the sonication process is optimized in terms of time and power. It also needs to be noted that the dispersion process is not linear, but follows an S-curve where temporal development of dispersion quality is related to quantity of un-dispersed solid.

Due to the re-agglomeration tendency of carbon nanotubes, it is necessary to use dispersion agents, i.e., surfactants, in manufacturing aqueous dispersions. If these dispersions are later used in conductive films, it is preferable to remove the surfactant to improve CNT network formation. Although carbon nanotubes are excellent conductors, CNT networks are not. This is due their high intertubular contact resistance. The contact points act essentially as a tunneling junction for electrons that is very sensitive to distance. The efficacy of surfactants is based on acting as a spacer between tubes, so any additional distance in a conductive network is detrimental to the conductivity itself.

4. Materials and Methods

Three-component systems containing nanocellulose, carbon nanotubes and surfactants are used in the strong, ecologically conscious nanocomposite films of this study. The CNTs add functionality

to the nanocellulose matrix and the surfactant enables percolation network to build and maximize conductivity properties.

In this study, the nanocellulose (NFC) production was based on mechanical disintegration of bleached hardwood kraft pulp (BHKP). First, dried commercial BHKP produced from birch was soaked in water at approximately 1.7 wt. % concentration and dispersed using a high-shear Ystral dissolver for 10 min at 700 rpm. The chemical pulp suspension was predefined in a Masuko grinder (Supermasscolloider MKZA10-15J, Masuko Sangyo Co., Tokyo, Japan) at 1500 rpm and fluidized with six passes through a Microfluidizer (Microfluidics M-7115-30, Microfluidics Corp., Newton, MA, USA) using 1800 MPa pressure. The final material appearance of NCF was a viscous and translucent gel.

Multiwall carbon nanotubes (MWCNT, Nanocyl 7000, Nanocyl SA., Sambreville, Belgium) were purchased from Nanocyl Inc. and the product was used in the state it was in when received. This type of nanotubes is produced via catalytic chemical vapor deposition (CCVD). Concentration of CNTs was kept constant at 16 wt. % in the nanocomposite films, so the effects of sonication energy and surfactant type to the conductivity properties are more visible.

Three surfactants were chosen based on their ionic nature and standard: non-ionic Triton X-100 and Pluronic F-127, and anionic cetyl triammonium bromide (CTAB). Surfactants were purchased from Sigma-Aldrich (Merck KGaA, Darmstadt, Germany). The surfactants were diluted in deionized water to form solutions with varying dissolutions (1, 2.5, 10 wt. %).

Preparation of NFC-CNT Aqueous Dispersion

The NFC and CNT were sonicated simultaneously and after sonication no centrifuge was used so that the preparation of aqueous dispersions could be achieved using a minimum amount of processing phases. NFC-CNT aqueous dispersions with a total volume of 80 mL were prepared. One set contained NFC (0.25 wt. %), CNTs (0.05 wt. %), deionized water and one of the selected surfactants (Triton X-100, 0.25 wt. %, Pluronic F-127, 0.09 wt. % and 0.3 wt. % and CTAB 0.30 wt. %). Details about preparation produce are showed as Figure 6.

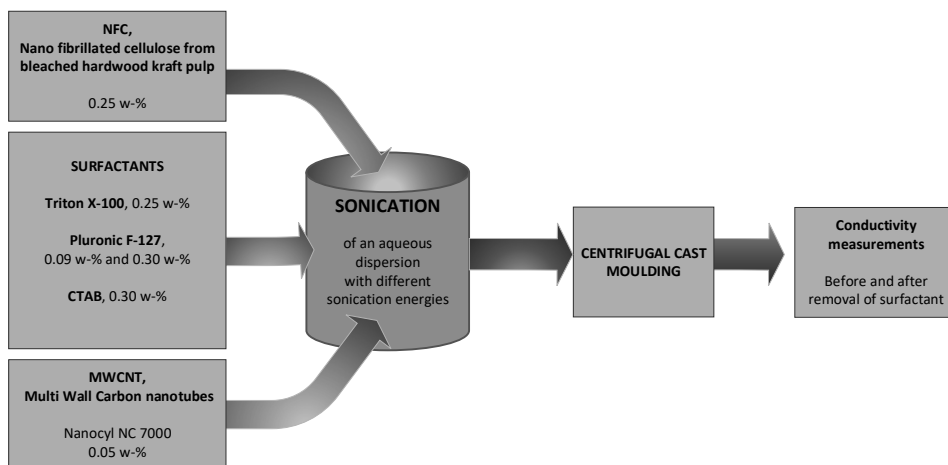


Figure 6. Preparation procedure of NFC-CNT dispersion and nanocomposite films.

The total dry mass for all the dispersions was 0.24 g. The sonication of the dispersion samples was performed with a tip horn (ϕ 12.7 mm) sonicator Q700 (QSonica LLC., Newton, CT, USA) in 100 mL glass beakers. The sonication amplitude of vibration (50%) was kept constant. The power output remained between 60 and 70 W for every sonication. The system included a water bath to keep

samples cool during the sonication so that temperature would not rise above 30 °C. The water bath was cooled by circulating cooling glycerol through a chiller (PerkinElmer C6 Chiller, PerkinElmer Inc., Waltham, MA, USA). Samples were sonicated for four different amounts of energies per dry mass, respectively 166, 333, 500 and 666 kJ/g, which corresponded to energies of 40, 80, 120 and 160 kJ. Unsonicated samples manufactured using all three surfactants were not homogenous, and this is why film formation was unsuccessful and not analyzed.

5. Conclusions

The typical approach to the manufacturing of conductive cellulose–CNT films has been to increase CNT weight percentage without optimizing the dispersion procedure. In this study, NFC and multiwall carbon nanotubes (MWCNT) were used to prepare composite films using a minimum number of processing phases (e.g., no centrifugal dispersion or pressing of the film were used), materials and chemicals. The amount of CNTs was 0.05 wt. % in dispersion and 16 wt. % in the film after the evaporation of water in ratio to dry mass content of NFC and CNT. The effect of surfactant type (Triton X-100, Pluronic F-127 and CTAB) and sonication energy on the electrical conductivity of NFC–CNT nanocomposite films was investigated to identify optimal processing conditions for high conductivity of the nanocomposite. A conductivity of 5.36 S/cm was achieved by using Pluronic F-127 surfactant and 666 kJ/g of sonication energy. In addition, removal of the surfactant from film and its effect on the electrical conductivity was studied. A dramatic increase in conductivity values from approximately 3.0 S/cm to a value of 8.42 S/cm was observed for films manufactured with surfactant Triton X-100. Conductivity diagrams of the nanocomposite films show that sonication affects the electrical performance of the films. SEM images of sonicated samples showed that the films sonicated at 166 kJ/g have a more porous structure than the films sonicated at higher energy. The imaging also showed that the CNTs form a more consistent network with a combination of high sonication energy and surfactant removal. It can be concluded that the following parameters significantly affect the conductivity of NFC–CNT nanocomposite films:

- (a) Surfactant type
- (b) Surfactant concentration
- (c) Sonication energy
- (d) Removal of the used surfactant
- (e) Film processing technique

To summarize, we manufactured nanocomposite films with exemplary conductivity in comparison to reported research and this was achieved by optimizing processing parameters and materials. Further research on the surfactant types and concentration can lead to better dispersion of the CNTs and therefore even higher conductivity.

Author Contributions: S.S. and P.K. conceived and designed the experiments; S.S. and A.R. performed the experiments and analyzed the data; V.K. and A.H. contributed materials; S.S., A.R., P.K., S.T. and K.R.R. wrote the paper. M.K. and J.V. coordinated the project aims in accordance to publication specific actions and delegation.

Funding: This research received no external funding.

Acknowledgments: This work was funded by Tekes (Finnish Funding Agency for Innovation) through a strategic opening entitled Design Driven Value Chains in the World of Cellulose (DWoC 2.0). We acknowledge the contributions of Jarmo Laakso and Essi Sarlin for SEM imaging.

Conflicts of Interest: The authors declare no conflict of interest.

References

1. Huang, J.C. Carbon black filled conducting polymers and polymer blends. *Adv. Polym. Technol.* **2002**, *21*, 299–313. [CrossRef]
2. Ma, P.C.; Siddiqui, N.A.; Marom, G.; Kim, J.K. Dispersion and functionalization of carbon nanotubes for polymer-based nanocomposites: A review. *Compos. Part A Appl. Sci. Manuf.* **2010**, *41*, 1345–1367. [CrossRef]

3. Pereira, C.; Nóvoa, P.J.R.O.; Calard, V.; Forero, S.; Hepp, F.; Pambaguian, L. Characterization of Carbon Nanotube Papers Infused with Cyanate-Ester Resin. In Proceedings of the ICCM International Conference on Composite Materials, Edinburgh, UK, 27–31 July 2009.
4. Layek, R.K.; Das, A.K.; Park, M.J.; Kim, N.H.; Lee, J.H. Enhancement of physical, mechanical, and gas barrier properties in noncovalently functionalized graphene oxide/poly(vinylidene fluoride) composites. *Carbon N. Y.* **2015**, *81*, 329–338. [CrossRef]
5. Palola, S.; Sarlin, E.; Kolahgar Azari, S.; Koutsos, V.; Vuorinen, J. Microwave induced hierarchical nanostructures on aramid fibers and their influence on adhesion properties in a rubber matrix. *Appl. Surf. Sci.* **2017**, *410*, 145–153. [CrossRef]
6. Hamed, M.M.; Hajian, A.; Fall, A.B.; Hkansson, K.; Salajkova, M.; Lundell, F.; Wgberg, L.; Berglund, L.A. Highly conducting, strong nanocomposites based on nanocellulose-assisted aqueous dispersions of single-wall carbon nanotubes. *ACS Nano* **2014**, *8*, 2467–2476. [CrossRef] [PubMed]
7. Tuukkanen, S.; Streiff, S.; Chenevier, P.; Pinault, M.; Jeong, H.J.; Enouz-Vedrenne, S.; Cojocar, C.S.; Pribat, D.; Bourgoin, J.P. Toward full carbon interconnects: High conductivity of individual carbon nanotube to carbon nanotube regrowth junctions. *Appl. Phys. Lett.* **2009**, *95*, 113108. [CrossRef]
8. Haghi, A.K.; Thomas, S. *Carbon Nanotubes: Theoretical Concepts and Research Strategies for Engineers*; Apple Academic Press: Waretown, NJ, USA, 2015.
9. Jung, R.; Kim, H.-S.; Kim, Y.; Kwon, S.-M.; Lee, H.S.; Jin, H.-J. Electrically Conductive Transparent Papers Using Multiwalled Carbon Nanotubes. *J. Polym. Sci. Part B Polym. Phys.* **2008**, *46*, 1235–1242. [CrossRef]
10. Haghi, A.K.; Zaikov, G.E. *Advanced Nanotube and Nanofiber Materials*; Nova Science Publishers, Inc.: New York, NY, USA, 2012; ISBN 978-1-62-081201-3.
11. Hoeng, F.; Denneulin, A.; Bras, J. Use of nanocellulose in printed electronics: A review. *Nanoscale* **2016**, *8*, 13131–13154. [CrossRef] [PubMed]
12. Gardner, D.J.; Oporto, G.S.; Mills, R.; Samir, M.A.S.A. Adhesion and surface issues in cellulose and nanocellulose. *J. Adhes. Sci. Technol.* **2008**, *22*, 545–567. [CrossRef]
13. Kuzmenko, V.; Naboka, O.; Haque, M.; Staaf, H.; Göransson, G.; Gatenholm, P.; Enoksson, P. Sustainable carbon nanofibers/nanotubes composites from cellulose as electrodes for supercapacitors. *Energy* **2015**, *90*, 1490–1496. [CrossRef]
14. Lehtimäki, S.; Tuukkanen, S.; Pörhönen, J.; Moilanen, P.; Virtanen, J.; Honkanen, M.; Lupo, D. Low-cost, solution processable carbon nanotube supercapacitors and their characterization. *Appl. Phys. A Mater. Sci. Process.* **2014**, *117*, 1329–1334. [CrossRef]
15. Lee, T.W.; Lee, S.E.; Jeong, Y.G. Carbon nanotube/cellulose papers with high performance in electric heating and electromagnetic interference shielding. *Compos. Sci. Technol.* **2016**, *131*, 77–87. [CrossRef]
16. Yun, S.; Kim, J. Multi-walled carbon nanotubes-cellulose paper for a chemical vapor sensor. *Sens. Actuators B Chem.* **2010**, *150*, 308–313. [CrossRef]
17. Qi, H.; Liu, J.; Pionteck, J.; Pötschke, P.; Mäder, E. Carbon nanotube-cellulose composite aerogels for vapour sensing. *Sens. Actuators B Chem.* **2015**, *213*, 20–26. [CrossRef]
18. Qi, H.; Mäder, E.; Liu, J. Unique water sensors based on carbon nanotube-cellulose composites. *Sens. Actuators B Chem.* **2013**, *185*, 225–230. [CrossRef]
19. Wang, M.; Anoshkin, I.V.; Nasibulin, A.G.; Korhonen, J.T.; Seitsonen, J.; Pere, J.; Kauppinen, E.I.; Ras, R.H.A.; Ikkala, O. Modifying native nanocellulose aerogels with carbon nanotubes for mechanoresponsive conductivity and pressure sensing. *Adv. Mater.* **2013**, *25*, 2428–2432. [CrossRef] [PubMed]
20. Oya, T.; Ogino, T. Production of electrically conductive paper by adding carbon nanotubes. *Carbon N. Y.* **2008**, *46*, 169–171. [CrossRef]
21. Hu, L.; Choi, J.W.; Yang, Y.; Jeong, S.; La Mantia, F.; Cui, L.-F.; Cui, Y. Highly conductive paper for energy-storage devices. *Proc. Natl. Acad. Sci. USA* **2009**, *106*, 21490–21494. [CrossRef] [PubMed]
22. Fugetsu, B.; Sano, E.; Sunada, M.; Sambongi, Y.; Shibuya, T.; Wang, X.; Hiraki, T. Electrical conductivity and electromagnetic interference shielding efficiency of carbon nanotube/cellulose composite paper. *Carbon N. Y.* **2008**, *46*, 1256–1258. [CrossRef]
23. Imai, M.; Akiyama, K.; Tanaka, T.; Sano, E. Highly strong and conductive carbon nanotube/cellulose composite paper. *Compos. Sci. Technol.* **2010**, *70*, 1564–1570. [CrossRef]
24. Yoon, S.H.; Jin, H.J.; Kook, M.C.; Pyun, Y.R. Electrically conductive bacterial cellulose by incorporation of carbon nanotubes. *Biomacromolecules* **2006**, *7*, 1280–1284. [CrossRef] [PubMed]

25. Toomadj, F.; Farjana, S.; Sanz-Velasco, A.; Naboka, O.; Lundgren, P.; Rodriguez, K.; Toriz, G.; Gatenholm, P.; Enoksson, P. Strain sensitivity of carbon nanotubes modified cellulose. *Procedia Eng.* **2011**, *25*, 1353–1356. [CrossRef]
26. Liu, Y.; Liu, D.; Ma, Y.; Sui, G. Characterization and properties of transparent cellulose nanowhiskers-based graphene nanoplatelets/multi-walled carbon nanotubes films. *Compos. Part A Appl. Sci. Manuf.* **2016**, *86*, 77–86. [CrossRef]
27. Chen, C.; Mo, M.; Chen, W.; Pan, M.; Xu, Z.; Wang, H.; Li, D. Highly conductive nanocomposites based on cellulose nanofiber networks via NaOH treatments. *Compos. Sci. Technol.* **2018**, *156*, 103–108. [CrossRef]
28. Hilding, J.; Grulke, E.; George Zhang, Z.; Lockwood, F. Dispersion of Carbon Nanotubes in Liquids. *J. Dispers. Sci. Technol.* **2003**, *24*, 1–41. [CrossRef]
29. Vaisman, L.; Wagner, H.D.; Marom, G. The role of surfactants in dispersion of carbon nanotubes. *Adv. Colloid Interface Sci.* **2006**, *128–130*, 37–46. [CrossRef] [PubMed]
30. Rastogi, R.; Kaushal, R.; Tripathi, S.K.; Sharma, A.L.; Kaur, I.; Bharadwaj, L.M. Comparative study of carbon nanotube dispersion using surfactants. *J. Colloid Interface Sci.* **2008**, *328*, 421–428. [CrossRef] [PubMed]
31. Bai, J.B.; Allaoui, A. Effect of the length and the aggregate size of MWNTs on the improvement efficiency of the mechanical and electrical properties of nanocomposites—Experimental investigation. *Compos. Part A Appl. Sci. Manuf.* **2003**, *34*, 689–694. [CrossRef]
32. Salajkova, M.; Valentini, L.; Zhou, Q.; Berglund, L.A. Tough nanopaper structures based on cellulose nanofibers and carbon nanotubes. *Compos. Sci. Technol.* **2013**, *87*, 103–110. [CrossRef]
33. Huang, Y.Y.; Terentjev, E.M. Dispersion and rheology of carbon nanotubes in polymers. *Int. J. Mater. Form.* **2008**, *1*, 63–74. [CrossRef]
34. Gimåker, M.; Östlund, M.; Östlund, S.; Wågberg, L. Influence of beating and chemical additives on residual stresses in paper. *Nord. Pulp Pap. Res. J.* **2011**, *26*, 445–451. [CrossRef]
35. Baez, C.; Considine, J.; Rowlands, R. Influence of drying restraint on physical and mechanical properties of nanofibrillated cellulose films. *Cellulose* **2014**, *21*, 347–356. [CrossRef]
36. Rosen, M.J. *Surfactants and Interfacial Phenomena*; John Wiley & Sons, Inc.: Hoboken, NJ, USA, 2004; ISBN 978-0-47-147818-8.
37. Keinänen, P.; Siljander, S.; Koivula, M.; Sethi, J.; Vuorinen, J.; Kanerva, M. Optimized dispersion quality of aqueous carbon nanotube colloids as a function of sonochemical yield and surfactant/CNT ratio. *Heliyon* **2018**, in press.
38. Blanch, A.J.; Lenehan, C.E.; Quinton, J.S. Optimizing Surfactant Concentrations for Dispersion of Single-Walled Carbon Nanotubes in Aqueous Solution. *J. Phys. Chem. B* **2010**, *114*, 9805–9811. [CrossRef] [PubMed]
39. Yu, J.; Grossiord, N.; Koning, C.E.; Loos, J. Controlling the dispersion of multi-wall carbon nanotubes in aqueous surfactant solution. *Carbon N. Y.* **2007**, *45*, 618–623. [CrossRef]
40. Islam, M.F.; Rojas, E.; Bergey, D.M.; Johnson, A.T.; Yodh, A.G. High weight fraction surfactant solubilization of single-wall carbon nanotubes in water. *Nano Lett.* **2003**, *3*, 269–273. [CrossRef]
41. Utsumi, S.; Kanamaru, M.; Honda, H.; Kanoh, H.; Tanaka, H.; Ohkubo, T.; Sakai, H.; Abe, M.; Kaneko, K. RBM band shift-evidenced dispersion mechanism of single-wall carbon nanotube bundles with NaDDBS. *J. Colloid Interface Sci.* **2007**, *308*, 276–284. [CrossRef] [PubMed]
42. Sun, Z.; Nicolosi, V.; Rickard, D.; Bergin, S.D.; Aherne, D.; Coleman, J.N. Quantitative Evaluation of Surfactant-stabilized Single-walled Carbon Nanotubes: Dispersion Quality and Its Correlation with Zeta Potential. *J. Phys. Chem. C* **2008**, *112*, 10692–10699. [CrossRef]
43. Maillaud, L.; Zakri, C.; Ly, L.; Pénicaud, A.; Poulin, P. Conductivity of transparent electrodes made from interacting nanotubes. *Appl. Phys. Lett.* **2013**, *103*, 263106. [CrossRef]
44. Bai, Y.; Lin, D.; Wu, F.; Wang, Z.; Xing, B. Adsorption of Triton X-series surfactants and its role in stabilizing multi-walled carbon nanotube suspensions. *Chemosphere* **2010**, *79*, 362–367. [CrossRef] [PubMed]
45. Calvaresi, M.; Dallavalle, M.; Zerbetto, F. Wrapping nanotubes with micelles, Hemimicelles, and cylindrical micelles. *Small* **2009**, *5*, 2191–2198. [CrossRef] [PubMed]
46. Geng, Y.; Liu, M.Y.; Li, J.; Shi, X.M.; Kim, J.K. Effects of surfactant treatment on mechanical and electrical properties of CNT/epoxy nanocomposites. *Compos. Part A Appl. Sci. Manuf.* **2008**, *39*, 1876–1883. [CrossRef]

47. Bystrzejewski, M.; Huczko, A.; Lange, H.; Gemming, T.; Büchner, B.; Rummeli, M.H. Dispersion and diameter separation of multi-wall carbon nanotubes in aqueous solutions. *J. Colloid Interface Sci.* **2010**, *345*, 138–142. [CrossRef] [PubMed]
48. Angelikopoulos, P.; Gromov, A.; Leen, A.; Nerushev, O.; Bock, H.; Campbell, E.E.B. Below the CMC. *J. Phys. Chem. C* **2010**, *114*, 2–9. [CrossRef]
49. Bonard, J.; Stora, T.; Salvétat, J.; Maier, F.; Stockli, T.; Duschl, C.; De Heer, W.A.; Forró, L.; Châtelain, A. Purification and Size-Selection of Carbon Nanotubes. *Adv. Mater.* **1997**, *9*, 827–831. [CrossRef]
50. Lu, P.; Hsieh, Y. Lo Multiwalled carbon nanotube (MWCNT) reinforced cellulose fibers by electrospinning. *ACS Appl. Mater. Interfaces* **2010**, *2*, 2413–2420. [CrossRef] [PubMed]
51. Rossell, M.D.; Kuebel, C.; Ilari, G.; Rechberger, F.; Heiligtag, F.J.; Niederberger, M.; Koziej, D.; Erni, R. Impact of sonication pretreatment on carbon nanotubes: A transmission electron microscopy study. *Carbon N. Y.* **2013**, *61*, 404–411. [CrossRef]
52. Yang, D.; Rochette, J.-F.; Sacher, E. Functionalization of Multiwalled Carbon Nanotubes by Mild Aqueous Sonication. *J. Phys. Chem. B* **2005**, *109*, 7788–7794. [CrossRef] [PubMed]
53. Dassios, K.G.; Alafogianni, P.; Antiohos, S.K.; Leptokaridis, C.; Barkoula, N.M.; Matikas, T.E. Optimization of sonication parameters for homogeneous surfactant assisted dispersion of multiwalled carbon nanotubes in aqueous solutions. *J. Phys. Chem. C* **2015**, *119*, 7506–7516. [CrossRef]
54. Fuge, R.; Liebscher, M.; Schröfl, C.; Oswald, S.; Leonhardt, A.; Büchner, B.; Mechtcherine, V. Fragmentation characteristics of undoped and nitrogen-doped multiwalled carbon nanotubes in aqueous dispersion in dependence on the ultrasonication parameters. *Diam. Relat. Mater.* **2016**, *66*, 126–134. [CrossRef]
55. Rajala, S.; Tuukkanen, S.; Halttunen, J. Characteristics of piezoelectric polymer film sensors with solution-processable graphene-based electrode materials. *IEEE Sens. J.* **2015**, *15*, 3102–3109. [CrossRef]
56. Xiao, W.; Wu, T.; Peng, J.; Bai, Y.; Li, J.; Lai, G.; Wu, Y.; Dai, L. Preparation, structure, and properties of chitosan/cellulose/multiwalled carbon nanotube composite membranes and fibers. *J. Appl. Polym. Sci.* **2013**, *128*, 1193–1199. [CrossRef]
57. Huang, H.D.; Liu, C.Y.; Zhang, L.Q.; Zhong, G.J.; Li, Z.M. Simultaneous reinforcement and toughening of carbon nanotube/cellulose conductive nanocomposite films by interfacial hydrogen bonding. *ACS Sustain. Chem. Eng.* **2015**, *3*, 317–324. [CrossRef]
58. Yamakawa, A.; Suzuki, S.; Oku, T.; Enomoto, K.; Ikeda, M.; Rodrigue, J.; Tateiwa, K.; Terada, Y.; Yano, H.; Kitamura, S. Nanostructure and physical properties of cellulose nanofiber-carbon nanotube composite films. *Carbohydr. Polym.* **2017**, *171*, 129–135. [CrossRef] [PubMed]
59. Mondal, S.; Ganguly, S.; Das, P.; Bhawal, P.; Das, T.K.; Nayak, L.; Khastgir, D.; Das, N.C. High-performance carbon nanofiber coated cellulose filter paper for electromagnetic interference shielding. *Cellulose* **2017**, *24*, 5117–5131. [CrossRef]



PUBLICATION

IV

**Conductive cellulose based foam formed 3D shapes—From innovation to
designed prototype**

S. Siljander, P. Keinänen, A. Ivanova, J. Lehmonen, S. Tuukkanen, M. Kanerva and
T. Björkqvist

Materials vol. 12.3 (2019), 430

Publication reprinted with the permission of the copyright holders

Article

Conductive Cellulose based Foam Formed 3D Shapes—From Innovation to Designed Prototype

Sanna Siljander ^{1,*}, Pasi Keinänen ¹, Anastasia Ivanova ², Jani Lehmonen ³, Sampo Tuukkanen ⁴, Mikko Kanerva ¹ and Tomas Björkqvist ¹

¹ Faculty of Engineering and Natural Sciences, Tampere University, P.O. Box 589, 33101 Tampere, Finland; pasi.keinanen@tuni.fi (P.K.); mikko.kanerva@tuni.fi (M.K.); tomas.bjorkqvist@tuni.fi (T.B.)

² Department of Design, Aalto University, P.O. Box 31000, 00076 Aalto, Finland; anastasia.ivanova@aalto.fi

³ VTT Technical Research Centre of Finland Ltd, P.O. Box 1000, 02044 VTT, Finland; jani.lehmonen@vtt.fi

⁴ Faculty of Medicine and Life Sciences, Tampere University; P.O. Box 589, 33101 Tampere, Finland; sampo.tuukkanen@tut.fi

* Correspondence: sanna.siljander@tuni.fi; Tel.: +358-503555777

Received: 7 December 2018; Accepted: 18 January 2019; Published: 31 January 2019



Abstract: In this article, we introduce for the first time, a method to manufacture cellulose based electrically conductive non-woven three-dimensional (3D) structures using the foam forming technology. The manufacturing is carried out using a minimum amount of processing steps, materials, and hazardous chemicals. The optimized solution applies a single surfactant type and a single predefined portion for the two main processing steps: (1) the dispersing of nanocellulose (NC) and carbon nanotubes (CNT) and (2) the foam forming process. The final material system has a concentration of the used surfactant that is not only sufficient to form a stable and homogeneous nanoparticle dispersion, but it also results in stable foam in foam forming. In this way, the advantages of the foam forming process can be maximized for this application. The cellulose based composite material has a highly even distribution of CNTs over the NC network, resulting a conductivity level of 7.7 S/m, which increased to the value 8.0 S/m after surfactant removal by acetone washing. Also, the applicability and a design product case ‘Salmiakki’ were studied where the advantages of the material system were validated for a heating element application.

Keywords: nanocellulose; carbon nanotube; foam forming; conductivity; Salmiakki

1. Introduction

Scientific and industrial research communities are giving considerable attention to smart and functional materials that are based on renewable bio-based resources and are processed in eco-friendly ways. Cellulose is a very potential substance as it is a bio-based material and it can be used as a matrix when manufacturing functional structures. In addition, scientific and technological development is mature for the emergence of controlled multi-length materials that take advantage of different forms of cellulose applied in optimal ways. The added functionality requires developing new manufacturing processes and, especially, adjusting the colloid dispersion upon material production [1,2]. Our innovation is to use nanocellulose (NC) as a carrier for carbon nanotubes (CNT) in the foam forming process. In this article, we introduce for the first time a method to manufacture cellulose based non-woven three-dimensional (3D) structures that are electrically conductive. The manufacturing of the conductive non-wovens is done using a minimum amount of processing steps, materials, and hazardous chemicals. Our target is to use the selected surfactant type and amount in both the dispersion processing step and in the foam forming step. The concentration of surfactant must be sufficient to form stable and homogeneous dispersion, but it should also allow the formation of stable foam.

The foam forming process has been studied since it was invented in the 1970s [3,4]. VTT Technical Research Centre of Finland has been active in the upscaling of foam forming technology and the first dynamic foam forming studies of the upscaling process were carried out with a modified semi-pilot scale former [5]. The foam forming technology enables the production and combination of a vast variety of fibre-based materials and the application of moulding technologies to form lightweight cellulosic 3D structures. In general, the foam forming technology utilizes aqueous foam instead of water as a carrier medium and the shear thinning behaviour of the foam makes it an excellent transport medium for fibres and particles, and it enables the excellent formation of the product being produced [6,7]. In addition, the air content of the carrier foam is 60–70% and it consists of air bubbles with a diameter below 100 μm . As stated in an article [8], interest is growing in the use of aqueous foam as a transporting medium of furnishes. By using the foam forming technology, a decrease in the cost of production and material savings can be achieved [6]. Furthermore, foam forming ensures structures that have excellent formation and, when combined with moulding technology, enables lightweight structures [9–11] and completely new functional product opportunities.

The functional cellulose based matrix structure can be done by adding organic or inorganic nanostructured components. As one of the numerous options, carbon nanotubes (CNT) provide excellent electrical properties. CNTs have potential applications in electronics, for example, as interconnects [12] or energy storages [13]. The true conductivity potential of CNTs can be uncovered when the dispersing step to a liquid medium is performed properly to form a percolation network. Recent studies have revealed that the process of dispersing CNTs in a water-based system can be optimised so that the outcome functionality increases exponentially [14,15]. It is reported in those articles that, when using sonication as a dispersing process, the applied sonication energy to the dispersion and a properly selected surfactant play a key role when optimizing conductivity properties and dispersion quality. In the event, where cellulose pulp and NC-CNT dispersion are combined in the foam forming process, it is crucial to have the right concentration of surfactant to ensure there is enough air in the foam. Thus, a highly homogeneous dispersion of pulp fibres must be reached. The selection of the surfactant must be based on a systematic study to ensure that it will function as a dispersing aid in the sonication process but also form stable foam upon foam forming.

One of the most commonly used surfactants for foam forming is the anionic surfactant sodium dodecyl sulphate (SDS), which is used in many industrial applications, such as shampoos, toothpastes, and shaving creams. The motive for the wide use is its relatively low price, foam stability, easy diffusion in water and therefore it can be used in rapid foaming [16]. However, SDS might still not be the optimal surfactant, since it has been shown that SDS as a surfactant of a water-CNT system does not disperse CNTs optimally to homogeneous dispersion, even if the higher sonication energy and concentration of surfactant are used [15]. The results in the cited study also clarify that, when surfactant Triton X-100 is used, stable homogeneous CNT-water dispersion can be achieved.

When the target is to form stable and homogeneous dispersion of CNTs and nano-fibrillated cellulose, basically two alternatives of non-ionic surfactants exist, in addition to the basic case where nanocellulose itself acts as a dispersing agent [17]. Based on the current literature [14,18], Pluronic F-127 and Triton X-100 surfactants have resulted in good conductivity values when NC-CNT dispersion is used to manufacture nanocomposite films with relatively low CNT concentration. Actually, the conductivity values of the nanocomposite film can be further increased by removing the surfactant e.g., by acetone washing. This effect was seen in samples when NC and CNTs were dispersed while using surfactant Triton X-100, but not in samples that were dispersed using Pluronic F-127. The reason for this might be that Pluronic F-127 surfactant prefers nanocellulose over carbon nanotubes and, respectively, Triton X-100 prefers carbon nanotubes. Removing Triton X-100 surfactant from the interfaces improves the conductivity values.

Nanocellulose interactions with different surfactant types are reported comprehensively in the review article [19]. In general, interaction between nanocellulose and surfactant has a dependency on nanocellulose isolation procedure, which affects the surface charge and crystalline level of cellulose

structure, which results as mobility in the wet state. Surface modification is needed to achieve interaction between different phases but often this is done at the cost of a given environmental effect, which is reached using nanocellulose as a structural component in composite structures. Using nanocellulose in papermaking processes has several advanced properties: it has a high aspect ratio, high strength along with good flexibility, an interaction potential via hydrogen bonding, and a tendency to form strong entangled networks. These properties mean that a high tensile strength is attainable at relatively low concentrations, lower than 5% with respect to pulp content [20,21]. Moreover, an increase in density has also been reported when nanocellulose is added to pulp. Nanocellulose attaches to the fibre surfaces as a layer and in this way a large contact area is formed, which increases the number of hydrogen bonds [22]. Using nanocellulose as a carrier for another material is mentioned in the patent filed by Tokushu Paper Manufacturing Co Ltd. They suggested using nanocellulose in tinted papers as a carrier for a dye or pigment [23]. Research group Hii et al. have reported in their article that microfibrillated cellulose contributed to the bonding of calcium carbonate filler in the fibre network of paper [24]. Nanocellulose is also suggested to be used as a biocarrier for controlled drug delivery [25].

The application of NC-CNT dispersions in the foam forming process enables the manufacturing of conductive 3D structures to almost any shape and size. Unfortunately, because of the nanoscale size of the CNTs, the formation with cellulose pulp alone does not occur efficiently enough to form the conductive percolation network during the foam forming process. When dispersion is prepared efficiently to form homogeneous dispersion without any aggregates present, the nanosized CNT particles flow through the cellulose fibre network in the vacuum assisted moulding with the foam. Our hypothesis is that nanocellulose can be used as a carrier for carbon nanotubes. It has been reported that nanocellulose can increase the strength of non-wovens that are manufactured using the foam forming process [6] and CNTs are good candidate to replace copper and aluminium as an interconnect material in the next generation electric devices [26].

When conductivity is reached to a certain level and an electric current is passaged through the structure, which acts like a resistive conductor, the system starts to heat due to its resistivity. This phenomenon is called resistive or Joule heating. Commonly personal heating elements are manufactured by inserting copper wire inside a seat heater or heating blanket. These types of multi-material structures are difficult to recycle, and heating occurs only near the conductive material. By harnessing carbon nanotubes as a conductive material for heating elements, it is possible to manufacture structures that do not create hot spots, act as a fire retardant, and the entire volume of the structure is functional (heating). Furthermore, it is possible to customize a maximum heating temperature of the heating element by adjusting the NC-CNT dispersion quality and the amount of CNTs in the foam formed structure.

2. Materials and Methods

In this study, nanocellulose production was based on the mechanical disintegration of bleached hardwood kraft pulp (BHKP). First, dried commercial BHKP produced from birch was soaked in water at approximately 1.7 wt % concentration and dispersed using a high shear Ystral dissolver for 10 min at 700 rpm. The chemical pulp suspension was preredefined in Masuko grinder (Supermasscolloider MKZA10-15), Masuko Sangyo Co., Kawaguchi, Japan) at 1500 rpm and then fluidized with eight passes through Microfluidizer (Microfluidics M-7115-30 Microfluidics Corp., Westwood, MA, USA) using 1800 MPa pressure. The final material appearance of NC was a viscous and opaque gel.

Multiwall carbon nanotubes were purchased from Nanocyl Inc. (MWCNT, Nanocyl 7000, Nanocyl SA., Sambreville, Belgium). CNTs were used as received, with-out pre-processing steps. This type of nanotubes is produced via catalytic chemical vapor deposition (CCVD).

The selection of used surfactant in this study was done based on the previous studies [14,15] and the requirement to reach an efficient foaming capability. Therefore, Triton X-100 was selected and it is a non-ionic surfactant that has a hydrophilic polyethylene oxide chain and an aromatic hydrophobic

group in its molecular structure. Triton X-100 was purchased from Sigma-Aldrich (Merck KGaA, Darmstadt, Germany).

The NC and CNT were sonicated simultaneously and after sonication no centrifuge was used so that the preparation of aqueous dispersions could be achieved using a minimum amount of processing steps. Two identical sets of NC-CNT aqueous dispersions with a total volume of 1800 mL were prepared. One set contained NC (0.15%), CNTs (0.3%), deionized water, and surfactant Triton X-100, 0.4% (Table 1). The total dry mass for the dispersions was 8.25 g. The sonication of the dispersions was performed using a tip horn (\varnothing 12.7 mm) sonicator Q700 with 20 kHz frequency (QSonica LLC., Newton, CT, USA) in 2000 mL glass beakers. The sonication amplitude of vibration (50%) was kept constant. The power output remained between 50 and 60 W for both sonications. The system included a water bath to keep dispersion cool during the sonication so that temperature would not rise above 30 °C. The water bath was cooled by circulating cooling glycerol through a chiller (PerkinElmer C6 Chiller, PerkinElmer Inc., Waltham, MA, USA). Dispersions were sonicated with energy per dry mass, respectively 700 kJ/g dry mass. The energy/dry mass indicates the total applied energy, not absorbed energy by dry mass. Part of the energy is used to heat the water and part is used to disperse nanoparticles. Also, part of the energy is used to degrade the sonicator itself and the vessel, to cause defects to the nanoparticles, and some energy is used to cause several different sonochemical reactions, like disintegration and the reorganization of water molecules [15,27].

Table 1. Material concentrations in different processing steps.

Material	Dispersion	Foam Forming
NC	0.15%	0.1%
CNT	0.3%	0.2%
Surfactant Triton X-100	0.4%	0.25%
Pulp	-	0.35%
Total volume	1800 mL	5500 mL

The cellulosic fiber material used in this study was gently refined bleached kraft pulp (Scots pine 3.7% dry mass), as obtained from a Finnish pulp mill.

In the foam forming process, two sets of NC-CNT dispersion each volume of 1800 mL were poured in to the foam forming 32 cm diameter cylindrical tank (Figure 1a), followed by water and pulp, so that total volume was 5.5 litres (Figure 1b). Concentrations of materials are listed in Table 1. Mechanical mixing was carried out at a rotation speed of 3500 rpm for 3.5 min. Foaming time resulted in 70% air content to the foam, meaning that the total foam volume was 19 l. The prepared foam containing NC-CNT and pulp was poured into a planar mould that has a perforated surface with area of 0.19 m², so that sheet formed 3D structure has a grammage of 100 g/m². Wet foam was removed using 0.5 bar vacuum suction and for maintaining constant local suction plastic film was placed on the top of the foam column. After vacuum assisted foam removal the 3D cellulosic fiber sheet was dried in a thermal cabinet at 70 °C for 12 h until dry. Also, reference sheets using bleached kraft pulp and Triton X-100 surfactant were processed using the same procedure.



Figure 1. (a) Laboratory scale foam forming equipment; (b) nanocellulose-carbon nanotubes (NC-CNT) dispersion, pulp, and water mixture before foaming.

The electrical conductivity of the foam formed non-wovens were measured using the four-probe measuring technique. With this method, it is possible to neglect the effect of contact resistances and thus provide more accurate conductivity measurements than using two-terminal measurement. The sheet resistances of prepared and cut foam formed non-wovens (size 30 mm × 30 mm) were measured using a four-point probe setup made in-house and a multimeter (Keithley 2002, Tektronix, Inc., Beaverton, OR, USA) in four-wire mode. The probes were placed in line, with equal 3 mm spacing. The four-probe setup is described elsewhere in detail [28]. The conductivity measurements were carried out using a 1 mA current and voltage was measured. Measurements were taken before and after the remaining surfactant was removed from samples by washing them in appropriate amount of acetone in room temperature (RT).

The mechanical testing (Testometric M500-25kN, Testometric Co Ltd, Rochdale, UK) of foam formed samples was done according to the standard EN 29073-3:1992 “Textiles. Test methods for non-wovens, Part 3: Determination of tensile strength and elongation”. From the foam formed non-wovens, ten sample pieces in total were cut (50 mm × 250 mm). Five of them were tested as such, while another set of five samples was washed in an appropriate amount of acetone in RT, so that the remaining surfactant Triton X-100 was removed. In general, the removal of surfactants from various nanocomposites can enhance the mechanical and electrical properties [14,29]. All of the non-woven samples were conditioned according to the standard ISO 139 before the tensile testing. The testing was performed by applying a constant rate of extension of 100 mm/min.

3. Results and Discussion

SEM imaging (FE-SEM, 3 kW, Zeiss ULTRaplus, Oberkochen, Germany) was used to investigate the CNT distribution in the foam formed non-wovens. The SEM images have been taken from a dry sample and the NC has generated a network where the dimensions for individual fibers are very difficult to determine. Two different magnifications in Figure 2 are illustrating the NC and the CNT interaction, and the formation of a homogeneous CNT coverage over cellulose fibers. Figure 2b describes a type of CNT coating on NC: the coverage has excellent distribution over the surface. This means that the dispersion process using the specific sonication parameters has been successful and a conductive percolation network of CNTs is formed.

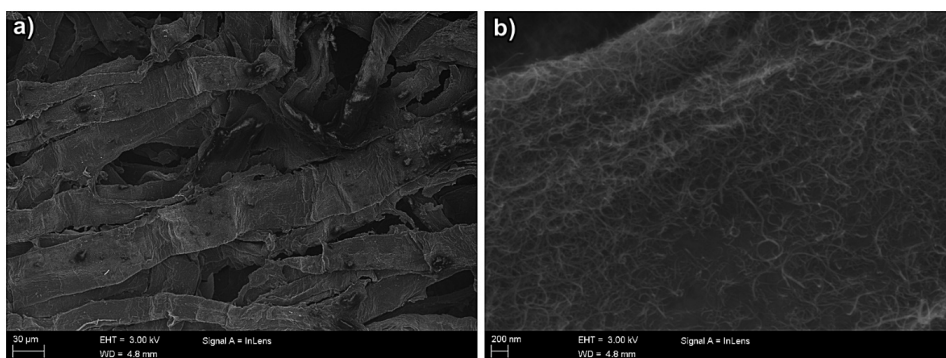


Figure 2. (a) Homogenous CNT coverage over cellulose fibers and (b) carbon nanotube percolation network on the surface of cellulose fiber.

The electrical conductivity and tensile testing of the foam formed non-woven material was measured before and after the removal of the surfactant. The non-woven material containing surfactant was determined to possess a conductivity of 7.7 S/m (± 1.32). After the removal of the surfactant, conductivity increases to a value of 8.0 S/m (± 1.34). The mechanical strength of the formed non-woven material is of essential importance for any practical application. Here, the tensile strength of the foam formed non-woven was 121 N (± 11.8). After surfactant was removed, the strength increased to a value of 142 N (± 6.1). In comparison, the tensile strength for foam formed reference non-woven made using the wood pulp, without nanocellulose or carbon nanotubes, is 9.4 N (± 0.5), and after acetone washing, to remove the surfactant, the value increased to 16.5 (± 1.7). This shows that nanocellulose and carbon nanotubes also increase the tensile strength of the non-woven composite structure. Also, the mechanical strength was expected to increase after removal of the surfactant, due to the increased entanglement and interactions of nanocellulose and carbon nanotubes.

The effect of surfactant removal by acetone washing is minimal to mechanical strength and conductivity values. The reason for this might be that a majority of the surfactant is already removed from the structure during the vacuum assisted moulding process. Results also show that adding NC-CNT dispersion in the foam forming procedure with wood pulp will increase the tensile values of the manufactured non-wovens. This three material system has over ten times higher tensile strength compared to one material pulp system when residue surfactant is still present in the non-woven structure.

The conductivity and mechanical performance of the final parameter set for the preparation led to results encouraging to the actual application verification. The high conductivity as well as mechanical strength mean that it is possible to manufacture conductive non-woven and utilize the innovated material system by using only two processing steps: (1) the sonication of the NC-CNT dispersion and (2) the foam forming of the final non-woven 3D structure.

4. Verification and Validation of Applicability: Heating Element “Salmiakki”

The verification study was carried out to manufacture a conductive 3D structure of a selected prototype using foam forming. The collaboration between designer and materials scientists has undergone the following steps:

1. Design briefing and setting the objective: a heating element
2. Research: material properties, benchmarking
3. Product innovation: user profiling (business case), user experience scenarios, product ideas, initial sketching, evaluation discussion, decision on the product features—heating element for indoor use and a device of a portable size and modular structure
4. Product design development: further sketching and paper mock-ups, evaluation discussion, decision on the visual form, clarifying the material specifications, testing of the material properties needed for the prototype manufacturing, CAD modelling, mold development for the foam forming process
5. Manufacturing and testing the prototype
6. Realistic rendering images of CAD model in interior settings
7. Establishing the outcomes of the collaborative process

Salmiakki, the heating element design taking advantage of conductive cellulose-based composite, is a result of close collaboration between a designer (A. Ivanova) and materials research scientists (S. Siljander and J. Lehmonen). The funding and targets of the product were a subtask in the national Design Driven Value Chains in the World of Cellulose (DWoC 2.0) project (www.cellulosefromfinland.fi). The objective was set to define the design of an electrical current-based heating element from newly developed conductive material that highlights the advantageous properties of this novel material and its production, provides a clear understanding of its future application possibilities, and emphasizes the local origin of raw materials that are used in the composite production. While features, such as high conductivity, no metal wires inside, temperature adjustability, mouldability, fire safety, light weight, soft material feeling, and recyclability make this material suitable for a variety of applications, several limiting factors, including restrictions in shape and color variations, needed to be considered to aim for the best performance and outlook.

Prior to the product ideation, a design research was conducted, which included benchmarking of existing indoor heating solutions, electrically-powered solutions, and solutions incorporating biomaterials. Benchmarking showed that a diverse variety of electrical interior heating designs are available on the market, however, biomaterials are seemingly not used for this type of applications. Based on a survey, no other product on the market offered bio-based, biodegradable indoor heating product solution with flexible temperature adjustment, and fabric-like tactile properties.

Product innovation was launched via creation of different user profiles. No in-depth user study was conducted prior to profile creation; the aim of profiles “personas”, was to serve as inspiration in the innovation and sketching the design process whilst helping to envision environments and situations where potential product’s users would benefit from the properties of conductive cellulose-based composite material. For instance, in addition to heating, such device could be used to keep places dry, serve as an acoustic element or room divider, and have a decorative purpose. As well as in home interiors, it could be used inside boats, cars, campervans, or other spaces that are protected from direct contact with water. Consequently, the decision was made to design a compact heating element of portable size and modular format, for indoor usage.

Visual design was initially carried out through the creation of sketches and scaled mock-ups, followed by full-scale paper models, which were discussed at the evaluation phase. Each paper model was considered for its functional and perceptual attributes, resulting in the choice of a diamond-like shape that has got the name “Salmiakki” due to its resemblance in shape and black color to a traditional Finnish candy.

For Salmiakki to be developed into a functional prototype, technical configurations of the material, direction of the electric current, and additional functional elements of the future heating device were outlined and observed when a CAD model was drawn. The CAD model was created for two major purposes: (1) to prepare a digital file for CNC-machinery of the mould for foam-forming process and (2) to create realistic 3D drawings to visualize the concept and plan modular compositions.

In order to manufacture the prototype a mould for foam forming process was sized and prepared. As a reference, the process of mould design for foam-formed cellulose fiber materials was considered, as described by Härkäsalmi et al. To ensure successful formability during the foam-forming process, the mould must have a sturdy structure withstanding the vacuum pressure (suction), and correct permeability allowing for water to pass through while capturing the cellulose fibers [8]. To achieve this, the structure was designed to consist of two parts, both being female moulds: load-bearing supporting structure machined from polystyrene foam and a smooth surface layer with micro-perforation, vacuum-formed from a polypropylene sheet with a 1.5 mm thickness. The prototype was manufactured at pilot plant of VTT Technical Research Centre of Finland located in the City of Jyväskylä.

Material concentrations and methods used were the same as in foam forming 3D sheets, only pulp concentration was increased to 85 g dry mass, meaning a concentration of 1.5% in foam forming. In Figure 3, a schematic flow of manufacturing of heating element Salmiakki is presented.

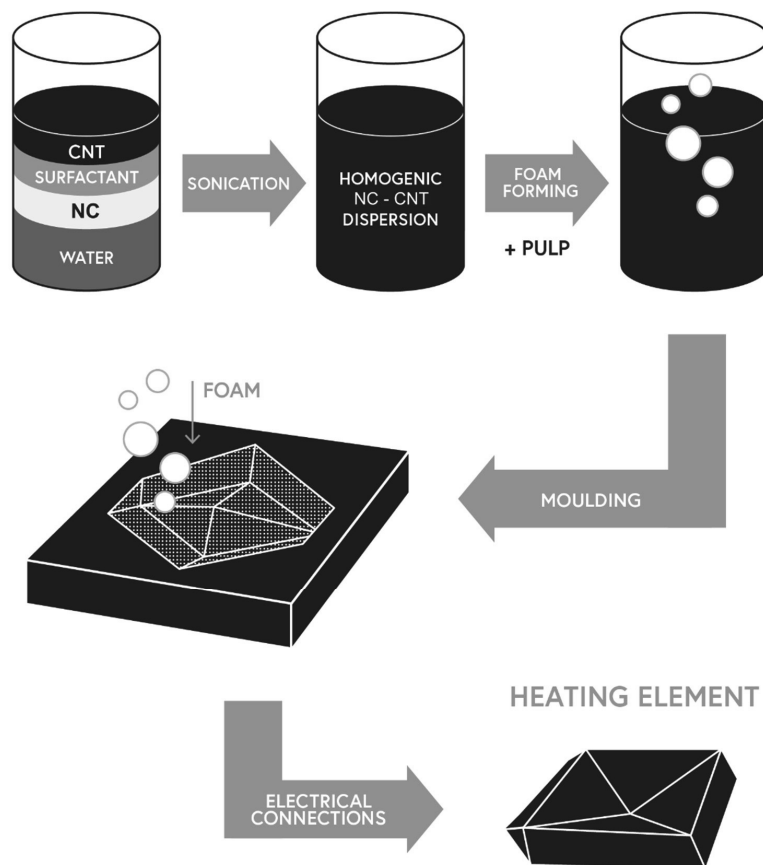


Figure 3. Manufacturing process of heating element prototype Salmiakki.

The sheet resistivity of the manufactured 3D shape was measured using the four-probe method before and after acetone washing. Average sheet resistances with standard deviation were, when measurements were performed from eight sample locations, $26.1 \Omega/\text{sq}$ (± 2.7), and after acetone washing, $25.8 \Omega/\text{sq}$ (± 2.0). Acetone washing did not decrease resistivity much, meaning that there is minimum amount of surfactant present in the structure that does not alter the conductivity of the carbon nanotubes. A post treatment option was studied to enhance the visual features and the conductivity. The final 3D structure was coated by the spray of NC-CNT dispersion that resulted darker, black finish and alongside, enhanced heating properties at a lower electrical voltage. If all electric energy P is converted into heat, then heater temperature can be evaluated using Joule's first law of heating $P = U^2 \times R^{-1}$, where U (electric voltage input, V) and R (resistance, Ω). Using the electric voltage input of 18.5 V with the resistivity of $25.8 \Omega/\text{sq}$, electric power of heating element is 13.2 W. After the post treatment spray layer of NC-CNT dispersion, the resistivity decreased to value $11.2 \Omega/\text{sq}$ (± 0.9), meaning that electric power is 30.6 W.

Finally, the cellulose fiber-based heating element was mounted in a plywood cover that was painted black using wood wax (Osmo Color 3169, Osmo Holz und Color GmbH & Co, Warendorf, Germany). The surface of the Salmiakki heating element was sprayed with varnish to gain glossy surface (Dupli-color Lackspray, Wolvega, Netherland) and electrical connections were installed. Copper tape forming the electrical connection are located on the opposing sides of the prototype Salmiakki and covering 18 cm^2 area per side. The distance between these copper connectors is 22 cm. As a power source Salmiakki is using 18.5 V, 3.5 A laptop charger (HP, Palo Alto, CA, USA). Infrared camera imaging was performed using a thermal camera (Fluke Ti400, Everett, WA, USA). In Figure 4, it can be observed that the temperature near copper tape conductors is $65\text{--}75 \text{ }^\circ\text{C}$ and a major part of Salmiakki heating element is heated to a comfortable $35\text{--}45 \text{ }^\circ\text{C}$ temperature at steady state in room temperature. Because of rapid heating and cooling properties of CNTs, the heating response of the whole element to steady state is in the order of minutes.

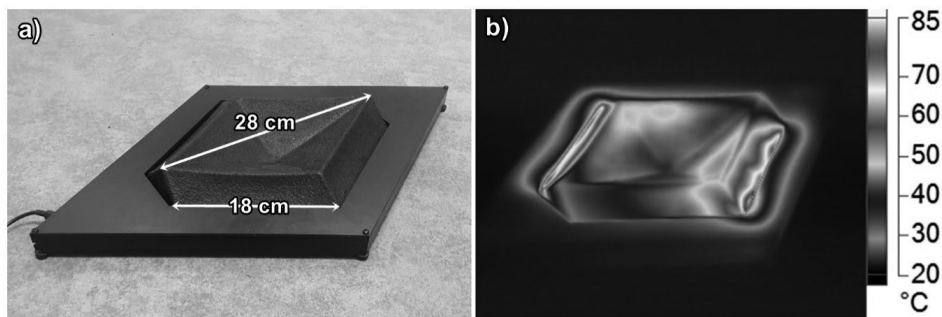


Figure 4. (a) Visual image of plywood mounted Salmiakki with dimensions and (b) Infrared camera image of heating element prototype Salmiakki at steady state in room temperature.

When calculated, based on the known pricing of raw materials, the total costs of Salmiakki heating element count less than four euros to manufacture the object (foaming plant investments not accounted for). In addition to the physical prototype, digital models that were rendered as realistic images of the heating element in use were produced to demonstrate how various modular compositions may be applied with various interior settings (see Figure 5).



Figure 5. Digital models of Salmiikki heating element.

The verification of the applicability via collaborative design, materials research, and prototype manufacturing process resulted in the following valid outcomes:

- Better understanding of application properties and overall possibilities of the novel conductive material
- Testing the foam-forming process of the conductive material into a complex three-dimensional object
- Effective dissemination of the research results for high technology readiness level (TRL) 6-7 through exhibiting of the physical prototype and sharing the digitally produced images.
- Deeper perspective of understanding the potential and possibilities of foam forming for producing functional 3D-structures.

5. Conclusions

This work focuses on the analysis of conductivity and mechanical strength of NC, CNT, and cellulose pulp based non-woven composite structure. Secondly, application of the foam forming process to prepare conductive non-woven sheets, where nanocellulose acts as a carrier for carbon nanotubes, is studied. Finally, the TRL 6-7 verification and validation programme is reported to establish industrial potential. The results show that it is possible to improve the surfactant selection, the sonication process of the NC-CNT dispersion, and foam forming to achieve the highly even coverage of CNT over the NC network, resulting in very high conductivity of 7.7 S/m. The effect of surfactant removal by acetone washing was studied, but the effects were not significant on the measured mechanical strength and conductivity values. Reason for this might be that the majority of surfactant is removed already during the vacuum assisted moulding process. The applicability and a design product case ‘Salmiikki’ were studied and the advantages of the material system were validated for a heating element application. The product case showed that it is possible to manufacture designed 3D heating element using a minimum amount of materials, processing steps, and hazardous chemicals.

These results mean that it is possible to manufacture conductive non-woven and utilize our innovation using only two processing steps: sonication of the NC-CNT dispersion and foam forming of the 3D structure. The whole process can be done using a minimum amount of materials and hazardous chemicals.

Author Contributions: S.S., P.K., A.I. and J.L. conceived and designed the experiments; S.S., P.K., A.I., J.L., and S.T. performed the experiments and analyzed the data; J.L. and A.I. contributed materials; S.S., P.K., A.I., J.L., S.T., M.K. and T.B. wrote the paper. M.K. and T.B. coordinated the projects aims in accordance to publication specific actions and delegation.

Funding: This work was funded by Tekes (Finnish Funding Agency for Innovation) through a strategic opening entitled Design Driven Value Chains in the World of Cellulose (DWoC 2.0) and Pirkanmaan liitto through project entitled BioÄly.

Acknowledgments: We acknowledge the contributions of Panu Lahtinen for cellulosic nanomaterial, Essi Sarlin for SEM imaging, Teija Joki for mechanical testing, Markus Kakkonen and Olli Tanhuanpää for all their help with manufacturing the heating element prototype “Salmiakki”.

Conflicts of Interest: The authors declare no conflict of interest.

References

- Klemm, D.; Schumann, D.; Kramer, F.; Hebler, N.; Koth, D.; Sultanova, B. Nanocellulose materials—Different cellulose, different functionality. *Macromol. Symp.* **2009**, *280*, 60–71. [CrossRef]
- Du, X.; Zhang, Z.; Liu, W.; Deng, Y. Nanocellulose-based conductive materials and their emerging applications in energy devices—A review. *Nano Energy* **2017**, *35*, 299–320. [CrossRef]
- Radvan, B.; Gatward, A.P.J. The Formation of wet-laid webs by a foaming process. *TAPPI J.* **1972**, *55*, 748.
- Punton, V.W. The use of an aqueous foam as a fibre-suspending medium in quality papermaking. In *Proceedings of a Symposium Organized by the Society of Chemical Industry. Colloid and Surface Chemistry Group, and Held at Brunel University*; Society of chemical industry: London, UK, 1975.
- Lehmonen, J.; Jetsu, P.; Kinnunen, K.; Hjelt, T. Potential of foam-laid forming technology in paper applications. *Nord. Pulp Pap. Res. J.* **2013**, 392–398. [CrossRef]
- Kinnunen, K.; Lehmonen, J.; Beletski, N.; Jetsu, P.; Hjelt, T. Benefits of foam forming technology and its applicability in high MFC addition structures. In *Proceedings of the 15th Pulp and Paper Fundamental Research Symposium*, Cambridge, UK, 8–13 October 2013.
- Smith, M.K.; Punton, V.W. Foam can improve formation. *Pulp Pap. Canada* **1975**, *76*, 55–58.
- Härkäsalmi, T.; Lehmonen, J.; Itälä, J.; Peralta, C.; Siljander, S.; Ketoja, J.A. Design-driven integrated development of technical and perceptual qualities in foam-formed cellulose fibre materials. *Cellulose* **2017**, *24*. [CrossRef]
- Madani, A.; Zeinoddini, S.; Varahmi, S.; Turnbull, H.; Phillion, A.B.; Olson, J.A.; Martinez, D.M. Ultra-lightweight paper foams: Processing and properties. *Cellulose* **2014**, *21*, 2023–2031. [CrossRef]
- Alimadadi, M.; Uesaka, T. 3D-oriented fiber networks made by foam forming. *Cellulose* **2016**, *23*, 661–671. [CrossRef]
- Haffner, B.; Dunne, F.F.; Burke, S.R.; Hutzler, S. Ageing of fibre-laden aqueous foams. *Cellulose* **2017**, *24*, 231–239. [CrossRef]
- Tuukkanen, S.; Streiff, S.; Chenevier, P.; Pinault, M.; Jeong, H.J.; Enouz-Vedrenne, S.; Cojocar, C.S.; Pribat, D.; Bourgoin, J.P. Toward full carbon interconnects: High conductivity of individual carbon nanotube to carbon nanotube regrowth junctions. *Appl. Phys. Lett.* **2009**, *95*. [CrossRef]
- Tuukkanen, S.; Välimäki, M.; Lehtimäki, S.; Vuorinen, T.; Lupo, D. Behaviour of one-step spray-coated carbon nanotube supercapacitor in ambient light harvester circuit with printed organic solar cell and electrochromic display. *Sci. Rep.* **2016**, *6*, 1–9. [CrossRef] [PubMed]
- Siljander, S.; Keinänen, P.; Rätty, A.; Ramakrishnan, K.R.; Tuukkanen, S.; Kunnari, V.; Harlin, A.; Vuorinen, J.; Kanerva, M. Effect of surfactant type and sonication energy on the electrical conductivity properties of nanocellulose-CNT nanocomposite films. *Int. J. Mol. Sci.* **2018**, *19*. [CrossRef] [PubMed]
- Keinänen, P.; Siljander, S.; Koivula, M.; Sethi, J.; Sarlin, E.; Vuorinen, J.; Kanerva, M. Optimized dispersion quality of aqueous carbon nanotube colloids as a function of sonochemical yield and surfactant/CNT ratio. *Heliyon* **2018**, *4*, e00787. [CrossRef] [PubMed]
- Al-Qararah, A.M. *Aqueous Foam as the Carrier Phase in the Deposition of Fibre Networks*; University of Jyväskylä: Jyväskylä, Finland, 2015.
- Hajian, A.; Lindström, S.B.; Pettersson, T.; Hamed, M.M.; Wågberg, L. Understanding the Dispersive Action of Nanocellulose for Carbon Nanomaterials. *Nano Lett.* **2017**, *17*, 1439–1447. [CrossRef] [PubMed]
- Rätty, A. Electro-mechanical integrity of nanocellulose-carbon nanotube films. Master’s Thesis, Tampere University of Technology, Tampere, Finland, 2017.
- Tardy, B.L.; Yokota, S.; Ago, M.; Xiang, W.; Kondo, T.; Bordes, R.; Rojas, O.J. Nanocellulose–surfactant interactions. *Curr. Opin. Colloid Interface Sci.* **2017**, *29*, 57–67. [CrossRef]
- Boufi, S.; González, I.; Delgado-Aguilar, M.; Tarrès, Q.; Mutjé, P. Nanofibrillated Cellulose as an Additive in Papermaking Process. In *Cellulose-Reinforced Nanofibre Composites Production, Properties and Applications*; Elsevier: Amsterdam, Netherlands, 2017; ISBN 9780081009659.

21. Kajanto, I.; Kosonen, M. The potential use of micro- and nanofibrillated cellulose as a reinforcement element in paper. *J. Sci. Technol. For. Prod. Process.* **2012**, *2*, 42–48.
22. Brodin, F.W.; Gregersen, Ø.W.; Syverud, K. Cellulose nanofibrils: Challenges and possibilities as a paper additive or coating material—A review. *Nord. Pulp Pap. Res. J.* **2014**, *29*, 156–166. [CrossRef]
23. Matsuda, Y.; Hirose, M.; Ueno, K. Super microfibrillated cellulose, process for producing the same, and coated paper and tinted paper using the same. United States Patent US 6183596 B1, 7 April 1995.
24. Hii, C.; Gregersen, Ø.W.; Chinga-Carrasco, G.; Eriksen, Ø. The effect of MFC on the pressability and paper properties of TMP and GCC based sheets. *Nord. Pulp Pap. Res. J.* **2012**, *27*, 388–396. [CrossRef]
25. Plackett, D.V.; Letchford, K.; Jackson, J.K.; Burt, H.M.; Jackson, J.; Burt, H. A review of nanocellulose as a novel vehicle for drug delivery. *Nord. Pulp Paper Res. J.* **2014**, *29*, 105–118. [CrossRef]
26. Ragab, T.; Basaran, C. Joule heating in single-walled carbon nanotubes. *J. Appl. Phys.* **2009**, *106*. [CrossRef]
27. Koda, S.; Kimura, T.; Kondo, T.; Mitome, H. A standard method to calibrate sonochemical efficiency of an individual reaction system. *Ultrason. Sonochem.* **2003**, *10*, 149–156. [CrossRef]
28. Rajala, S.; Tuukkanen, S.; Halttunen, J. Characteristics of piezoelectric polymer film sensors with solution-processable graphene-based electrode materials. *IEEE Sens. J.* **2015**, *15*, 1–8. [CrossRef]
29. Keinänen, P.; Das, A.; Vuorinen, J. Further Enhancement of Mechanical Properties of Conducting Rubber Composites Based on Multiwalled Carbon Nanotubes and Nitrile Rubber by Solvent Treatment. *Materials (Basel)* **2018**, *11*, 1806. [CrossRef]



© 2019 by the authors. Licensee MDPI, Basel, Switzerland. This article is an open access article distributed under the terms and conditions of the Creative Commons Attribution (CC BY) license (<http://creativecommons.org/licenses/by/4.0/>).

PUBLICATION

V

The effect of multi-wall carbon nanotube morphology on electrical and mechanical properties of polyurethane nanocomposites

J. Sethi, E. Sarlin, S. S. Meysami, R. Suihkonen, A. R. S. S. Kumar, M. Honkanen,
P. Keinänen, N. Grobert and J. Vuorinen

Composites Part A: Applied Science and Manufacturing vol. 102.(2017), 305–313

Publication reprinted with the permission of the copyright holders



The effect of multi-wall carbon nanotube morphology on electrical and mechanical properties of polyurethane nanocomposites



Jatin Sethi^a, Essi Sarlin^a, Seyyed Shayan Meysami^b, Reija Suihkonen^a, Arunjunai Raja Shankar Santha Kumar^a, Mari Honkanen^a, Pasi Keinänen^a, Nicole Grobert^b, Jyrki Vuorinen^{a,*}

^a Department of Materials Science, Tampere University of Technology, P.O. Box 589, FI-33101 Tampere, Finland

^b Department of Materials, University of Oxford, Oxford OX1 3PH, UK

ARTICLE INFO

Article history:

Received 17 November 2016
Received in revised form 1 June 2017
Accepted 11 August 2017
Available online 14 August 2017

Keywords:

A. Carbon nanotubes and nanofibres
A. Nanocomposites
B. Electrical properties
B. Mechanical properties

ABSTRACT

In this study, we examine the effect of multi-wall carbon nanotubes (MWCNT) morphology on electrical and mechanical properties of MWCNT-filled polyurethane (PU) nanocomposites. The main objective of this study is to understand the role of aspect ratio and length of MWCNTs in determining the performance of nanocomposites. Highly aligned MWCNTs were prepared by aerosol-assisted chemical vapour deposition method and compared to commercially available MWCNTs in PU matrix for ease of dispersibility and performance. We observed opposing influence of the MWCNT on electrical and mechanical behaviour of the nanocomposites. The electrical properties were proportional to length of the MWCNTs whereas the mechanical properties were dependent on the aspect ratio of the MWCNTs. Moreover, thicker nanotubes (approximately 40 nm) with a higher aspect ratio (approximately 225) are less prone to shortening and impart better tensile and storage modulus along with improved electrical and therefore are more suitable for the MWCNT nanocomposites.

© 2017 Elsevier Ltd. All rights reserved.

1. Introduction

Carbon nanotubes (CNTs) have excellent mechanical and physical properties such as strength, elastic modulus, and electrical and thermal conductivity [1]. They are an excellent candidate as reinforcements for nanocomposites, as they can improve mechanical strength and physical properties of polymeric matrix [1]. In nanocomposite applications, it is important to understand how the structure and the properties of nanotubes affect the mechanical properties such as strength and stiffness, and physical properties such as electrical and thermal conductivity of resulting composite. This field is rather less explored when it comes to CNTs.

The central thesis of this paper is to address the degree of uncertainty around understanding the effect of MWCNT morphology on the properties of MWCNT-filled nanocomposites. For electrical conductivity, it has consistently been reported that the aspect ratio is the most important parameters in determining the percolation threshold of nanocomposites [2–6]. On the other hand, some researchers have reported that length is the critical

factor in determining the percolation threshold [7,8]. Lima *et al.* found that longer MWCNTs result in lower percolation thresholds [9]. For electrical properties, the published findings seem to be contradictory and relevance of the aspect ratio appears to be debatable. On the other hand, for the mechanical properties of CNT-polymer composites, the aspect ratio has been proven to be reliable in estimating behaviour of nanocomposites [6,10–12]. However, there seems to be a gap in the evaluation of the mechanical and electrical properties of CNT-polymer composites simultaneously taking into account both the aspect ratio and the length of the CNTs. Moreover, a large number of studies looking at the effect of CNT morphology (aspect ratio, length) on properties of nanocomposites have not considered the effect of processing methods [5,6,13,14]. Commonly used processing methods such as sonication and melt processing are known to shorten the MWCNTs, hence leading to the reduction of their aspect ratio [15,16]. Therefore, a detailed study that evaluates the impact of actual morphology on electrical and mechanical properties of nanocomposites is needed.

In this paper we address the controversy arising from contradicting results published on effect of length and aspect ratio on performance of MWCNT filled nanocomposites, by designing an

* Corresponding author.

E-mail address: jyrki.vuorinen@tut.fi (J. Vuorinen).

experiment which simultaneously studies effect of length and aspect ratio on performance of the nanocomposites.

2. Experimental

Three types of MWCNTs of different aspect ratio were used: two of them were prepared using aerosol assisted chemical vapour deposition (AACVD) [17] and one commercially available. These MWCNTs were sonicated in water and Triton X-100, a commonly used surfactant, and the MWCNT length and diameter were determined using both scanning and transmission electron microscopy (SEM and TEM). MWCNTs with average aspect ratios of 110, 210 and 225 were then dispersed in water based polyurethane and solution casted to obtain nanocomposites. MWCNT/PU nanocomposites were evaluated for their electrical and mechanical properties.

3. Materials

Details of the MWCNT AACVD synthesis are described elsewhere [17–24]. Briefly, the AACVD setup consisted of a piezo-driven aerosol generator and a quartz reactor heated to 800–850 °C. A mixture of toluene ($C_6H_5CH_3$; Fluka; 99.7%) or ethylbenzene ($C_6H_5CH_2CH_3$; Sigma-Aldrich 99%) with ferrocene (5 wt%; $C_{10}H_{10}Fe$; Sigma-Aldrich 98%; purified by sublimation at 95 °C) was used as the precursor solutions. Prior to the synthesis, the aerosol generator unit was flushed with argon at room temperature. The aerosol was then carried into the reactor using argon with flow rates between 1.0 and 2.5 L/min. Table 1 contains the list of MWCNT samples and corresponding synthesis parameters, and their properties.

Commercially available MWCNTs Nanocyl NC 7000 (Nanocyl s. a., Belgium) were used as received without further processing in all experiments described in this article. They were selected for this study due to their high dispersibility which can be attributed to their loosely packed structure [25]. Specifications of all nanotubes used in this study are shown in Table 1. The MWCNTs are referred according to their aspect ratio after sonication, e.g., in-house generated MWCNTs are referred to as AR 110 and AR 225, whilst commercial MWCNTs (Nanocyl NC 7000) are labeled as AR 210, where AR stands for aspect ratio.

The characteristics of anionic aliphatic polyester-polyurethane dispersion Bayhydro[®] UH 240 in water are listed in Table 2. The polyurethane was selected for this study due to its versatility and current use in wide range of industrial applications such as adhesives [26], coatings [27], elastomers [28], biomedical applications [29] and foams [30].

Triton X-100, a non-ionic, octylphenoxyethylate surfactant was chosen for this study because it has been reported as most suitable and efficient surfactant for dispersion of MWCNTs in water [31,32].

Table 1
List of the MWCNT samples, corresponding synthesis parameters (reactor size, synthesis temperature, time and flow rate of carrier gas); and properties of MWCNTs (mean outer diameter, thickness of the carpets, Raman I_D/I_G , thermogravimetric analysis (TGA) temperature of 50% mass loss [20] and residual catalyst content).

Property	AR 110	AR 225	AR 210 (Nanocyl NC 7000)
Reactor size	60 cm long; 2.1 cm ID	120 cm long; 9.5 cm ID	Not known
Synthesis temperature (°C)	800	800	Not known
Synthesis time (min)	60	30	Not known
Argon flow rate (L/min)	1	2.5	Not known
Diameter	40–60 nm	30–50 nm	5–14 nm
Length	500–1000 μ m	300–800 μ m	1–3 μ m
Raman I_D/I_G	~0.4	~0.3	1.18–1.84 [56–59]
Residual Fe	~3 wt%	5–6 wt%	~10 wt% ^a
TGA T50%	~600 °C	600–620 °C	~580 °C[60]

^a Provided by manufacturer.

Table 2

Characteristics of Bayhydro[®] UH240 polymer dispersion in water as provided in technical data sheet provided by supplier [61].

Property	Value
Non-volatile content	40 ± 1 wt%
pH	6–8
Flow time at 23 °C, 4 mm cup	Max. 70 s
Appearance	Milky, cloudy
Density @ 20 °C	Approx. 1.1 g/cm ³
Mean particle size	210 nm

3.1. Preparation of MWCNT dispersions

For all samples, 0.6 wt% of MWCNTs were dispersed in 1.2 wt% solution of Triton X-100 in water using a Soniprep 150 plus with cylindrical titanium tip (diameter 9.5 mm) at a frequency of 23 kHz and a constant power of 20 W. The sonication was continued until maximum dispersion was achieved, determined by method reported by Grossiord *et al.* [33] whereby 3 μ l of the dispersion was collected after regular intervals of sonication, which was then further diluted in water with a factor of 750. UV absorbance was measured over a range of 250–500 nm with a sampling interval of 0.2 nm using a Shimadzu UV-1601 UV-VIS spectrometer. Sonication was stopped when the maximum absorbance value remained constant in two consecutive samples. The amount of surfactant was kept constant for all the MWCNTs because it affects the electrical and mechanical properties of polymeric composites [34–36] and we aimed to keep MWCNT morphology as the only variable.

3.2. Electron microscopy

Scanning and transmission electron microscopy (SEM and TEM) were used to determine the aspect ratio of the MWCNTs. Samples were prepared by drop casting the MWCNT dispersions in water on a copper grid (300 mesh) with a holey carbon film and air dried for 24 h. The length of MWCNTs after dispersion was determined by measuring the length of 50 MWCNTs using a Zeiss UTRApplus operated at 3.00 kV in conjunction with imageJ image analysis software by taking an average. For diameter measurements, a Jeol JEM 2100 TEM operating at 200 kV was used for imaging the MWCNTs and an average diameter of MWCNTs was determined again by measuring the diameter of 50 MWCNTs using imageJ image analysis software and taking an average. It was assumed that the diameter of MWCNTs was same before and after sonication. This assumption was made according to findings reported in previous work [37] [38]. Grossiord *et al.* mentioned that prolonged and intense sonication leads only to localized damage in SWCNT walls under intense sonification [37], therefore it can be inferred the diameter

remained the same. Similarly, Chen *et al.* reported that nitric acid treated CNTs are susceptible to damage, which induces notches in the outer layer, not removal of MWCNT walls [38]. This research has utilized mild sonication for a relatively short time. MWCNTs used in this work were not treated with chemicals such as nitric acid, so we believe that it is safe to assume that the diameter is not altered during the process. We should stress that for original aspect ratio calculations, the original length (before sonication) for AR 210 was calculated from the data provided by the manufacturer, as the supplied nanotubes were in bundle form and cannot be separated without damaging the original length. Similar limitation was observed for AR 110 and AR 225, in their case, the length was calculated by measuring the thickness of grown carpets in AACVD setups and taking average.

3.3. Preparation of nanocomposite

Composite films were prepared by solution casting on a glass Petri dish. The thickness of the films was approximately 800 μm measured by digital caliper. The concentration of MWCNTs was kept between 0 and 2 wt%. The MWCNT dispersion was mixed with a fixed amount of polymer solution and sonicated using the ultrasonic tip for 15 min before casting into a glass mould with a diameter of 10 cm. For measuring the influence of the aspect ratio on the performance of the composite, the MWCNT dispersions were also sonicated for 15 min to expose them to same amount of energy as the MWCNTs in the nanocomposites. After casting, the solution was stored overnight and to allow complete evaporation of water films were then annealed at 110 °C until the weight became constant, approximately 6 h. Before any testing, samples were conditioned in 50% relative humidity and at 20 °C temperature for 96 h. After conditioning, the water content was ca. 0.25 wt%, as measured using thermogravimetric analysis (TGA), see Fig. 11. The amount of surfactant in nanocomposite films was twice the amount of MWCNT films, for example 2 wt% MWCNT nanocomposite has 1 wt% MWCNT, 2 wt% surfactant and 97 wt% polyurethane.

3.4. Characterization of nanocomposites

Surface resistivity was measured by MetrISO 2000 resistance meter (Wolfgang Warmbier, Hilzingen, Germany); 100 V was applied through a surface resistance probe on a circular sample with diameter of approximately 10 cm. All measurements were performed at room temperature. The reported resistivity is an average of 5 measurements for each sample.

Stress-strain measurements were conducted on dog bone-shaped samples (type iV; ISO 37:2005) in order to analyse the mechanical behaviour of the composites. Tensile tests were carried out according to ISO 37:2005, using a Messphysik (midi 10-20/411, Messphysik Materials Testing GmbH, Fürstenfeld, Austria) universal testing machine at room temperature (23 °C). The crosshead speed was kept at 100 mm/min. The elastic modulus was measured in the linear region between 5 and 15%. Three samples were tested and reported as average.

PerkinElmer PYRIS Diamond DMA equipment was used for dynamic mechanical analysis of the samples. The operational mode was sinusoidal tension/compression with the amplitude of 40 μm and frequency of 1 Hz. The heating rate was kept constant at 3 °C/min.

4. Results and discussions

4.1. Effect of sonication

According to previous studies, sonication energy, not the sonication time is more precise parameter in determining the optimum dispersion state of carbon nanotubes [33,39]. Sonication energy (E) is defined by the following equation:

$$E = P * t / V$$

where P is output power in watts, t is time of sonication in seconds, and V is total volume of liquid in millilitres. This topic has been extensively researched by Grossiord and co-workers. According to them, characterizing the dispersion state with sonication energy provides reproducible results [40,41]. Additionally, Dutta and co-workers have comprehensively worked on effects of sonication on MWCNTs. They suggested “destruction reduced sonication protocol” which involves “mild sonication” for obtaining stable MWCNTs dispersion in organic solvent [42].

Ultrasonication has reported to effectively shorten CNTs [15]. However, extent of damage is not commonly comprehensively quantified in research papers. The effect of mild sonication on MWCNTs is given in Table 3 (by comparing average length and aspect ratio before and after sonication). It can be observed that sonication, even at low power, results in extreme shortening of MWCNTs. AR 110 shortened to 5.5 μm from 750 μm of average length. On the other hand, average length of AR 225 MWCNTs was down to 8 μm from pre-sonication average length of 550 μm . However, AR 210 suffered no loss in length, one of the possible reasons might be lower sonication time (energy) required for dispersion of AR 210 and their easy dispersibility (due to their loosely packed structure and low density [43,44]). AR 225 and AR 110 took more time (energy) to disperse because they are extra-long and highly-aligned.

Despite the fact that more defective CNTs are presumably more prone to ultrasound-induced shortening [45,46], no clear correlation between the defect density (Raman D/G) and shortening ($\frac{\text{length before sonication}}{\text{length after sonication}}$) was observed. AR 210 with highest density of structural defects showed negligible sensitivity to sonication, while AR110 and AR 225 with low defect densities dramatically shortened. Therefore, it seems that the effect of ultrasonication on the length of MWCNTs, as a critical processing parameter, requires further investigation.

Additionally, it is apparent that MWCNTs with large diameters can break more easily. AR 110, with diameters of ca. 50 nm were shortened by a factor of 140. On the other hand, the length of AR 225, which has an average diameter of 40 nm, was shortened by a factor of 70. The difference in diameter of MWCNTs can be observed in Fig. 2. Our results are in agreement with Heller *et al.*,

Table 3

Effect of sonication, extent of damage and aspect ratio measurements illustrating the extensive damage in MWCNTs even at low sonication energy.

Nanotubes	Approximate aspect ratio (Before Sonication)	Average diameter (nm)	Average length (after sonication) (μm)	Approximate aspect ratio (after sonication)	Sonication energy imparted (J/ml)
AR 225	13750	35 \pm 9	8 \pm 2.1	225	3900
AR 210	158 ^a	9.5 \pm 2.5	2 \pm 0.8	210	1500
AR 110	15,000	49 \pm 8	5.5 \pm 2	110	2700

^a Based on data provided by manufacturer.

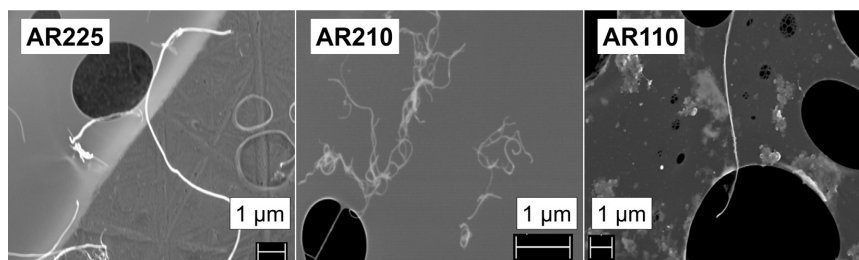


Fig. 1. SEM images (taken at different magnification) of MWCNTs after sonication treatment depicting the difference in morphology; an interesting observation is significantly difference in morphology; an interesting observation is significantly different appearance of the samples AR 225 and AR 210, revealing the uncertain nature of the aspect ratio. AR 210 are short, thin and twisted; AR 225 are thick and straight, although their aspect ratio is comparable.

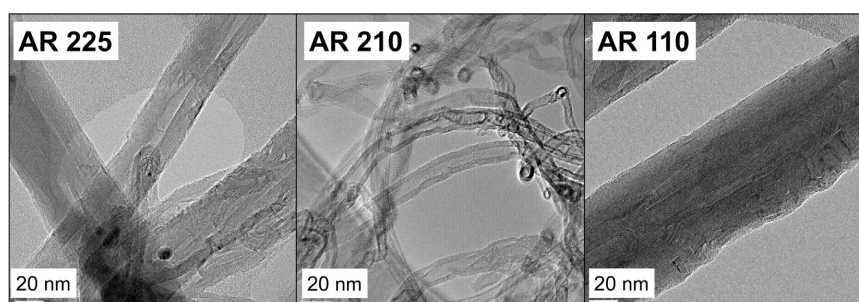


Fig. 2. TEM images showing the difference in nanotube width of the samples. AR 225 and AR 110 are straight and thick while AR 210 is curved and entangled.

who have reported that scission of nanotubes as a result of sonication is diameter sensitive, which means that MWCNTs with largest diameter are most affected [47].

The difference in aspect ratio can be easily seen in Fig. 1; AR 225 and AR 110 are clearly visible with thick thread like appearance; AR 210 is in the form of fine filaments. All the dispersions prepared for this study were stable (monitored by visual observation) for at least 4 weeks without any sedimentation, indicating that MWCNTs were finely dispersed in water.

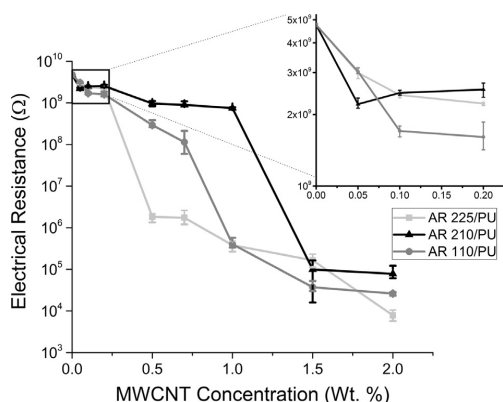


Fig. 3. Surface resistivity of MWCNT/PU samples with respect to concentration. The inset figure shows the region at low MWCNT concentration (up to 0.2 wt%). MWCNTs with longer length (AR 225 and AR 110) show a steep decrease in electrical resistivity, indicating ease of achieving percolation.

4.2. Electrical resistivity of nanocomposites

The electrical resistivity of nanocomposites at different MWCNT concentration is shown in Fig. 3. The steep decrease in resistivity values clearly indicates that an interconnected conductive network is formed with all types of MWCNTs [48]. The results strongly indicate that the percolation threshold is affected by the length of nanotubes. Among the longer nanotubes, In sample AR 225 percolation is achieved between 0.2 and 0.5 wt% whereas AR 110 has a percolation threshold of 0.6–1 wt%. The shorter AR 210 has percolation threshold of 1–1.5 wt% (Table 4). Moreover, the minimum resistivity is also lowest for the nanocomposite containing the longest nanoantubes (AR 225), which are one-third of the length of AR 110, and one-tenth of the AR 210 sample. It is apparent that the aspect ratio is not suitable for an approximation of the percolation threshold. The correlational analysis of performance (electrical and mechanical) against length and aspect ratio is presented in Figs. 6 and 7. In this particular case length, not aspect ratio, is more accurate to determine the electrical properties.

The percolation threshold of non-spherical fillers in matrix materials is theoretically estimated by the concept of excluded volume. The percolation threshold is related to the aspect ratio in following way [49]:

$$\varphi_p = \frac{1}{2AR} \quad (1)$$

where φ_p is the percolation threshold and AR is aspect ratio. It has been reported that a good agreement between experimental and theoretical values is observed [16,49]. However, our results contradict this theory as they strongly suggest that the aspect ratio, is not always inversely proportional to the percolation threshold. It appears that estimating the percolation threshold is a complicated

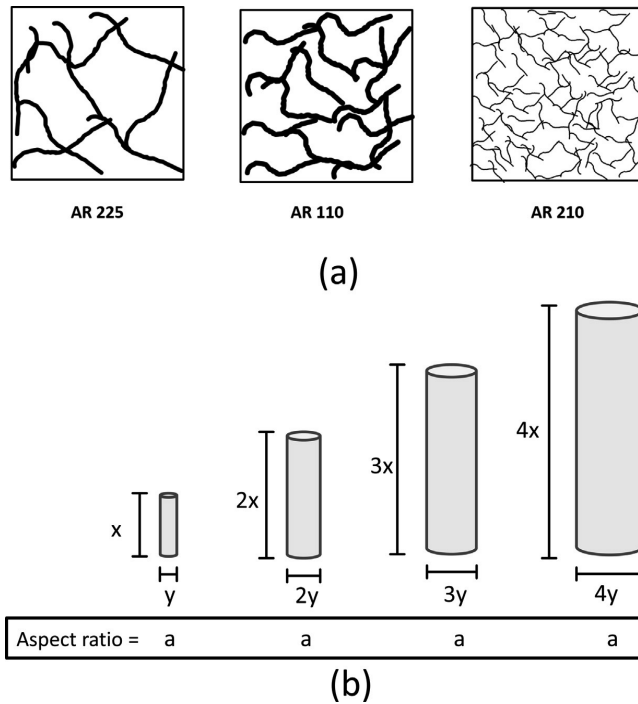


Fig. 4. Relative representation of aspect ratio: (a) Image depicting a possible orientation of nanotubes during formation of interconnected network in the polymeric matrix, clearly indicating that aspect ratio can be misleading in some cases. The image is drawn to scale keeping results from Table 4 in consideration. The graphic scale for MWCNTs portrayed in this image is different in length and width directions. (Scale Explanation- Length of MWCNTs: $1 \mu\text{m} = 0.46 \text{ cm}$, Width of MWCNTs: $1 \text{ nm} = 0.035 \text{ cm}$). (b) Image again further confirming the misleading nature of aspect ratio. All the hypothetical rod-shaped fillers have same the aspect ratio but significant difference in length and diameter. (For the interpretation of the references to colour in this figure legend, the reader is referred to the web version of this article.)

Table 4

Percolation and minimum resistivity data of MWCNT-filled nanocomposites indicating the proportional increase with respect of length of MWCNTs. The longest MWCNTs ($8 \mu\text{m}$) has 10-fold better electric current conduction in comparison to shortest MWCNT ($2 \mu\text{m}$).

MWCNT type	Average aspect ratio in matrix	Average length in matrix (μm)	Percolation threshold (wt%)	Minimum resistivity (Ω)
AR 225	225	8	0.2–0.5	7840
AR 210	210	2	1–1.5	78,200
AR 110	110	5.5	0.6–1	26,200

task and for a particular nanotube, it can depend on the aspect ratio or on the length of the nanotubes. (as in our results).

Fig. 4a depicts a sketch of a possible arrangement of well-dispersed MWCNTs (of proportional length and width of MWCNTs used in this study) embedded in an insulating matrix to show that interpreting percolation thresholds on the basis of aspect ratios can be misleading. It can be clearly observed that sample AR 210 contains significantly more MWCNTs AR 225 and AR 110, which explains our experimental results that AR 210 has a higher percolation threshold than AR 225 and AR 110. The dependency of electrical properties on MWCNT length observed in this study can be explained as follows: First and foremost, smaller nanotubes are likely to have more contacts thus resulting in significant increase in cumulative contact resistance. It can be clearly observed in

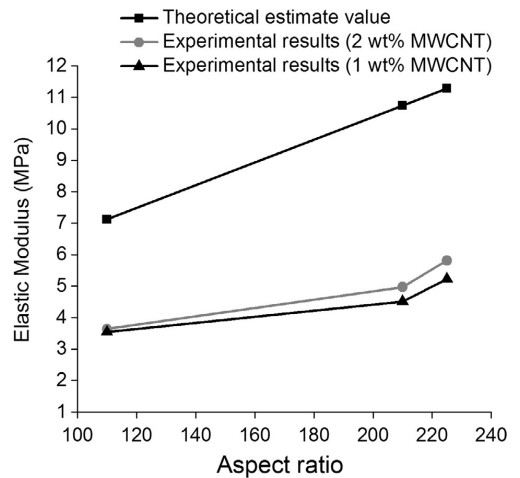


Fig. 5. Graph depicting an theoretical estimate and experimental results of the elastic modulus with respect to various aspect ratios. The linearity in the results is conforming a trend in aspect ratio; however, the experimental values are less than theoretical values which might be explained by imperfect interfacial bonding and inability to achieve the perfect dispersion.

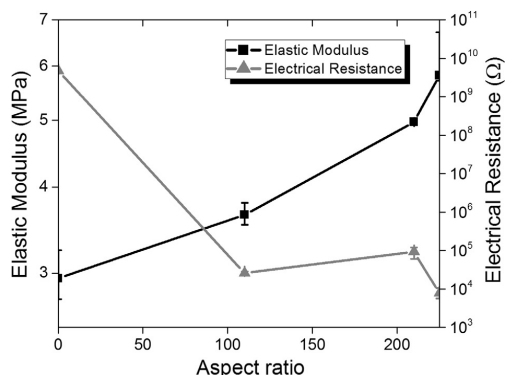


Fig. 6. Co-relational analysis of tensile properties and electric properties with variation of aspect ratio for 2 wt.% MWCNT/PU nanocomposites, clearly indicating that elastic modulus is proportional to aspect ratio of MWCNTs, and surface resistivity have no ordered behaviour with respect to the aspect ratio. (For interpretation of the references to colour in this figure legend, the reader is referred to the web version of this article.)

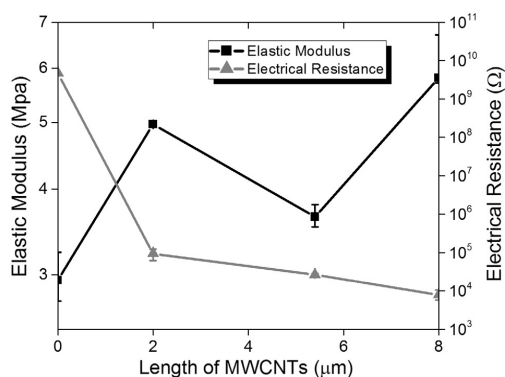


Fig. 7. Co-relational analysis of tensile properties and electric properties with variation of length for 2 wt.% MWCNT/PU nanocomposites, clearly indicating that surface resistivity is proportional to the length of MWCNTs, and the elastic modulus is not correlated to length.

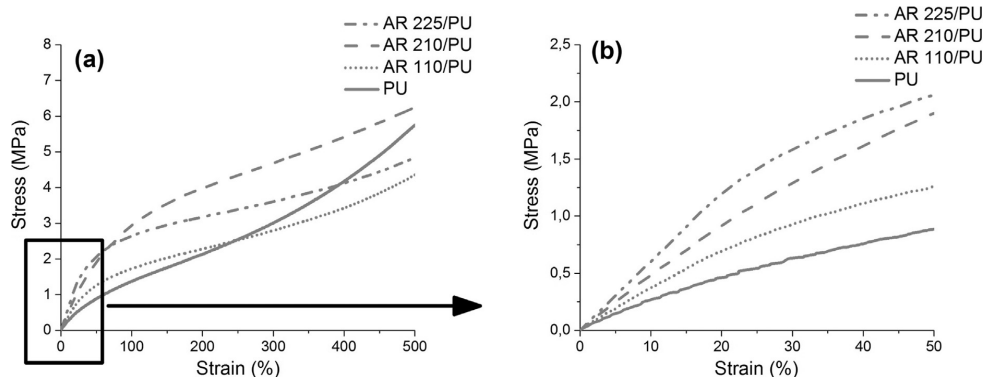


Fig. 8. Stress-strain curves for 2 wt.% MWCNT nanocomposites: (a) Indicates behaviour on high strain values (till 500%). The strain of all the samples was more than 500%. (b) Indicates the magnified area indicated, to clearly depict the increase in elastic modulus with increase of aspect ratio.

Fig. 4a, that shorter MWCNTs (AR 210) are more abundant in the matrix than the longer MWCNTs (AR 225 and AR 110), thus will have higher contact resistance overall caused by numerous junctions ultimately resulting in decreased electrical properties. Secondly, it has also been mentioned that longer nanotubes bridge the smaller agglomerates that are also present in the matrix thus improving the percolation behaviour [50]. Thirdly, the diameter also plays a significant role in the orientation of the nanotubes in polymer matrix. For a given volume of MWCNTs larger quantities of thinner nanotubes are required giving rise to higher van der Waals forces due to increased surface area enhancing the probability of agglomeration. This agglomeration is likely to result in lower electrical conductivity, as bundled nanotubes will behave as spherical microfillers, rather than cylindrical particles capable of forming interconnected networks. This tendency of thinner nanotubes to aggregate can be observed in Fig. 1, where AR 210 nanotubes are present in entangled state. On the other hand, AR 110 and AR 225 does not exhibit any such tendency. Tendency for aggregation of thinner nanotubes with respect to thicker ones has also been confirmed by Dubnikova *et al.* [51]. Finally, it has been mentioned that thinner nanotubes get twisted during processing which leads to reduction in effective aspect ratio [51,52].

Another premise that can be used to explain the unanticipated results in this study is the relative nature of aspect ratio, making it not completely trustworthy. It is quite possible that two nanotubes having similar aspect ratio can have a big difference in actual length and diameter. Fig. 4b explains the relative nature of aspect ratio. It can be observed that all the four hypothetical rod-shaped nanofillers have the same aspect ratio but have very different physical dimensions. Such significant difference in the morphology, at the nanoscale, is likely to cause contrasting response, because other factors such as van der Waals forces can vary significantly at that level. Therefore, all the above-mentioned factors need to be considered separately when estimating percolation threshold on the basis of MWCNT morphology.

Table 5

Quantitative data for the stress-strain analysis of 2 wt%, 1 wt% and 0.5 wt% nanocomposites for AR 225, AR 210 and AR 110.

	E (2 wt%)	E (1 wt%)	E (0.5 wt%)
AR225	5.81 ± 1	5.22 ± 0.9	4.48 ± 0.2
AR210	4.97 ± 0.1	4.51 ± 0.2	3.78 ± 0.3
AR 110	3.64 ± 0.1	3.54 ± 0.1	3.81 ± 0.4

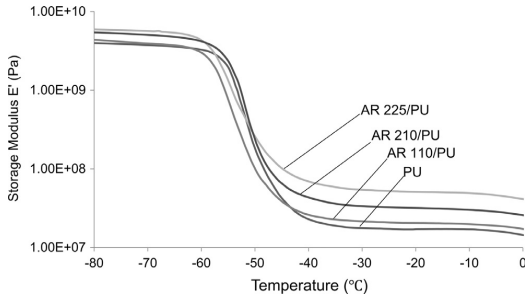


Fig. 9. Storage modulus as a function of temperature for 2 wt% MWCNT/PU samples indicating the reinforcement efficiency of MWCNTs with various aspect ratio. The reinforcing efficiency is clearly higher above Tg of polymer (around -55 °C).

4.3. Tensile properties

Fig. 5 shows the elastic modulus variation with aspect ratio from MWCNT reinforced PU samples at 2 wt% and 1 wt% MWCNT concentration. The Tsai-Halpin model was used in order to evaluate the difference in experimental results and theoretical predictions. According to theory, the maximum elastic modulus (assuming uniform distribution and strong interface) is described by

$$E_c = \left(\frac{3}{8} \frac{1 + 2AR\eta_l V_f}{1 - \eta_l V_f} + \frac{5}{8} \frac{1 + 2\eta_r V_f}{1 - \eta_r V_f} \right) E_m \tag{2}$$

in which

$$\eta_l = \frac{E_f/E_m - 1}{E_f/E_m + 2AR} \tag{3}$$

and

$$\eta_r = \frac{E_f/E_m - 1}{E_f/E_m + 2} \tag{4}$$

where E_c , E_m and E_f are the elastic modulus of the composite, matrix and fibre respectively. The AR is aspect ratio and V_f stands for fibre volume fraction. The elastic modulus of nanotubes was assumed to be 200 GPa. This value, which is considerably less than the widely reported value of 1 TPa, was selected as CVD grown MWCNTs are far less stiff due to the inevitable presence of relatively large number of defects, structural disorders (such as knees and twists), and inclusions (catalyst particles) [53,54]. The comparisons of theoretical and practical results are also presented in Fig. 5. The results

clearly indicate that the theoretical values are considerably higher than those that were found experimentally. This difference can be explained by inability of the processing method to achieve dispersions containing individual MWCNTs. The results also indicate that the difference between theoretical and experimental values increases with the aspect ratio. However, it is worth mentioning that our results are in disagreement with Ayatollahi *et al.*, who reported that with higher aspect ratio the difference between theoretical and practical values decreases [6].

Fig. 6 presents the variation in tensile properties and electric properties with respect to the aspect ratio. Fig. 7, on the other hand, presents the variation in tensile properties and electric properties with respect to the MWCNT length. Fig. 6 clearly portrays the linear variation of tensile modulus with respect to the aspect ratio; and the zigzag-shaped graph displays the electric properties. Opposite behaviour can be observed in Fig. 7, where electric properties are proportional to nanotube length whilst the tensile modulus follows no clear trend.

Fig. 8 presents the stress strain curve for the 2 wt% samples. Pure PU has elastic modulus of 2.9 MPa approximately, indicating its elastomeric nature. Quantitatively, the elastic modulus of 2 wt% MWCNT nanocomposites is increased by 100% for AR 225/PU, 70% for AR 210/PU and 25% for AR 110 (when compared to pure PU), suggesting that in this particular case, the aspect ratio correlates with the elastic modulus, not the length. The elastic modulus appears to be also linearly dependent on the aspect ratio. The quantitative results of stress-strain analysis is provided in Table 5. Similar patterns were observed in 1 wt% MWCNT nanocomposites. Unfortunately, the data for 0.5 wt% MWCNT samples were not statistically significant.

4.4. Dynamic mechanical analysis (DMA)

DMA was conducted to confirm the findings of tensile testing and to study the temperature dependent mechanical properties of nanocomposites. Since the polyurethane used in this study was an elastomer, DMA was conducted over sub-zero temperatures. Storage modulus curves of samples with 2 wt% MWCNT content are presented in Fig. 9. All samples containing MWCNTs showed an increase in storage modulus as a result of the stiffening effect of MWCNTs and the interfacial interactions between MWCNTs and matrix [55]. Fig. 10(a and b) presents the variation of storage modulus with increasing aspect ratio and length, respectively. The pattern in Fig. 10 indicates that the storage modulus, like the tensile modulus, is also dependent on aspect ratio, confirming the finding of the tensile testing.

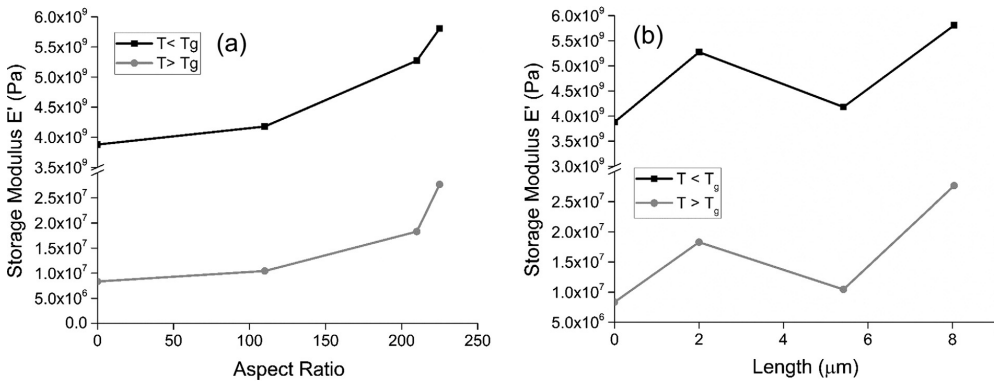


Fig. 10. Variation of storage modulus 20 °C (above Tg) and -75 °C (below Tg) for 2 wt% MWCNT/PU nanocomposites: (a) With aspect ratio of MWCNTs. (b) With length of MWCNT. Storage modulus increases with aspect ratio and follows a trend; however, length follows no definite correlating pattern with storage modulus.

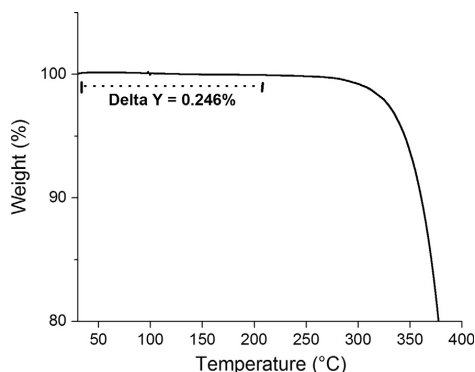


Fig. 11. TGA graph used to estimate the equilibrium moisture content of nanocomposite films, which was ca. 0.246%.

5. Conclusion

In this study, the effect of MWCNT morphology on electrical and mechanical properties of PU nanocomposites was studied. We have shown that longer nanotubes exhibit better electrical conductivity, and the percolation threshold is dependent on length, not on the aspect ratio. The MWCNTs in PU matrix with lengths of 8 μm , 5.5 μm , and 2 μm resulted in percolation thresholds of 0.2–0.5 wt %, 0.6–1 wt %, and 1–1.5 wt % respectively, with minimum resistivity of 7840 Ω , 26,200 Ω , and 78,200 Ω respectively at a concentration of 2 wt%. On the other hand, the modulus is found to be dependent on the aspect ratio, as expected. The tensile modulus of the samples with 2 wt% MWCNT in a PU matrix with aspect ratio 225, 210, and 110 corresponds to 100%, 70%, the 25% over pure PU, following a linear increase. A similar pattern was observed in results obtained by DMA analysis. We suggest that aspect ratio should not be interpreted as the universal parameter for characterization of MWCNTs. Depending on the materials employed it is possible that the length of the MWCNTs can more appropriately fit the predicted pattern, rather than their aspect ratio. Our results are naturally specific to a particular case where two nanotubes have same aspect ratio but different lengths. Nevertheless, they provide valuable information regarding the unreliability of the aspect ratio as an inherent parameter for characterization of nanocomposites.

Acknowledgements

The authors would like to thank Kosti Rämö and Sinikka Pohjonen for their help with dynamic mechanical analysis. We are also grateful for the financial support received from the European Community's Seventh Framework Programme (FP7/2007–2013): The Marie Curie CONTACT Project under grant agreement no. 238363; The Royal Society, European Research Council (ERC-2009-StG 240500 DEDIGROWTH; ERC-2012-PoC 309786 DEVICE, and ERC-2015-POC-680559 CONDUCT); the UK Government for Engineering and Physical Sciences Research Council (EPSRC) Pathways to Impact grants.

References

- Ajayan PM, Tour JM. Materials science: nanotube composites. *Nature* 2007;447:1066–8. <http://dx.doi.org/10.1038/4471066a>.
- Li J, Ma PC, Chow WS, To CK, Tang BZ, Kim J-K. Correlations between percolation threshold, dispersion state, and aspect ratio of carbon nanotubes. *Adv Funct Mater* 2007;17:3207–15. <http://dx.doi.org/10.1002/adfm.200700065>.
- Bao HD, Sun Y, Xiong ZY, Guo ZX, Yu J. Effects of the dispersion state and aspect ratio of carbon nanotubes on their electrical percolation threshold in a polymer. *J Appl Polym Sci* 2013;128:735–40. <http://dx.doi.org/10.1002/app.37554>.
- Rosca ID, Hoa SV. Highly conductive multiwall carbon nanotube and epoxy composites produced by three-roll milling. *Carbon* 2009;47:1958–68. <http://dx.doi.org/10.1016/j.carbon.2009.03.039>.
- Rahaman M, Thomas SP, Hussein IA. Dependence of electrical properties of polyethylene nanocomposites on aspect ratio of carbon nanotubes. *Polym Compos* 2013;494–9. <http://dx.doi.org/10.1002/polb>.
- Ayatollahi MR, Shadlou S, Shokrieh MM, Chitsazzadeh M. Effect of multi-walled carbon nanotube aspect ratio on mechanical and electrical properties of epoxy-based nanocomposites. *Polym Test* 2011;30:548–56. <http://dx.doi.org/10.1016/j.polymertesting.2011.04.008>.
- Singh I, Verma A, Kaur I, Bharadwaj LM, Bhatia V, Jain VK, et al. The effect of length of single-walled carbon nanotubes (SWNTs) on electrical properties of conducting polymer-SWNT composites. *J Polym Sci B Polym Phys* 2009;48:89–95. <http://dx.doi.org/10.1002/polb.21847>.
- Singh BP, Saini K, Choudhary V, Teotia S, Pande S, Saini P, et al. Effect of length of carbon nanotubes on electromagnetic interference shielding and mechanical properties of their reinforced epoxy composites. *J Nanopart Res* 2013;16:2161. <http://dx.doi.org/10.1007/s11051-013-2161-9>.
- Lima MD, Andrade MJ, Skákalová V, Bergmann CP, Roth S. Dynamic percolation of carbon nanotubes in liquid medium. *J Mater Chem* 2007;17:4846. <http://dx.doi.org/10.1039/b710417k>.
- Wu D, Wu L, Zhou W, Sun Y, Zhang M. Relations between the aspect ratio of carbon nanotubes and the formation of percolation networks in biodegradable polylactide/carbon nanotube composites. *J Polym Sci B Polym Phys* 2010;48:479–89. <http://dx.doi.org/10.1002/polb.21909>.
- Abbasi SH, Al-juhani AA, Ul-hamid A, Hussein IA. Effect of aspect ratio, surface modification and compatibilizer on the mechanical and thermal properties of ldpe-mwcnt nanocomposites. *E-Polymers* 2011;11:722–38. <http://dx.doi.org/10.1515/epoly.2011.11.1.722>.
- Thomas SP, Rahaman M, Hussein I a. Impact of aspect ratio and CNT loading on the dynamic mechanical and flammability properties of polyethylene nanocomposites. *E-Polymers* 2014;14:57–63. <http://dx.doi.org/10.1515/epoly-2013-0019>.
- Dang ZM, Shehzad K, Zha JW, Hussain T, Jun N, Bai J. On refining the relationship between aspect ratio and percolation threshold of practical carbon nanotubes/polymer nanocomposites. *Jpn J Appl Phys* 2011;50:080214. <http://dx.doi.org/10.1143/JJAP.50.080214>.
- Martone A, Faiella G, Antonucci V, Giordano M, Zarrelli M. The effect of the aspect ratio of carbon nanotubes on their effective reinforcement modulus in an epoxy matrix. *Compos Sci Technol* 2011;71:1117–23. <http://dx.doi.org/10.1016/j.compscitech.2011.04.002>.
- Lu KL, Lago RM, Chen YK, Green MLH, Harris PJF, Tsang SC. Mechanical damage of carbon nanotubes by ultrasound. *Carbon* 1996;34:814–6.
- Guo J, Liu Y, Prada-Silvy R, Tan Y, Azad S, Krause B, et al. Aspect ratio effects of multi-walled carbon nanotubes on electrical, mechanical, and thermal properties of polycarbonate/MWCNT composites. *J Polym Sci B Polym Phys* 2014;52:73–83. <http://dx.doi.org/10.1002/polb.23402>.
- Meysami SS, Koós AA, Dillon F, Dutta M, Grobert N. Aerosol-assisted chemical vapour deposition synthesis of multi-wall carbon nanotubes: III. Towards upscaling. *Carbon* NY 2015. <http://dx.doi.org/10.1016/j.carbon.2015.02.045>.
- Meysami SS. Development of an aerosol-CVD technique for the production of CNTs with integrated online control. University of Oxford 2013.
- Meysami SS, Dillon F, Koós AA, Aslam Z, Grobert N. Aerosol-assisted chemical vapour deposition synthesis of multi-wall carbon nanotubes: I. Mapping the reactor. *Carbon* NY 2013;58:151–8. <http://dx.doi.org/10.1016/j.carbon.2013.02.044>.
- Meysami SS, Koós AA, Dillon F, Grobert N. Aerosol-assisted chemical vapour deposition synthesis of multi-wall carbon nanotubes: II. An analytical study. *Carbon* NY 2013;58:159–69. <http://dx.doi.org/10.1016/j.carbon.2013.02.041>.
- Meysami SS, Snoek LC, Grobert N. Versatile in situ gas analysis apparatus for nanomaterials reactors. *Anal Chem* 2014;86:8850–6. <http://dx.doi.org/10.1021/ac502288x>.
- Koós AA, Dowling M, Jurkschat K, Crossley A, Grobert N. Effect of the experimental parameters on the structure of nitrogen-doped carbon nanotubes produced by aerosol chemical vapour deposition. *Carbon* NY 2009;47:30–7. <http://dx.doi.org/10.1016/j.carbon.2008.08.014>.
- Koós AA, Dillon F, Obratsova EA, Crossley A, Grobert N. Comparison of structural changes in nitrogen and boron-doped multi-walled carbon nanotubes. *Carbon* NY 2010;48:3033–41. <http://dx.doi.org/10.1016/j.carbon.2010.04.026>.
- Nicholls RJ, Britton J, Meysami SS, Koós AA, Grobert N. In situ engineering of NanoBud geometries. *Chem Commun (Camb)* 2013;49:10956–8. <http://dx.doi.org/10.1039/c3cc46064a>.
- Müller MT, Krause B, Kretzschmar B, Pötschke P. Influence of feeding conditions in twin-screw extrusion of PP/MWCNT composites on electrical and mechanical properties. *Compos Sci Technol* 2011;71:1535–42. <http://dx.doi.org/10.1016/j.compscitech.2011.06.003>.
- Orgilés-Calpena E, Arán-Aís F, Torró-Palau A.M, Orgilés-Barceló C. Effect of amount of carbon nanotubes in polyurethane dispersions. In: *Macromolecular Symposia* 2012;321–322:135–9. <http://dx.doi.org/10.1002/masy.201251123>.
- Fiori DE. Two-component water reducible polyurethane coatings. *Prog Org Coatings* 1997;32:65–71.

- [28] Oprea S. Effect of the long chain extender on the properties of linear and castor oil cross-linked PEG-based polyurethane elastomers. *J Mater Sci* 2011;46:2251–8.
- [29] Gurunathan T, Rao CRK, Narayan R, Raju KVS. Polyurethane conductive blends and composites: synthesis and applications perspective. *J Mater Sci* 2012;48:67–80. <http://dx.doi.org/10.1007/s10853-012-6658-x>.
- [30] Heintz AM, Duffy DJ, Nelson CM, Hua Y, Hsu SL, Suen W, et al. A spectroscopic analysis of the phase evolution in polyurethane foams. *Macromolecules* 2005;38:9192–9.
- [31] Rastogi R, Kaushal R, Tripathi SK, Sharma AL, Kaur I, Bharadwaj LM. Comparative study of carbon nanotube dispersion using surfactants. *J Colloid Interface Sci* 2008;328:421–8. <http://dx.doi.org/10.1016/j.jcis.2008.09.015>.
- [32] Kumar P, Bohidar HB. Aqueous dispersion stability of multi-carbon nanoparticles in anionic, cationic, neutral, bile salt and pulmonary surfactant solutions. *Colloids Surf A Physicochem Eng Aspects* 2010;361:13–24. <http://dx.doi.org/10.1016/j.colsurfa.2010.03.009>.
- [33] Grossiord N, Regev O, Loos J, Meuldijk J, Koning CE. Time-dependent study of the exfoliation process of carbon nanotubes in aqueous dispersions by using UV-visible spectroscopy. *Anal Chem* 2005;77:5135–9. <http://dx.doi.org/10.1021/ac050358j>.
- [34] Yu J, Lu K, Sourty E, Grossiord N, Koning CE, Loos J. Characterization of conductive multiwall carbon nanotube/polystyrene composites prepared by latex technology. *Carbon NY* 2007;45:2897–903. <http://dx.doi.org/10.1016/j.carbon.2007.10.005>.
- [35] Gong X, Liu J, Baskaran S, Voise RD, Young JS. Surfactant-assisted processing of carbon nanotube/polymer composites. *Chem Mater* 2000;12:1049–52. <http://dx.doi.org/10.1021/cm9906396>.
- [36] Lovell CS, Wise KE, Kim J-W, Lülehei PT, Harrison JS, Park C. Thermodynamic approach to enhanced dispersion and physical properties in a carbon nanotube/polypeptide nanocomposite. *Polymer (Guildf)* 2009;50:1925–32. <http://dx.doi.org/10.1016/j.polymer.2009.02.016>.
- [37] Grossiord N, Loos J, Regev O, Koning CE. Toolbox for dispersing carbon nanotubes into polymers to get conductive nanocomposites. *Chem Mater* 2006;18:1089–99. <http://dx.doi.org/10.1021/cm051881h>.
- [38] Chen H, Jacobs O, Wu W, Rüdiger G, Schädel B. Effect of dispersion method on tribological properties of carbon nanotube reinforced epoxy resin composites. *Polym Test* 2007;26:351–60. <http://dx.doi.org/10.1016/j.polymertesting.2006.11.004>.
- [39] Yang K, Yi Z, Jing Q, Yue R, Jiang W, Lin D. Sonication-assisted dispersion of carbon nanotubes in aqueous solutions of the anionic surfactant SDBS: the role of sonication energy. *Chin Sci Bull* 2013;58:2082–90. <http://dx.doi.org/10.1007/s11434-013-5697-2>.
- [40] Grossiord N. A Latex-based concept for making carbon nanotube/polymer nanocomposites. Eindhoven: Technische Universiteit Eindhoven; 2007.
- [41] Grossiord N, Claire HM, Koning C. Polymer carbon nanotube composites the polymer latex concept. Pan Stanford Publishing; 2012.
- [42] Dutta M. Development of a spray process for manufacturing carbon nanotube films. University of Oxford, 2015.
- [43] Sathyanarayana S, Hübner C. Structural Nanocomposites. Berlin, Heidelberg: Springer; 2013. <http://dx.doi.org/10.1007/978-3-642-40322-4>.
- [44] Krause B, Mende M, Pötschke P, Petzold G. Dispersibility and particle size distribution of CNTs in an aqueous surfactant dispersion as a function of ultrasonic treatment time. *Carbon NY* 2010;48:2746–54. <http://dx.doi.org/10.1016/j.carbon.2010.04.002>.
- [45] Weydemeyer EJ, Sawdon AJ, Peng CA. Controlled cutting and hydroxyl functionalization of carbon nanotubes through autoclaving and sonication in hydrogen peroxide. *Chem Commun (Cambridge, United Kingdom)* 2015;51:5939–42. <http://dx.doi.org/10.1039/C5CC01115A>.
- [46] Huang W, Lin Y, Taylor S, Gaillard J, Rao AM, Sun YP. Sonication-assisted functionalization and solubilization of carbon nanotubes. *Nano Lett* 2002;2:231–4. <http://dx.doi.org/10.1021/nl010083x>.
- [47] Heller Da, Mayrhofer RM, Baik S, Grinkova YV, Urey ML, Strano MS. Concomitant length and diameter separation of single-walled carbon nanotubes. *J Am Chem Soc* 2004;126:14567–73. <http://dx.doi.org/10.1021/ja046450z>.
- [48] Allaoui A, Jin B, Rieux N. Dielectric properties of composites of multi-walled carbon nanotubes in a resin matrix. *Polym Polym Compos* 2003;11:171–8.
- [49] Bauhofer W, Kovacs JZ. A review and analysis of electrical percolation in carbon nanotube/polymer composites. *Compos Sci Technol* 2009;69:1486–98. <http://dx.doi.org/10.1016/j.compscitech.2008.06.018>.
- [50] Bai JB, Allaoui A. Effect of the length and the aggregate size of MWNTs on the improvement efficiency of the mechanical and electrical properties of nanocomposites—experimental investigation. *Compos A Appl Sci Manuf* 2003;34:689–94. [http://dx.doi.org/10.1016/S1359-835X\(03\)00140-4](http://dx.doi.org/10.1016/S1359-835X(03)00140-4).
- [51] Dubnikova I, Kuvardina E, Krashenninikov V, Lomakin S, Tchmutin I, Kuznetsov S. The effect of multiwalled carbon nanotube dimensions on the morphology, mechanical, and electrical properties of melt mixed polypropylene-based composites. *J Appl Polym Sci* 2010;117:18–21. <http://dx.doi.org/10.1002/app>.
- [52] Nan CW, Shi Z, Lin Y. A simple model for thermal conductivity of carbon nanotube-based composites. *Chem Phys Lett* 2003;375:666–9. [http://dx.doi.org/10.1016/S0009-2614\(03\)00956-4](http://dx.doi.org/10.1016/S0009-2614(03)00956-4).
- [53] Lukić B, Seo JW, Couteau E, Lee K, Građečak S, Berkecz R, et al. Elastic modulus of multi-walled carbon nanotubes produced by catalytic chemical vapour deposition. *Appl Phys A* 2005;80:695–700. <http://dx.doi.org/10.1007/s00339-004-3100-5>.
- [54] Guhadós G, Wan W, Sun X, Hutter JL. Simultaneous measurement of Young's and shear moduli of multiwalled carbon nanotubes using atomic force microscopy. *J Appl Phys* 2007;101:33514. <http://dx.doi.org/10.1063/1.2433125>.
- [55] Montazeri A. The effect of functionalization on the viscoelastic behaviour of multi-wall carbon nanotube/epoxy composites. *Mater Des* 2013;45:510–7. <http://dx.doi.org/10.1016/j.matdes.2012.09.013>.
- [56] Pevzner S, Pri-Bar I, Regev O. Solid-state solvent-free catalyzed hydrogenation: enhancing reaction efficiency by spillover agents. *J Mol Catal A Chem* 2013;376:48–52. <http://dx.doi.org/10.1016/j.molcata.2013.04.007>.
- [57] Milakin KA, Yaremko IA, Smirnova AV, Pyshkina OA, Sergeev VG. Effect of multiwall carbon nanotubes surface on polymerization of aniline and properties of its products. *Russ J Gen Chem* 2015;85:1146–51. <http://dx.doi.org/10.1134/S1070363215050242>.
- [58] Figarol A, Pourchez J, Boudard D, Forest V, Berhanu S, Tulliani J-M, et al. Thermal annealing of carbon nanotubes reveals a toxicological impact of the structural defects. *J Nanopart Res* 2015;17:1–14. <http://dx.doi.org/10.1007/s11051-015-2999-0>.
- [59] Che BD, Nguyen BQ, Nguyen LTT, Nguyen HT, Nguyen VQ, Van Le T, et al. The impact of different multi-walled carbon nanotubes on the X-band microwave absorption of their epoxy nanocomposites. *Chem Cent J* 2015;9:10. <http://dx.doi.org/10.1186/s13065-015-0087-2>.
- [60] White CM, Banks R, Norton B, Hamerton I, Watts JF. Development of an anti-static coating incorporating multi-walled carbon nanotubes as an alternative to graphite. *Adhes Soc Annu Meet* 2013;500:4–6.
- [61] TDS. Bayer Materials Science, Bayhydrol UH 240. n.d. <http://www.coatings.covestro.com/en/Products/Bayhydrol/ProductListBayhydrol/201503030528/Bayhydrol-UH-240; 2016> [accessed November 4].

